AD_____

Award Number: DAMD17-98-1-8603

TITLE: Radiation and Angiostatin Target the Tumor Vasculature: A New Paradigm for Prostate Cancer Treatment

PRINCIPAL INVESTIGATOR: Ralph R. Weichselbaum, M.D.

CONTRACTING ORGANIZATION: The University of Chicago
Chicago, Illinois 60637

REPORT DATE: October 2000

TYPE OF REPORT: Final

PREPARED FOR: U.S. Army Medical Research and Materiel Command
Fort Detrick, Maryland 21702-5012

REPORT DOCUMENTATION PAGE

Form Approved
OMB No. 074-0188

1. AGENCY USE ONLY (Leave blank)	2. REPORT DATE	3. REPORT TYPE AND DATES COVERED
	October 2000	Final (1 Oct 98 - 30 Sep 00)

4. TITLE AND SUBTITLE
Radiation and Angiostatin Target the Tumor Vasculature: A New Paradigm for Prostate Cancer Treatment

5. FUNDING NUMBERS
DAMD17-98-1-8603

6. AUTHOR(S)
Ralph R. Weichselbaum, M.D.

7. PERFORMING ORGANIZATION NAME(S) AND ADDRESS(ES)
The University of Chicago
Chicago, Illinois 60637

E-MAIL:
rrw@rover.bsd.uchicago.edu

8. PERFORMING ORGANIZATION REPORT NUMBER

9. SPONSORING / MONITORING AGENCY NAME(S) AND ADDRESS(ES)
U.S. Army Medical Research and Materiel Command
Fort Detrick, Maryland 21702-5012

10. SPONSORING / MONITORING AGENCY REPORT NUMBER

11. SUPPLEMENTARY NOTES

12a. DISTRIBUTION / AVAILABILITY STATEMENT
Approved for public release; Distribution unlimited

12b. DISTRIBUTION CODE

13. ABSTRACT *(Maximum 200 Words)*

Our laboratory has investigated the interaction of angiostatin and ionizing radiation (IR) both *in vivo* and *in vitro*. We proposed the hypothesis that interactive killing between angiostatin and fractionated radiation in murine tumors and human xenografts may overcome radioresistance by targeting the prostate tumor neovasculature. We have demonstrated enhanced tumor regression in PC3 (human prostate carcinoma) xenografts and in murine Lewis lung carcinomas (LLC) treated with the combination of angiostatin and IR when compared with either treatment alone. We have shown *in vitro* that angiostatin was cytotoxic to endothelial cells but not to tumor cells. Additive cytotoxicity was seen in endothelial cells when angiostatin was combined with IR. This cytotoxic interaction was absent in tumor cells treated with angiostatin and IR suggesting specificity of targeting tumor endothelium. We investigated the hypothesis that DNA damaging agents other than IR will interact with angiostatin. Cyclophosphamide was employed in combination with angiostatin to assess primary tumor regression using PC3 xenografts and LLC tumors and to assess growth of metastases using LLC. These data may lead to increased efficacy of localized radiotherapy for prostate cancer and may be beneficial in the adjuvant treatment of prostate cancer and possibly in some forms of metastatic prostate cancer.

14. SUBJECT TERMS
Prostate Cancer

15. NUMBER OF PAGES
59

16. PRICE CODE

17. SECURITY CLASSIFICATION OF REPORT	18. SECURITY CLASSIFICATION OF THIS PAGE	19. SECURITY CLASSIFICATION OF ABSTRACT	20. LIMITATION OF ABSTRACT
Unclassified	Unclassified	Unclassified	Unlimited

Table of Contents

Original proposal title: Radiation and Angiostatin Target the Tumor Vasculature: A New Paradigm for Prostate Cancer Treatment

Original Award Category: Idea Development Award

Principal Investigator: Ralph R. Weichselbaum, MD
Phone: (773) 702-0817
FAX: (773) 834-7233
Email: rrw@rover.bsd.uchicago.edu

Institution: University of Chicago
5801 S. Maryland Ave., MC 1105
Chicago, IL 60637
USA

Introduction

Angiogenesis, the formation of new capillaries from pre-existing vessels, is essential for tumor progression. (1, 2, 3, 4, 5) Angiostatin, a proteolytic fragment of plasminogen(6), inhibits angiogenesis and thereby growth of primary(7) and metastatic tumors(8, 9, 10). Radiotherapy is important in the treatment of human cancers but is often unsuccessful due to tumor cell radioresistance(11, 12). We proposed the hypothesis that interactive killing between angiostatin and fractionated radiation in murine tumors and human xenografts may overcome radioresistance by targeting the prostate tumor neovasculature. This hypothesis is based on the fact that tumor endothelium is derived from normal host tissue, and unlike neoplastic tissue, is genetically stable. Furthermore, one tumor vessel may supply as many as 10^1-10^4 tumor cells. We hypothesize that concepts from our investigations of targeting the tumor vasculature with DNA damaging agents and angiogenesis inhibitors may be beneficial in some forms of prostate cancer.

Radiation and Angiostatin Target the Tumor Vasculature: A New Paradigm for Prostate Cancer Research
Ralph R. Weichselbaum, MD

Body

Task 1: Angiostatin and radiation exert an interactive tumor killing effect in human prostate carcinoma xenografts by inhibiting tumor angiogenesis. For the first twelve months of the proposal we proposed to use purified angiostatin (AS) and ionizing radiation (IR) to assess the anti-tumor effect of combined treatment in prostate cancer. PC-3 prostate cancer cells were injected into the flank of nude mice and tumors grown to a mean size of 770 mm^3. The animals were divided into four treatment groups: control (n=8), IR (n=10), AS (n=10), combined AS+IR (n=10). AS was injected intraperitoneally (IP) at a dose of 25 mg/kg/day. IR was delivered over two weeks at a fraction of 500 cGy per day to a total dose of 4000 cGy. Animals receiving combined treatment were injected with AS four hours prior to IR. The tumors were measured twice weekly with calipers. The animals treated with AS alone grew at the same rate as the controls and both groups were euthanized at day 21 due to tumor burden. The animals treated with IR and AS+IR showed similar tumor regression through day 24. From day 24 to day 42 the IR treated tumors began regrowth while the AS+IR treated tumors continued regressing. At day 42 the difference in means is statistically significant ($P<0.001$). (Figure 1)

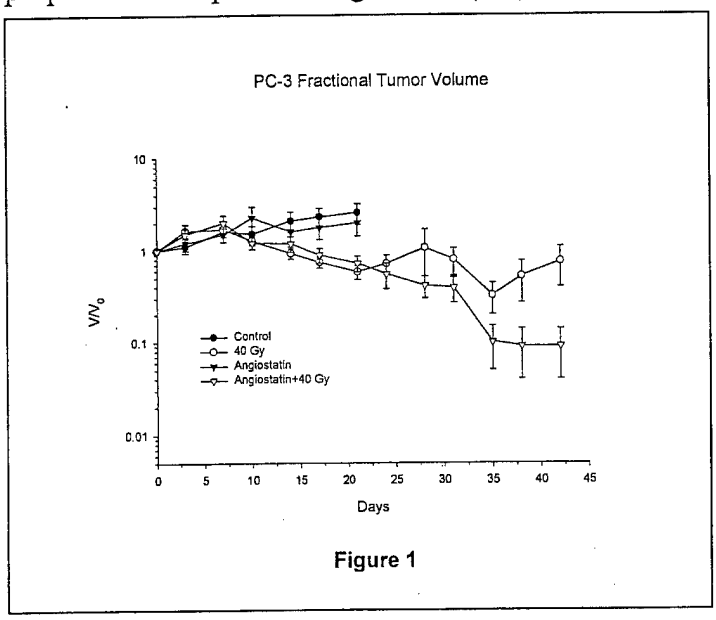

Figure 1

We also used the Lewis lung carcinoma (LLC) model to study the interaction of AS and IR. LLC cells were injected ($5x10^5$) into C57BL/6 mice. The tumors grew to a mean volume of 1104 mm^3. 28 mice were divided into treatment groups, untreated control (n=7), 40 Gy (20+20 Gy days 0 and 1) (n=7), AS (n=7), and AS+40 Gy (n=7). AS was injected IP beginning at day 0 at a dose of 25 mg/kg/day divided into two daily injections and continued for fourteen days. The untreated control and AS alone animals were euthanized on day 9. The time to tumor regrowth is extended in the AS+IR treatment group compared to the IR alone. At day nine the difference in mean tumor volumes is statistically significant ($P<0.05$). (Figure 2) To determine the effects of treatment on tumor neovascularization, representative tissue sections from LLC tumors were stained using anti-CD-31 antibody and standard immunohistochemical techniques. The number of tumor vessels per high power field was reduced following treatment with AS+IR compared with all other treatments. To demonstrate that the PC-3 tumor cells are not the target of the AS/IR interaction, PC-3 cells were treated with AS+IR *in vitro* employing the clonogenic assay. Cells treated with AS have identical surviving fractions to those cells treated with IR alone. This demonstrates that the *in vivo* interaction of AS and IR is not attributable to the direct killing of the PC-3 cells but suggests that endothelial cells are the target of the AS+IR interaction. My laboratory has

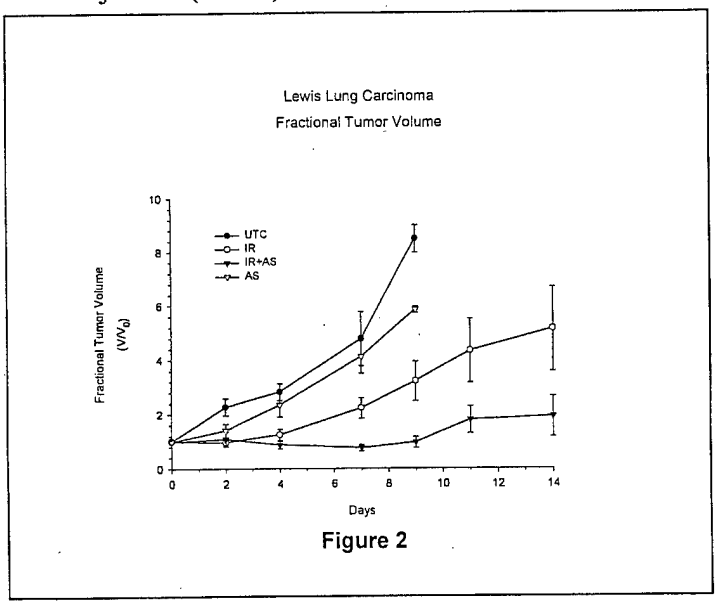

Figure 2

demonstrated that the AS/IR response is directed at the endothelial cells. HUVEC were treated with 1, 10, 100, and 1000 ng/ml AS. There is an initial rapid decrease in surviving fraction which levels off at 100 ng/ml (0.47 surviving fraction) and remains comparable when HUVEC are treated with concentrations of AS as high as 1000 ng/ml (0.44 surviving fraction). We then studied the effects of treatment with AS followed by IR on HUVEC. In order to conserve the limited AS supply, we chose to use an AS concentration of 100 ng/ml (since the surviving fraction was the same as 1000 ng/ml) added to the cultures 18 hours after plating. IR was delivered four hours after addition of AS. These experiments demonstrate the additive cytotoxic interaction of AS and IR in HUVEC. In order to elucidate whether the mechanism of this killing by AS was due in part to increased apoptosis in AS treated cells, we determined the percentage of HUVEC undergoing apoptosis after treatment with 1000 ng/ml AS, 10Gy, or the combination when compared to controls at 0, 12, 24, and 48 hours. We chose to use the 7-AAD staining method as it stained both early and late apoptotic cells. There is no increase in apoptosis in HUVEC treated with AS when compared with control. Also, the cells treated with AS prior to 10 Gy had the same percentage of apoptotic cells as the cells treated with 10 Gy alone. This leads us to conclude that AS does not kill cells through apoptosis, and that the interaction of AS and IR is not mediated by apoptosis, but the cytotoxicity observed is due to a mitotic cell death. **Task 2: Angiostatin and radiation are potentially an effective therapy against metastases from prostate cancer.** From 12 months to the present we have been investigating the interaction between a DNA damaging agent, cyclophosphamide (CTX), and AS. We have studied this interaction using the PC3 xenograft and LLC tumor model and its effects on primary tumor growth delay. Figure 3 shows the results of treatment of PC3 xenografts treated with AS, CTX, and AS+CTX. A small tumor growth delay was seen in the AS+CTX treatment group compared to CTX alone. LLC tumors were established as outlined above. For the first experiment, the treatments began seven days after injection with tumors having a mean volume of 228 mm^3. The pattern of growth in the AS group was similar to

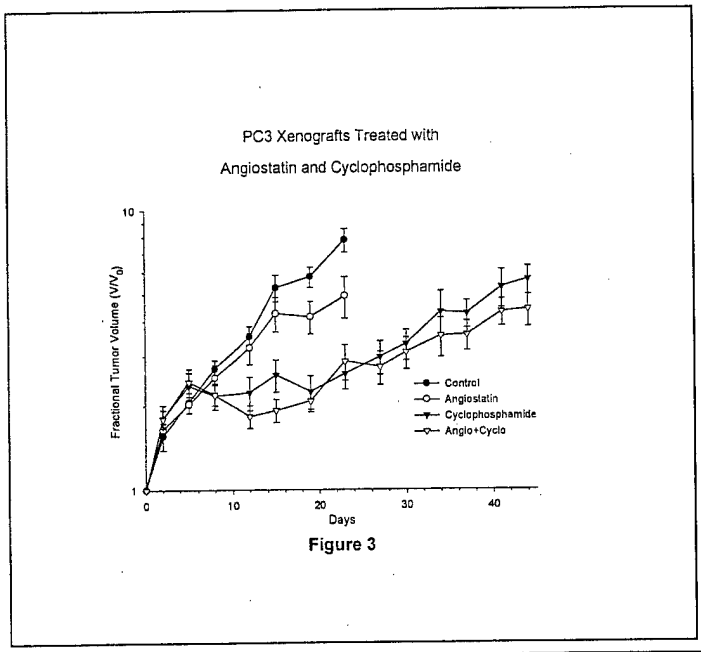

Figure 3

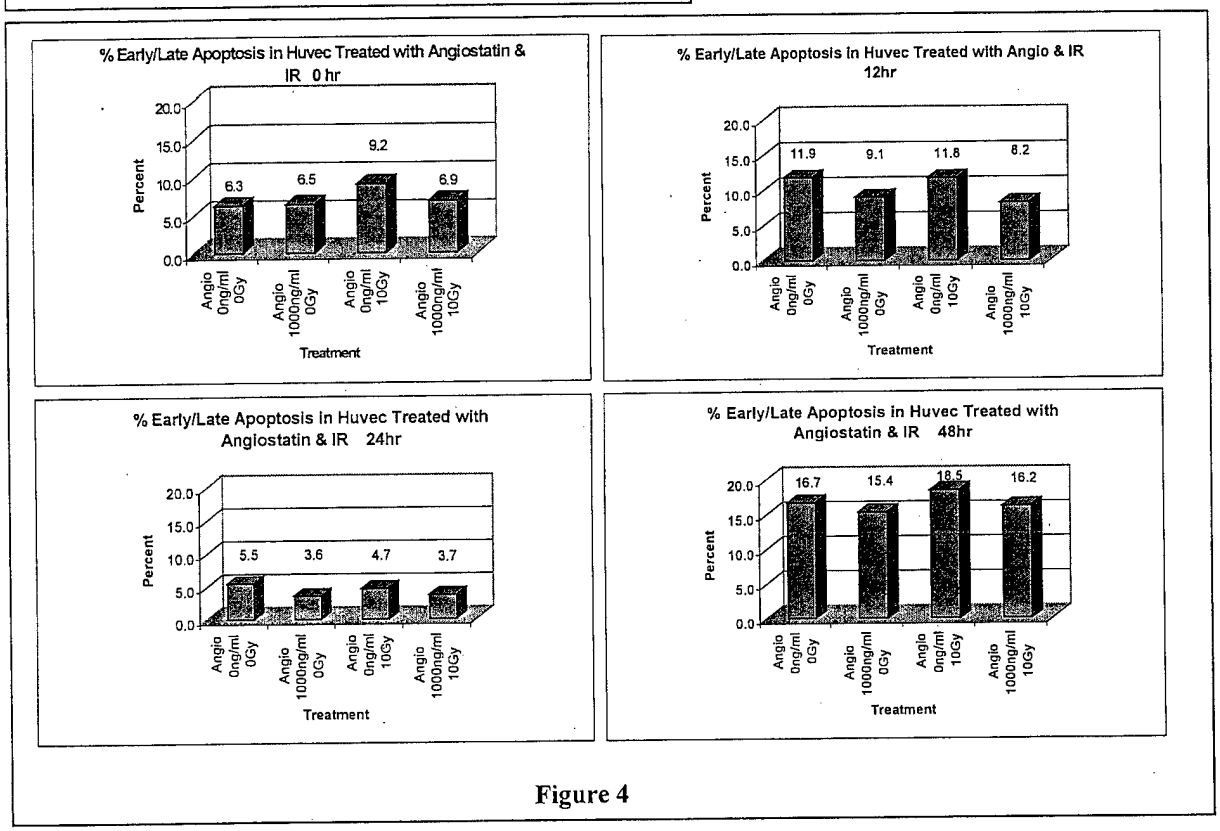

Figure 4

that of PBS injected mice. Although growth was delayed by three days in the groups treated with CTX alone and the combination, at day 14 we did not observe any difference in the primary tumor growth of mice treated with CTX alone or with CTX+AS.

Table 1: The mean number of lung metastases in mice bearing LLC tumors that were treated with PBS (Control), Angiostatin, Cyclophosphamide, and Angiostatin + Cyclophosphamide.

Time (Days)	Control	Angiostation	Cyclophosphamide	Angiostatin + Cyclophosphamide
10	0.5	2.3	0.67	0
12	1.5	4.3	0	0.33
14	2.8	5.2	0.86	0.67
17	49.75	30	3.8	1.17
19	89.86	88	5.88	0.67
21	134.9	74.86	15.22	2.56
				(P=0.024)

Because the Lewis lung carcinoma begins neoangiogenesis about day 4 post tumor implantation (Scan. Electron Microsc. (pt. 2): 557, (1986)), we chose day 3 in the subsequent study to initiate treatment with AS. We also evaluated the effects of the treatments on distant disease in the lungs by determining the number of metastasized colonies. The mice were injected with LLC cells and randomized into four treatment groups as described. 3 days later, treatment began. Control tumors were injected with PBS (200 µl daily for 7 days). Mice treated with CTX received a total dose of 300 mg divided into four treatments of 75 mg/kg delivered on days 4, 5, 6, and 7. Animals in the AS group received 5 mg/kg of AS on days 3, 4, 5, 6, 7, 8, and 9. Primary tumor volumes were determined as before and mean tumor volumes were recorded. Tumors were measurable in all the groups at day 7. Primary tumor volumes in the CTX group (mean 92.4 $\pm$ 8.97 mm^3) and the combined treatment groups (88.5 $\pm$ 8.3 mm^3) were smaller than the control (139 $\pm$ 12.89 mm^3) and AS treated groups (103.7 $\pm$ 12.65 mm^3). Tumors continued to grow in all the groups throughout the experiment. Tumor volumes of mice in the PBS and AS treated groups tripled at day 10 while those in the CTX and the combined treatment group had doubled. The control group reached a tumor volume of 3000 mm^3 by day 17 with tumors in the AS group reaching a comparable size. Tumors of mice treated with CTX alone and those with AS+CTX reached a mean volume of 1000 mm^3 at day 17. This study was repeated to confirm the results obtained. While the AS and AS+CTX treatment did not alter the growth of the primary tumor, the number of lung metastases (Table 1) was reduced in the AS treated group as compared to the controls at day 21. The number of lung metastases was lower in the CTX treated group as compared to the AS treated group. Interestingly, the number of lung metastases was markedly reduced in the group treated with AS+CTX (p=0.024). This reduction in metastases in tumors treated with CTX+AS is relevant to the development of adjuvant treatment of prostate cancer. To determine which stages of angiogensis were altered by the treatment with angiostatin + cyclophosphamide, we employed the in vitro assays for interactive cell killing, migration and tube formation. Figures 5A and 5B demonstrate that there is no increase in cytotoxicty of PC-3 and HUVEC treated with the combination of angiostatin and 4-HC when compared to cells treated with 4-HC. Figure 6 shows that migration was not affected in HUVEC treated with angiostatin, 4-HC, or the combination of angiostatin and 4-HC. However, we found that tube formation, although not effected by either agent alone, demonstrated inhibition when angiostatin was combined with cyclophophamide (Figure 7). These data indicate that exposure of endothelial cells to the combination of angiostatin and cyclophosphamide show no increase in cell killing, allow endothelial cells to migrate normally, but act by inhibiting the formation of vessels. **Task 3: Angiostatin and x-irradiation induce p53 and lower the apoptotic threshold in endothelial cells when**

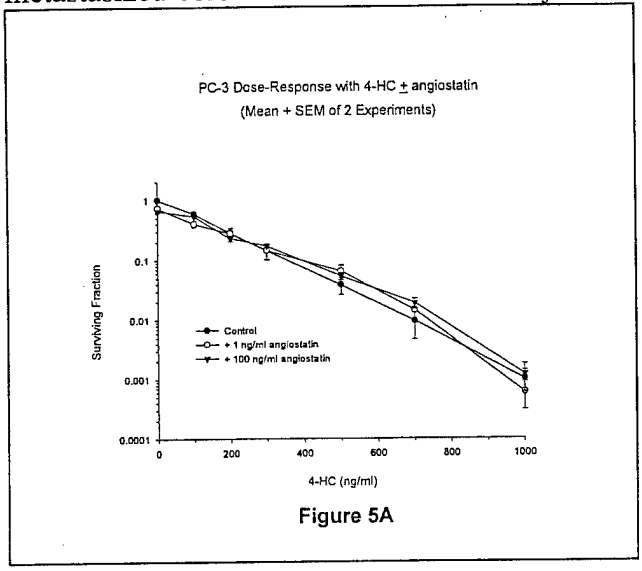

Figure 5A

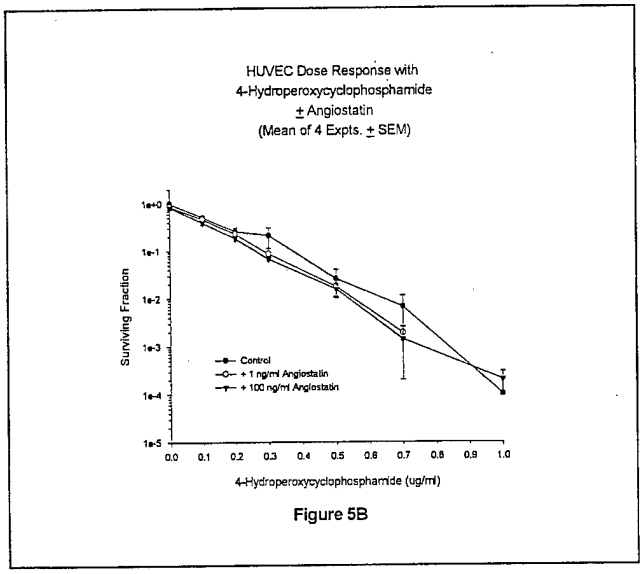

Figure 5B

compared to x-irradiation or angiostatin alone. We have analyzed whether the enhanced killing effect of AS+IR is due, in part, to increased apoptosis by a p53 dependent mechanism. As stated above, we found no increase in apoptosis in control versus AS treated HUVEC, and no increase in IR versus AS+IR treated HUVEC. We further analyzed the *in vitro* levels of p53 in endothelial cells using western analysis. We found no difference in p53 levels in control versus AS treated endothelial cells, and no increase in IR versus AS+IR

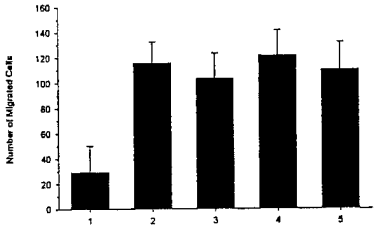

Figure 6: HUVEC migration assay. 1) negative control, 2) positive control, 3) angiostatin, 4) 4-HC, 5) angiostatin + 4-HC

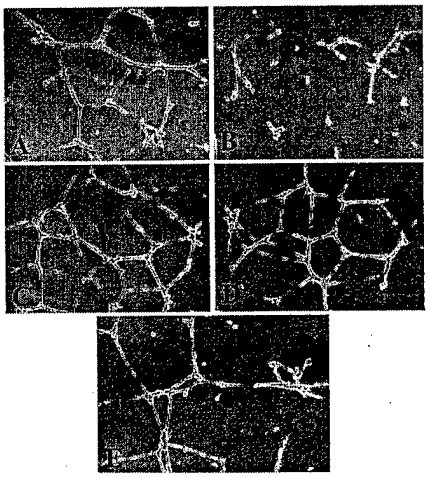

Figure 7: Tube formation assay. HUVEC treated with A) positive control, B) negative control, C) angiostatin, D) 4-HC, E) angiostatin + 4-HC

treated endothelial cells. Cell cycle analysis confirmed these data with no differences in the cell cycle phases in control versus AS treated endothelial cells and in the IR versus AS+IR treated endothelial cells. **Task 4: Angiostatin interacts with IR by inhibiting activation of PKCα or PKCβ_{II} proliferative isoforms of PKC or activating PKCδ, a pro-apoptotic isoform of PKC.** HUVEC were incubated with angiostatin and cells were harvested at 0, 6, 12, 18, 24 and 36 hours for protein isolation and western analysis with PKCα, PKCβ_{II}, and PKCδ. Figure 7A shows the western blot for PKCα and figure 7B the western blot for PKCβ_{II}. The results show no inhibition of either PKC isoform. PKCδ showed no induction or increased activation by appearance of cleavage products in HUVEC exposed to angiostatin. These data further support our evidence that angiostatin does not enhance the radiation-induced apoptosis of endothelial cells.

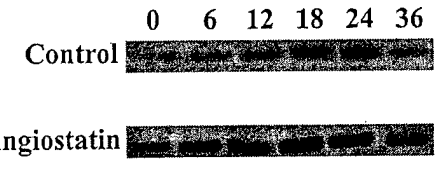

Figure 7A: PKCα western blot of HUVEC following exposure to angiostatin.

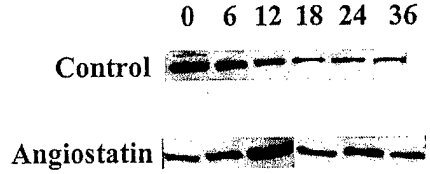

Figure 7B: PKCβII western blot of HUVEC following exposure to angiostatin.

The data we have generated during the duration of this funding period may lead to increased efficacy of localized radiotherapy for prostate cancer and expand the use of angiogenesis inhibitor/radiation combinations. Also the discovery that DNA damaging agents in combination with angiogenesis inhibitors decrease metastatic disease in animals may be beneficial in the adjuvant treatment of prostate cancer and possibly in some forms of metastatic prostate cancer.

Key Research Accomplishments

- PC-3 prostate cancer cell xenografts treated with angiostatin + IR produce a significant increase in tumor regression and delayed tumor regrowth than xenografts treated with angiostatin or IR alone.
- The effects of treatment with angiostatin + IR is directed to the tumor endothelium and not the PC-3 cancer cells.
- The number of tumor vessels was reduced in LLC tumor sections following treatment with angiostatin + IR compared with either treatment alone.
- The interaction of angiostatin + IR is additive.
- The interaction of angiostatin + IR is not mediated by apoptosis.
- There is no interactive effect on growth of LLC tumors treated with angiostatin + cyclophosphamide.
- There is a dramatic decrease in the number of lung metastases in animals bearing LLC tumors treated with angiostatin + cyclophosphamide compared to cyclophosphamide alone.
- There is no interactive effect *in vitro* in PC-3 and HUVEC treated with angiostatin + cyclophosphamide.
- p53 levels were not different in control versus angiostatin treated endothelial cells or IR versus angiostatin+IR treated endothelial cells.
- The interaction of angiostatin and IR is not mediated by the inhibition of PKCα or PKCβ_{II}, or the induction or cleavage of PKCδ.

Reportable Outcomes

1. Mauceri, H. J., Hanna, N. N., Beckett, M. A., Gorski, D. H., Staba, M. J., Stellato, K. A., Bigelow, K., Heimann, R., Gately, S., Dhanabal, M., Soff, G. A., Sukhatme, V. P., Kufe, D. W., and Weichselbaum, R. R. (1998). Combined effects of angiostatin and ionizing radiation in antitumour therapy. Nature *394*, 287-291.
2. Gorski, D. H., Mauceri, H. J., Salloum, R. M., Gately, S., Hellman, S., Beckett, M. A., Sukhatme, V. P., Soff, G. A., Kufe, D. W., and Weichselbaum, R. R. (1998). Potentiation of the antitumor effect of ionizing radiation by brief concomitant exposures to angiostatin. Cancer Res *58*, 5686-5689.
3. Gorski, D. H., Beckett, M. A., Jaskowiak, N. T., Calvin, D. P., Mauceri, H. J., Salloum, R. M., Seetharam, S., Koons, A., Hari, D. M., Kufe, D. W., and Weichselbaum, R. R. (1999). Blockage of the vascular endothelial growth factor stress response increases the antitumor effects of ionizing radiation. Cancer Res *59*, 3374-3378.
4. Seetharam, S., Staba M-J., Schumm, L.P., Schreiber, K., Schreiber, H., Kufe, D.W., and Weichselbaum, R.R. (1999) Enhanced eradication of local and distant tumors by genetically produced interleuken-12 and radiation. Int. J. Onc. *15*, 769-773.
5. Mauceri, H.J., Beckett, M.A., Seetharam, S., Kufe, D.W., and Weichselbaum, R.R. (2000) Gene therapy targeted by ionizing radiation targets both tumor cells and tumor vasculature. Proceedings of the 11th International Congress of Radiation Research *2*, 672-675.
6. Colorado, P.C., Torre, A., Kamphaus. G., Maeshima, Y., Hopfer, H., Takahashi, K., Volk, R., Zamborsky, E.D., Herman, S., Sarkar, P.K., Eridksen, M.B., Dhanabal, M., Simons, M., Post, M., Kufe, D.W., Weichselbaum, R.R., Sukhatme, V.P., Kalluri, R. (2000) Antiangiogenic cues from vascular basement membrane collagen. Cancer Res *60*, 2520-2526.
7. Hari, D., Beckett, M.A., Sukhatme, V.P., Dhanabal, M., Lu, H., Mauceri, H.J., Kufe, D.W., and Weichsebaum, R.R. (2000) Angiostatin induces mitotic cell death of proliferating endothelial cells. Mol. Cell. Biol. Res. Commun. *3*, 277-282.
8. Hanna, N.N., Mauceri, H.J., Seetharam, S., Beckett, M.A., Jaskowiak, N.T., Salloum, R.M., Hari, D., Dhanabal, M., Ramchandran, R., Colorado,P.C., Kalluri, R., Sukhatme, V.P., Kufe, D.W., and Weichselbaum, R.R. Antitumor interaction of short course endostatin and ionizing radiation. The Cancer Journal from The Scientific American (In Press).
9. Seetharam, S., Mauceri, H.J., Beckett, M.A., Gupta, V., Koons, A., Schumm, P., Sukhatme, V.P., Dhanabal, M., Lu, H., Kufe, D.W., and Weichsebaum, R.R. Angiostatin in combination with cyclophosphamide inhibits lung metastases but not primary tumor growth. (Manuscript in preparation)

Conclusions: We demonstrate that the combined treatment with AS+IR produces a significant increase in tumor regression and delayed regrowth in PC-3 prostate cancer cell xenografts. We also show that effect of this combined treatment is directed to the endothelial cells and not to the PC-3 prostate cancer cells. Our data demonstrate that the percentage of apoptotic endothelial cells does not increase when treated with AS, IR, and AS+IR *in vitro*. We conclude, therefore, that the interaction of AS and IR is not mediated by p53 dependent apoptosis but is likely due to a mitotic cell death. We further demonstrate that the interaction is not due to increased apoptosis by showing no inhibition of PKCα or PKCβII or induction of the pro-apoptotic isoform, PKCδ. We demonstrate that combined treatment with a DNA damaging agent (CTX) in combination with AS has little effect on the growth of the primary tumor when compared with either treatment alone. However, there is a decrease in the number of lung metastases in the combined treatment group. In vitro we demonstrated that the combination of angiostatin and CTX had no increase in cell killing compared to CTX alone, did not inhibit migration, but did inhibit tube formation. These data may lead to increased efficacy of localized radiotherapy for prostate cancer and expand the use of angiogenesis inhibitor/radiation combinations. Also the discovery that DNA damaging agents in combination with angiogenesis inhibitors decrease metastatic disease in animals may be beneficial in the adjuvant treatment of prostate cancer and possibly in some forms of metastatic prostate cancer.

References

1. J. Folkman, Y. Shing, *J Biol Chem* 267, 10931-4 (1992).
2. I. J. Fidler, L. M. Ellis, *Cell* 79, 185-8 (1994).
3. J. Folkman, *Nat Med* 1, 27-31 (1995).
4. D. Hanahan, J. Folkman, *J Natl Cancer Inst* 88, 1091-2 (1996).
5. J. W. Rak, B. D. St Croix, R. S. Kerbel, *Anticancer Drugs* 6, 3-18 (1995).
6. Y. Cao, et al., *J Biol Chem* 271, 29461-7 (1996).
7. M. O'Reilly, L. Holmgren, C. Chen, J. Folkman, *Nat Med* 2, 689-92 (1996).
8. M. O'Reilly, et al., *Cancer Res* 54, 6083-6 (1994).
9. L. Holmgren, O. R. MS, J. Folkman, *Nat Med* 1, 149-53 (1995).
10. B. K. Sim, et al., *Cancer Res* 57, 1329-34 (1997).
11. R. R. Weichselbaum, et al., *Proc Natl Acad Sci U S A* 83, 2684-8 (1986).
12. R. R. Weichselbaum, M. A. Beckett, W. Dahlberg, A. Dritschilo, *Int J Radiat Oncol Biol Phys* 14, 907-12 (1988).

Appendices

Combined effects of angiostatin and ionizing radiation in antitumour therapy

Helena J. Mauceri*, Nader N. Hanna*, Michael A. Beckett*, David H. Gorski†, Mary-Jane Staba‡, Kerri Anne Stellato*, Kevin Bigelow*, Ruth Heimann*, Stephen Gately§, Mohanraj Dhanabal‖, Gerald A. Soff§, Vikas P. Sukhatme‖, Donald W. Kufe¶ & Ralph R. Weichselbaum*

* *Department of Radiation and Cellular Oncology,* † *Department of Surgery,* ‡ *and Department of Pediatrics, University of Chicago, Chicago, Illinois 60637, USA*

§ *Department of Medicine, Division of Hematology/Oncology, Northwestern University Medical School, Chicago, Illinois 60611, USA*

‖ *Renal Division, Beth Israel Deaconess Medical Center, Boston, Massachusetts 02115, USA*

¶ *Dana Farber Cancer Institute and Harvard Medical School, Boston, Massachusetts 02115, USA*

Angiogenesis, the formation of new capillaries from pre-existing vessels, is essential for tumour progression[1–5]. Angiostatin, a proteolytic fragment of plasminogen[6] that was first isolated from the serum and urine of tumour-bearing mice[7], inhibits angiogenesis and thereby growth of primary[8] and metastatic[7,9,10] tumours. Radiotherapy is important in the treatment of many human cancers, but is often unsuccessful because of tumour cell radiation resistance[11,12]. Here we combine radiation with angiostatin to target tumour vasculature that is genetically stable and therefore less likely to develop resistance[13–15]. The results show an antitumour interaction between ionizing radiation and angiostatin for four distinct tumour types, at doses of radiation that are used in radiotherapy. The combination produced no increase in toxicity towards normal tissue. *In vitro* studies show that radiation and angiostatin have combined cytotoxic effects on endothelial cells, but not tumour cells. *In vivo* studies show that these agents, in combination, target the tumour vasculature. Our results provide support for combining ionizing radiation with angiostatin to improve tumour eradication without increasing deleterious effects.

To assess the effects of human angiostatin on primary tumour growth, we treated mice with murine Lewis lung carcinoma (LLC)

tumours with 25 or 50 mg angiostatin per kg per day. The former dose produced a 38% decrease in mean tumour volume and the latter dose reduced mean tumour volume by 54%, as compared with untreated controls (day 9; $P = 0.026$). We selected a dose of 25 mg human angiostatin per kg per day for subsequent studies to allow optimal evaluation of a potential interaction between angiostatin and ionizing radiation.

We examined the effects of human angiostatin and ionizing radiation in LLC tumours and in three human-tumour xenograft models (D54, SQ-20B and PC3). These tumour cell lines, which differ in radiation sensitivities and growth kinetics, are derived from tumours in which local failure of the primary tumour results in morbidity and mortality. The tumour volumes at the start of treatment ranged from 386 to 1,104 mm^3 and represented a tumour burden of 2–5.5% of body weight. The dose of 25 mg human angiostatin per kg per day produced only modest growth inhibition compared with ionizing radiation alone. In contrast, combined treatment with human angiostatin and ionizing radiation produced significant growth inhibition (determined at the nadir; Fig. 1) compared with either treatment alone (Table 1).

In other experiments, we treated mice with LLC tumours with recombinant murine angiostatin. By day 5, 25 mg per kg per day of

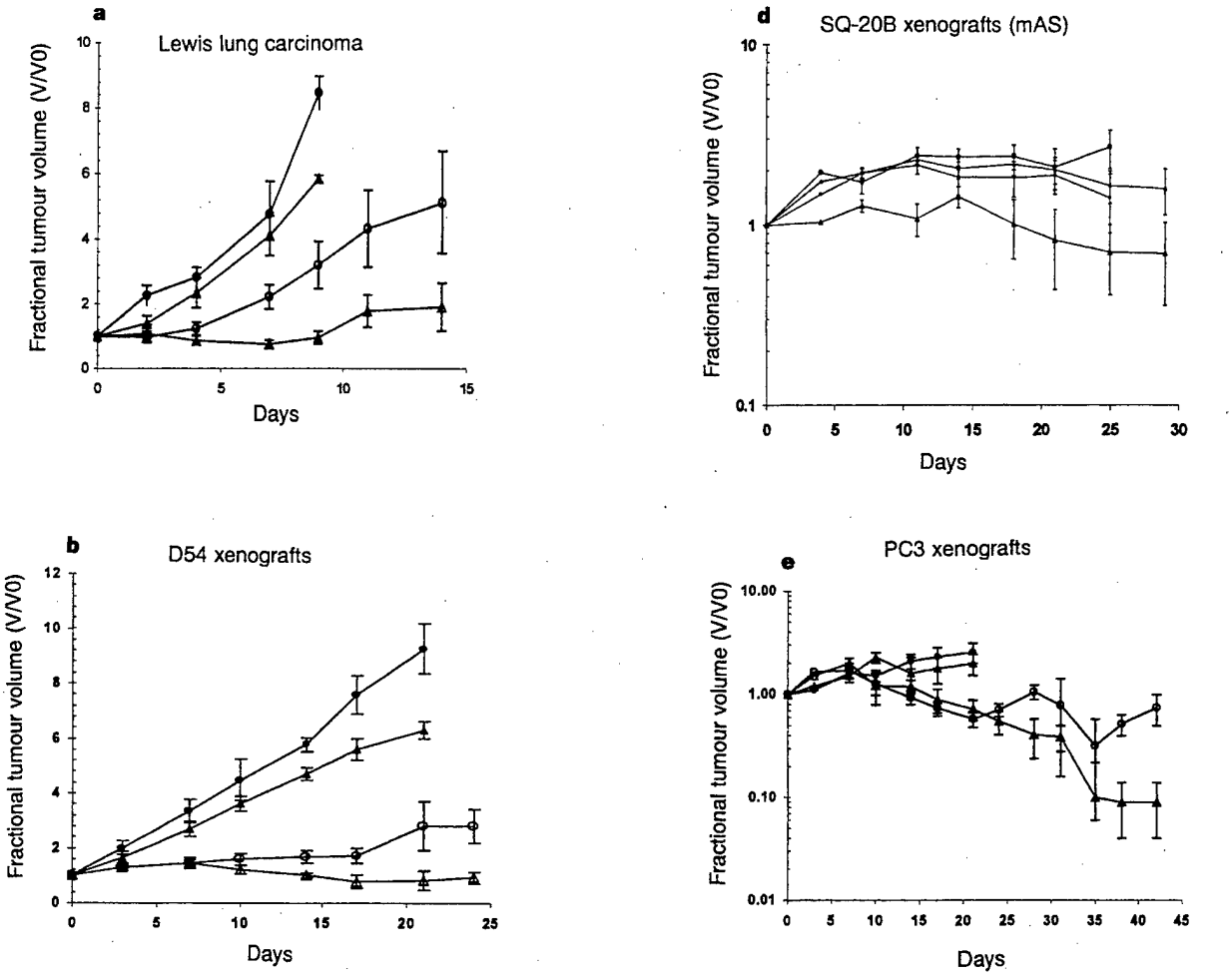

Figure 1 Tumour growth following combined treatment with angiostatin and radiation (XRT). Open triangles represent untreated controls; filled triangles represent treatment with XRT; open circles represent treatment with angiostatin; filed circles represent treatment with angiostatin and XRT. **a**, LLC growth. C57Bl/6 mice with LLC tumours (1104 ± 97.9 mm^3) were injected daily for 14 days with human angiostatin and received two 20 Gy doses (on days 0 and 1). **b**, D54 growth. Female nude mice with human glioblastoma tumours (385.8 ± 48.2 mm^3) were injected with human angiostatin 2 h before XRT treatment (5 Gy per day to 30 Gy). **c**, SQ-20B growth (treatment with human angiostatin, hAS). Athymic nude mice with SQ-20B xenografts (675.8 ± 74.7 mm^3) received human angiostatin (25 mg per kg per day) 2 h before XRT treatment (5 Gy per day, to 50 Gy). **d**, SQ-20B growth (treatment with murine angiostatin, mAS). Mice with SQ-20B tumours (535 ± 29.5 mm^3) were injected with murine angiostatin (2.5 mg kg per day) 2 h before XRT treatment (5 Gy per day, to 50 Gy). **e**, PC3 growth. Mice with PC3 xenografts (769.5 ± 69.5 mm^3) were treated with human angiostatin 2 h before XRT treatment (5 Gy per day, to 40 Gy). Combined treatment with angiostatin and XRT produced significant tumour regression in all tumour types (LCC day 9, $P < 0.05$; D54 day 21, $P < 0.005$; SQ-20B hAS day 21, $P < 0.005$; SQ-20B mAS day 21, $P < 0.001$; PC3 day 42, $P < 0.001$).

murine angiostatin significantly decreased ($P = 0.007$) mean tumour volume by 29% ($1,680 \pm 111\,mm^3$) as compared with control tumours ($2,370 \pm 169\,mm^3$; data not shown). In mice with SQ-20B xenografts (Fig. 1d) treatment with murine angiostatin (2.5 mg per kg per day) and ionizing radiation significantly reduced mean tumour volume by 64% (day 21; $P < 0.001$) as compared with angiostatin alone (16% reduction) or ionizing radiation alone (18% reduction). These studies, in which we used murine angiostatin at a tenfold lower dose than of human angiostatin, confirmed the interactive antitumour effects of combined treatment with angiostatin and ionizing radiation.

Table 1 Summary of fractional tumour volume as a function of treatment

Tumour designation	Control	Radiation	Human angiostatin	Human angiostatin + radiation	
LLC day 9 ($n = 28$)	8.49 ±0.51	3.21 ±0.73 (40 Gyr)	5.85 ±0.12	0.96 ±0.20	$P < 0.05$
D54 day 21 ($n = 20$)	9.25 ±0.91	2.78 ±0.89 (30 Gy)	2.94 ±0.07	0.38 ±0.16	$P < 0.005$
SQ-20B day 21 ($n = 31$)	2.17 ±0.50	1.05 ±0.31 (50 Gy)	2.94 ±0.07	0.38 ±0.16	$P < 0.005$
PC3 day 42 ($n = 38$)	*2.55 ±0.05	0.75 ±0.35 (40 Gy)	*1.98 ±0.55	0.09 ±0.05	$P < 0.001$

The interactive anti-tumour effects of combined treatment with human angiostatin and ionizing radiation are greater than additive when compared with the expected effects of combined treatment. In LLC tumours the mean fractional tumour volume of 3.21 mm^3 (radiation-treated group) represents a 62.2% volumetric reduction. If this percentage is analysed with the 31.1% reduction in tumour size in the angiostatin-treated group, then the expected volumetric reduction in the tumour size in the combined treatment group should be 74%. However, the per cent reduction in the combined treatment group is 88.7%, suggesting greater-than-additive treatment effects. Greater-than-additive treatment effects are also observed for D54 tumours (expected, 90.4%; actual, 95.9%), SQ-20B tumours (expected, 34.4%; actual, 82.5%) and PC3 tumours (expected, 77.2%; actual, 96.5%). Data are mean tumour volume ± s.e.m. per group. Day, nadir of regression; n, total number of animals. * These mice were killed at day 21 because of tumour burden.

To determine the effects of treatment on tumour neovascularization, we examined representative tissue sections from LLC, D54 and SQ-20B tumours using anti-CD31 antibody and standard immunohistochemical techniques (Fig. 2). The number of LLC and D54 tumour vessels per high-power field was reduced following exposure to combined treatment with human angiostatin and ionizing radiation compared with exposure to all other treatments. The number of vessels per high-power field was also reduced in SQ-20B tumours exposed to combined treatment with angiostatin and ionizing radiation compared with those exposed to ionizing radiation alone ($P = 0.04$). Significant interactive treatment effects were observed in all tumour types (LLC, day 14, $P = 0.06$; D54, day 24, $P = 0.011$; and SQ-20B, day 28, $P = 0.003$; ANOVA).

To explore potential cytotoxic effects of combining angiostatin with ionizing radiation we studied clonogenic survival of human aortic endothelial cells (HAECs) and human umbilical vein endothelial cells (HUVECs) exposed to ionizing radiation. Clonogenic assays demonstrated 30–40% cell killing of HAECs and HUVECs exposed to human angiostatin (10 and 100 ng ml^{-1}). There was no difference in the amount of apoptosis, as measured by staining of HUVEC with 4,6-diamidino-2-phenylindole (DAPI), at 4, 8, 12 or 24 hours of treatment with angiostatin (6.03–9.92% apoptosis) compared with control HUVEC (6.03–10.57%). Inter-

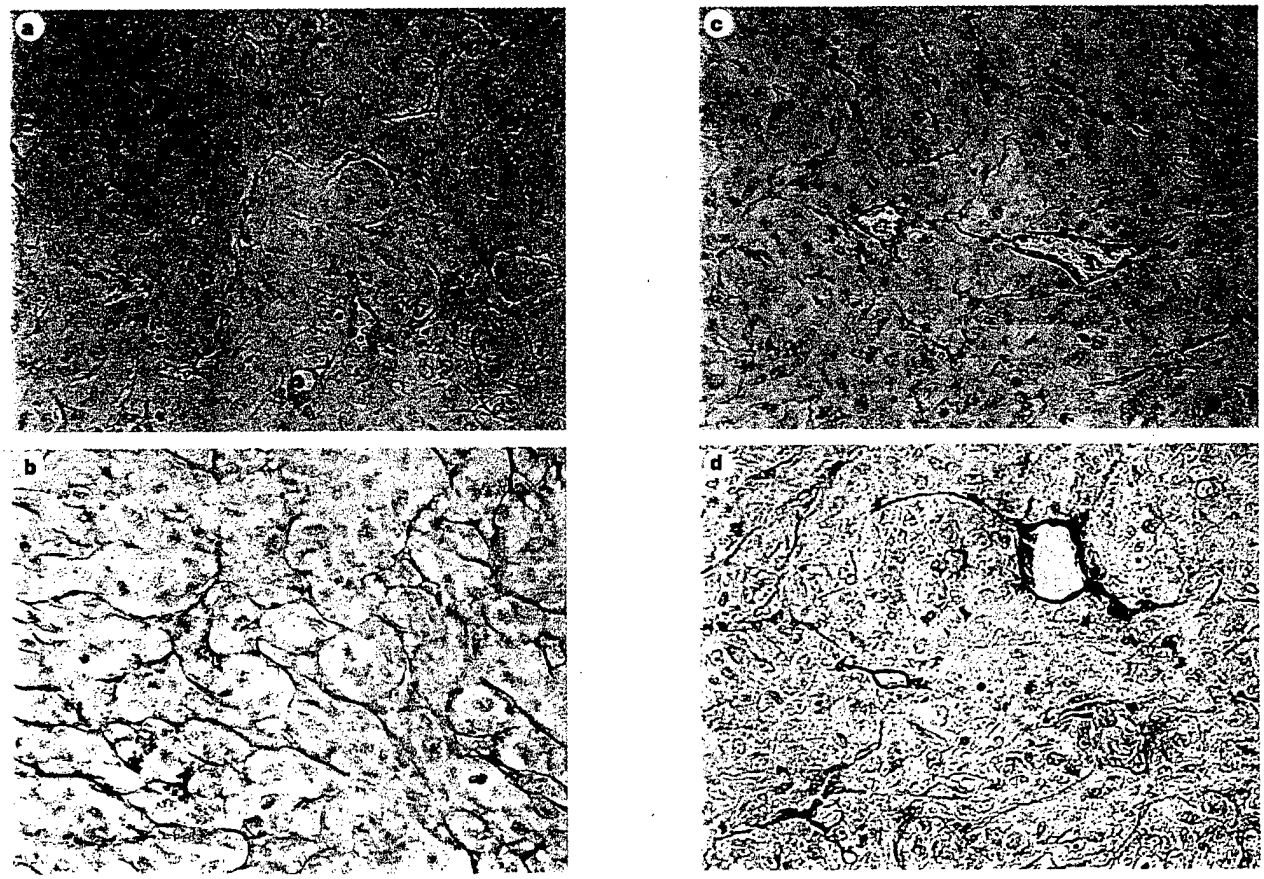

Figure 2 Visualization of the tumour vasculature using anti-CD31 immunohistochemistry. Micrographs are of representative sections from D54 glioblastoma xenografts (day 24) following treatment with human angiostatin and ionizing radiation. Microvessels were visualized in paraffin-embedded tissue sections using a monoclonal antibody against CD31, and developed using the avidin-biotin peroxidase technique. **a**, Untreated control. **b**, 30 Gy ionizing radiation. **c**, Angiostatin alone. **d**, Angiostatin + 30 Gy ionizing radiation.

active cytotoxicity was observed when HAECs and HUVECs were treated with angiostatin and exposed to 100, 200 or 900 cGy (Fig. 3). Similar results were obtained when we treated bovine aortic endothelial cells (BAECs) with human angiostatin and ionizing radiation. In contrast, no cytotoxicity was observed when tumour cell lines were treated with human angiostatin, and no interactive killing was observed following exposure to angiostatin and ionizing radiation (Fig. 4). No increase in apoptosis was observed when HUVEC cultures were treated with angiostatin and ionizing radiation (maximum of 21.58% apoptosis at 4 h) compared with ionizing radiation alone (maximum of 22.54% apoptosis at 4 h). These findings indicate that the interactive cytotoxic effects of human angiostatin and ionizing radiation *in vitro* are selective for endothelial cells and not mediated by apoptosis.

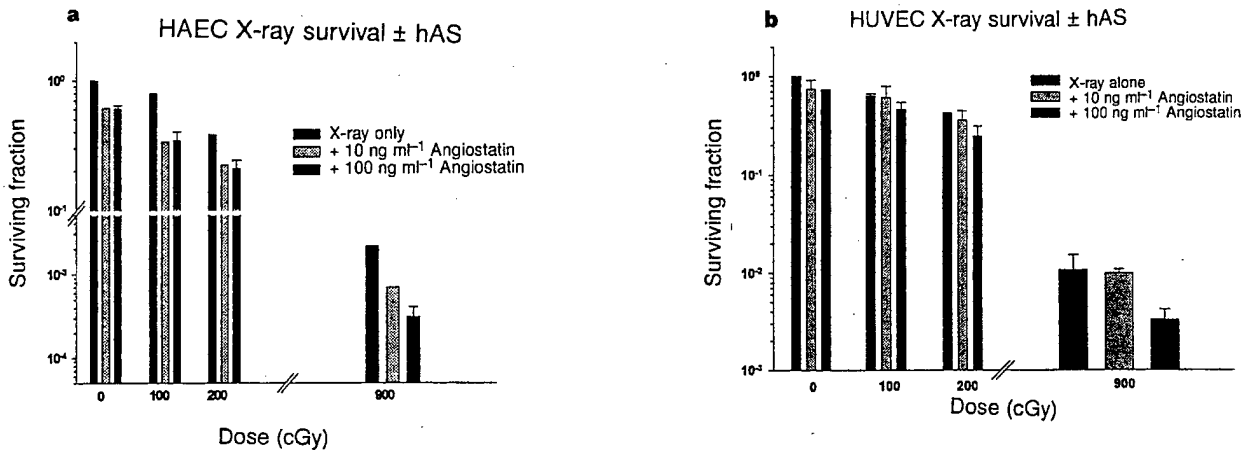

Figure 3 *In vitro* clonogenic survival of **a**, HAECs, and **b**, HUVECs on exposure to X-rays in the presence of human angiostatin (hAS). Cells were plated and exposed to angiostatin 4 hours before a single dose of X-ray irradiation. Colonies were stained and the surviving fraction was determined. Data represent the mean of two separate experiments ± s.e.m.

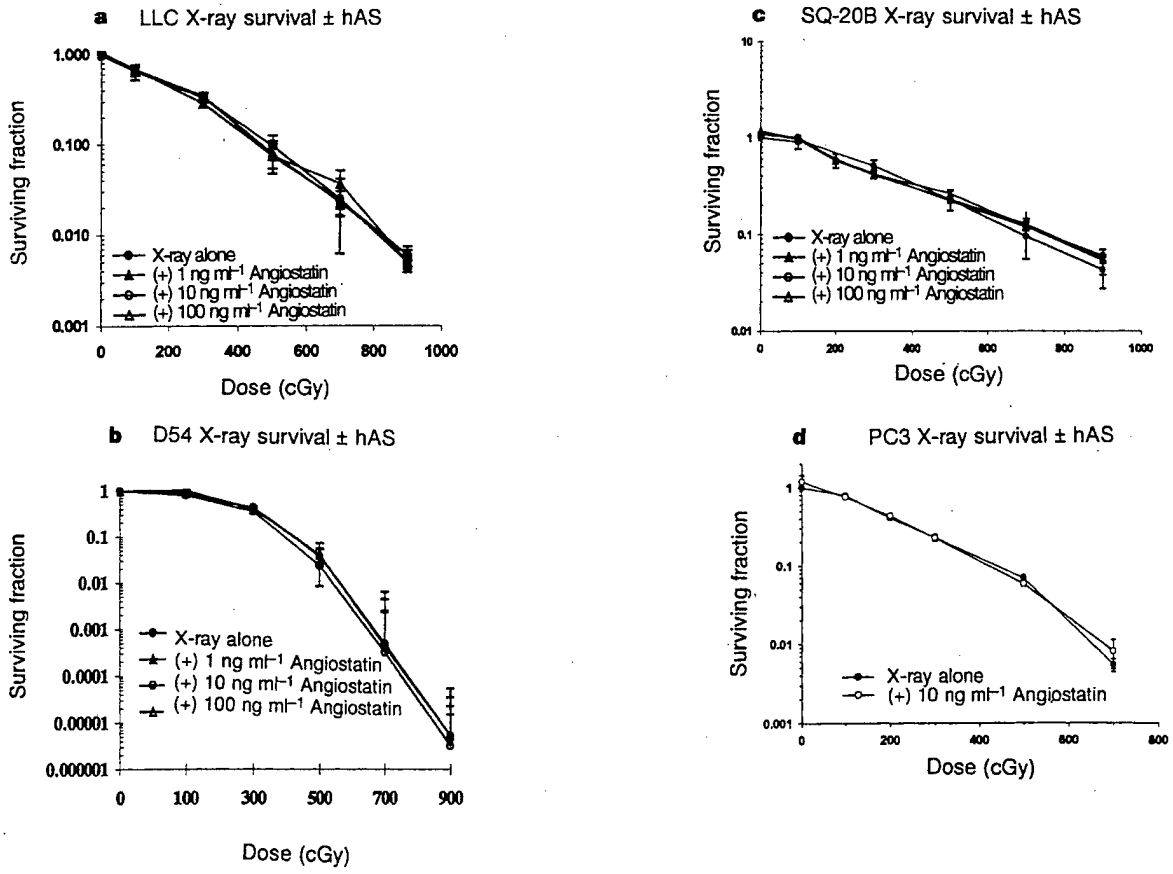

Figure 4 *In vitro* clonogenic survival of **a**, Lewis lung carcinoma cell line (LLC), **b**, human malignant glioma cell line (D54), **c**, human squamous cell carcinoma cell line (SQ-20B), and **d**, human prostate adenocarcinoma cell line (PC3) in response to angiostatin. Cells were plated and exposed to human angiostatin (hAS) 4 h before a single dose of X-ray irradiation. Colonies were stained and the surviving fraction was determined as described (see Methods). Data are represented as the mean ± s.e.m.

The interaction of the antitumour effects of angiostatin and ionizing radiation was observed at concentrations of angiostatin that had modest effects on primary tumour growth. We used angiostatin for a relatively short period of time (to coincide with radiotherapy) and used lower doses than those used previously[8]. The relative lack of treatment effects when angiostatin was used as a single agent may be related to the large tumour volumes used here compared with in other studies[9,10]. Analysis of histological sections of tumours treated with angiostatin and ionizing radiation indicates that newly forming vessels may be the target of the observed antitumour effects. This hypothesis is supported by *in vitro* studies, which show interactive killing of endothelial cell lines by angiostatin and ionizing radiation. Further support for the endothelial cell as a target of the radiation–angiostatin interaction is provided by experiments that show no cytotoxic action or radiosensitizing effects of angiostatin in tumour cell lines. Angiostatin inhibits endothelial cell proliferation *in vitro*; however, this is to our knowledge the first report of clonogenic killing of endothelial cells by angiostatin and synergistic antitumour effects using angiostatin as a radiation modifier. Angiostatin has great potential to enhance the therapeutic ratio in combined-modality cancer treatment. □

Methods

Cell culture. Lewis lung carcinoma cells (LLC-LM) (a gift from J. Folkman) were maintained in DMEM medium (Gibco) with 10% heat-inactivated fetal bovine serum (Intergen) and penicillin/streptomycin (Gibco). Human malignant glioma (D54) cells (a gift from D. D. Bigner) were cultured in 50% DMEM, 50% F-12 medium (Gibco), 7% fetal bovine serum and penicillin/streptomycin. SQ-20B squamous cell carcinoma cells derived from a patient with recurrent squamous cell carcinoma of the larynx were maintained in DMEM: F-12 (3:1), 20% fetal bovine serum, 0.4 $\mu g\,ml^{-1}$ hydrocortisone (Sigma) and penicillin/streptomycin. PC3 prostate adenocarcinoma tumour cells (American Type Culture Collection) were maintained in RPMI-1640 medium (Gibco) containing 10% fetal bovine serum and penicillin/streptomycin. HAECs and HUVECs were maintained in EGM-2 medium (Clonetics Corp.).

Mouse studies. LLC cells were injected subcutaneously (s.c.) into the right hind limb (5×10^5 cells in 100 μl PBS) of C57B1/6 female mice (Frederick Cancer Research Institute). D54 (1×10^6), SQ-20B (5×10^6) and PC3 cells (2×10^7) were injected into female nude mice. Tumours grew for 17–28 days. Tumour volume was determined by direct measurement with calipers and calculated by the formula (length × width × depth/2). Mice treated with human angiostatin[16] were injected intraperitoneally (i.p.) twice daily (except for SQ-20B) at a total dose of 25 mg per kg per day. Mice with SQ-20B xenografts received a single injection of human angiostatin (25 mg per kg) 2 h before X-ray irradiation. We found no difference in the response to human angiostatin if it was given in one or two injections daily. One group of mice with LLC tumours was injected i.p. twice daily with a dose of 50 mg angiostatin per kg per day. Mice treated with murine angiostatin received a single injection of either 2.5 mg per kg per day (SQ-20B xenografts) or 25 mg per kg per day (LLC tumours). The care and treatment of experimental animals was in accordance with institutional guidelines. Data are reported as percentages of the original (day 0) tumour volume and plotted as fractional tumour volume ± s.e.m..

Angiostatin production. Affinity-purified human angiostatin was generated as a cell-free preparation as described[16]. No endotoxin was present in any of the preparations, as shown using the QCL-1000 limulus amebocyte lysate assay (BioWhittaker).

The gene encoding murine angiostatin was cloned and expressed using a yeast expression system (M.D. and V.P.S., unpublished data). Briefly, a complementary DNA encoding mouse plasminogen (ATCC) was amplified using Vent DNA polymerase. The primers used were designed with the appropriate restriction sites to allow cloning directly into the yeast shuttle plasmid pPICZαA, which contains *Eco*RI and *Not*I restriction sites. Use of this vector permitted secretion of the recombinant protein into the culture medium. Positive clones were grown in 25 ml BMGY medium containing 100 $\mu g\,ml^{-1}$ Zeocin at 30 °C for 18–24 h. The overnight grown culture (A_{600}, 2–6) was used to inoculate 2-litre flasks containing 500 ml buffered glycerol medium. Cells were grown for 2 days at 30 °C (A_{600} 16–20), then centrifuged at 500 r.p.m. for 10 min, and resuspended in 300–400 ml buffered methanol induction medium. The cell-free supernatant was collected on days 2, 3 and 4 and concentrated using ammonium precipitation (70%), dissolved in 50 mM phosphate buffer, pH 7.4, and dialysed at 4 °C. Proteins were purified using a lysine–Sepharose 4B column (Pharmacia) equilibrated with 50 mM phosphate buffer, pH 7.4. Recombinant angiostatin was eluted with 0.2 M c-amino-*N*-caproic acid, pH 7.4. Fractions with maximum absorbency were pooled and dialysed for 25 h against PBS, pH 7.4, at 4 °C, with three changes at intervals of 6–8 h. The dialysed sample was further concentrated by ultrafiltration using an Amicon concentrator (YM 10). Protein concentration was determined using the micro BCA assay (BioRad).

Immunohistochemistry. At day 24, mice were killed and tumours were excised and fixed in 10% neutral buffered formalin. After embedding in paraffin, 5 μm sections were cut and tissue sections were mounted. Briefly, sections were dried, deparaffinized and rehydrated. After quenching endogenous peroxidase activity and blocking with bovine serum albumin, slides were incubated at 4 °C overnight with a 1:50 dilution of rat anti-mouse-CD31 monoclonal antibody (Pharmingen), and were then incubated for 1 h with biotinylated rabbit anti-rat immunoglobulin (Vector Laboratories). Localization of blood vessels was visualized using the Vectastain elite ABC kit, Vector PK-6100 (Vector). Slides were dipped in 0.125% osmium tetroxide (Sigma) to enhance positivity and counterstained with 1% methyl green (Trevigen). Ten high-power fields (×400) were examined for each tumour section using a Nikon Microphot-FX microscope equipped with a Sony digital camera. Vessels were counted using Macintosh Image Pro-Plus imaging software.

Clonogenic assay. Endothelial cells (HAECs and HUVECs) were grown in EGM-2 medium (Clonetics). Tumour cell lines (LLC, D54, SQ-20B and PC3) were grown as described. To account for radiation killing, increasing numbers of cells (10^2 to 5×10^4) were plated in 100-mm tissue-culture dishes. Eighteen hours after plating, angiostatin was added at concentrations of 10 $ng\,ml^{-1}$ and 100 $ng\,ml^{-1}$. Four hours later, cells were irradiated with doses of 0–900 cGy using a GE Maxitron X-ray generator operating at 250 kV, 26 mA, with a 0.5 mm copper filter, at a dose rate of 118 $cGy\,min^{-1}$. Cultures were returned to the incubator for 14–17 days, after which they were stained with crystal violet, colonies were counted, and the surviving fraction was determined. Colonies containing >50 cells were scored as positive.

Statistical analysis. Statistical significance was determined using one-way analysis of variance (ANOVA) or the Kruskal–Wallis test.

Received 1 April; accepted 13 May 1998.

1. Folkman, J. & Shing, Y. Angiogenesis. *J. Biol. Chem.* **267**, 10931–10934 (1992).
2. Fidler, I. J. & Ellis, L. M. The implications of angiogenesis for the biology and therapy of cancer metastasis. *Cell* **79**, 185–188 (1994).
3. Folkman, J. Angiogenesis in cancer, vascular, rheumatoid and other disease. *Nature Med.* **1**, 27–31 (1995).
4. Hanahan, D. & Folkman, J. Patterns and emerging mechanisms of the angiogenic switch during tumorigenesis. *J. Natl Cancer Inst.* **88**, 1091–1092 (1996).
5. Rak, J. W., St Croix, B. D. & Kerbel, R. S. Consequences of angiogenesis for tumor progression, metastasis and cancer therapy. *Anticancer Drugs* **6**, 3–18 (1995).
6. Cao, Y. *et al.* Kringle domains of human angiostatin. Characterization of the anti-proliferative activity on endothelial cells. *J. Biol. Chem.* **271**, 29461–29467 (1996).
7. O'Reilly, M. Angiostatin: a novel angiogenesis inhibitor that mediates the suppression of metastases by a Lewis lung carcinoma. *Cell* **79**, 315–328 (1994).
8. O'Reilly, M., Holmgren, L., Chen, C. & Folkman, J. Angiostatin induces and sustains dormancy of human primary tumors in mice. *Nature Med.* **2**, 689–692 (1996).
9. Holmgren, L., O'Reilly, M. S. & Folkman, J. Dormancy of micrometastases: balanced proliferation and apoptosis in the presence of angiogenesis suppression. *Nature Med.* **1**, 149–153 (1995).
10. Sim, B. K. *et al.* A recombinant human angiostatin protein inhibits experimental primary and metastatic cancer. *Cancer Res.* **57**, 1329–1334 (1997).
11. Weichselbaum, R. R. *et al.* Radiation-resistant and repair-proficient human tumor cells may be associated with radiotherapy failure in head- and neck-cancer patients. *Proc. Natl Acad. Sci. USA* **83**, 2684–2688 (1986).
12. Weichselbaum, R. R., Beckett, M. A., Dahlberg, W. & Dritschilo, A. Heterogeneity of radiation response of a parent human epidermoid carcinoma cell line and four clones. *Int. J. Radiat. Oncol. Biol. Phys.* **14**, 907–912 (1988).
13. Kerbel, R. S. Inhibition of tumor angiogenesis as a strategy to circumvent acquired resistance to anti-cancer therapeutic agents. *BioEssays* **13**, 31–36 (1991).
14. Kakeji, Y. & Teicher, B. A. Preclinical studies of the combination of angiogenic inhibitors with cytotoxic agents. *Invest. New Drugs* **15**, 39–48 (1997).
15. Teicher, B. A., Sotomayor, E. A. & Huang, Z. D. Antiangiogenic agents potentiate cytotoxic cancer therapies against primary and metastatic disease. *Cancer Res.* **52**, 6702–6704 (1992).
16. Gately, S. *et al.* The mechanism of cancer-mediated conversion of plasminogen to the angiogenesis inhibitor angiostatin. *Proc. Natl Acad. Sci. USA* **94**, 10868–10872 (1997).

Acknowledgements. We thank S. Hellman and R. Salloum for discussions.

Correspondence and requests for materials and reprints should be addressed to R.R.W. (e-mail: rrw@rover.uchicago.edu).

[CANCER RESEARCH 58, 5686–5689, December 15, 1998]

Potentiation of the Antitumor Effect of Ionizing Radiation by Brief Concomitant Exposures to Angiostatin[1]

David H. Gorski, Helena J. Mauceri, Rabih M. Salloum, Stephen Gately, Samuel Hellman, Michael A. Beckett, Vikas P. Sukhatme, Gerald A. Soff, Donald W. Kufe, and Ralph R. Weichselbaum[2]

Departments of Radiation and Cellular Oncology [D. H. G., H. J. M., S. H., M. A. B., R. R. W.] and Surgery [R. M. S.], University of Chicago, Chicago, Illinois 60637; Division of Hematology and Oncology, Department of Medicine, Northwestern University, Chicago, Illinois 60611 [S. G., G. A. S.]; Renal Division, Beth Israel Deaconness Medical Center, [V. P. S.]; and Dana Farber Cancer Institute, Harvard Medical School [D. W. K.], Boston, Massachusetts 02115

Abstract

Angiostatin, a proteolytic fragment of plasminogen, inhibits the growth of primary and metastatic tumors by suppressing angiogenesis. When used in combination with ionizing radiation (IR), angiostatin demonstrates potent antitumor synergism, largely caused by inhibition of the tumor microvasculature. We report here the temporal interaction of angiostatin and IR in Lewis lung carcinoma (LLC) tumors growing in the hind limbs of syngeneic mice. Tumors with an initial mean volume of 510 ± 151 mm^3 were treated with IR alone (20 Gy × 2 doses on days 0 and 1), angiostatin alone (25 mg/kg/day divided twice daily) on days 0 through 13, or a combination of the two as follows: (*a*) IR plus angiostatin (days 0 through 13); (*b*) IR plus angiostatin (days 0 and 1); and (*c*) IR followed by angiostatin beginning on the day after IR completion and given daily thereafter (days 2 through 13). By day 14, tumors in untreated control mice had grown to 6110 ± 582 mm^3, whereas in mice treated with: (*a*) IR alone, tumors had grown to 2854 ± 338 mm^3 ($P < 0.05$ compared with untreated controls); and (*b*) angiostatin alone, tumors had grown to 3666 ± 453 mm^3 ($P < 0.05$ compared with untreated controls). In combined-treatment groups, in mice treated with: (*a*) IR plus longer-course angiostatin, tumors reached 2022 ± 282 mm^3 ($P = 0.036$ compared with IR alone); (*b*) IR followed by angiostatin, tumors reached 2677 ± 469 mm^3 ($P > 0.05$ compared with IR alone); and (*c*) IR plus short-course angiostatin, tumors reached 1032 ± 78 mm^3 ($P < 0.001$ compared with IR alone). These findings demonstrate that the efficacy of experimental radiation therapy is potentiated by brief concomitant exposure of the tumor vasculature to angiostatin.

Introduction

Tumor cells express pro-angiogenic factors that include vascular endothelial cell growth factor (1), basic fibroblast growth factor (2), and certain angiogenesis-promoting peptides (3). Experimental evidence from transgenic mouse models suggest that angiogenesis is necessary early in tumor development (4, 5). The angiogenic "switch" hypothesis is based on a change in the balance between pro- and anti-angiogenic factors toward a pro-angiogenic state as being essential to tumor progression (3, 5). Further support for the importance of angiogenesis in human tumor progression comes from correlations of increasing tumor vascularity with more aggressive clinical behavior in human tumors (6) and the demonstration that pro-angiogenic factors are up-regulated during tumor progression (3, 4, 7).

Inhibition of angiogenesis has emerged as a promising strategy to treat both primary and metastatic tumors by shifting the balance from a pro-angiogenic toward an anti-angiogenic state (3, 4, 7). Strategies using monoclonal antibodies or soluble receptors to pro-angiogenic cytokines such as vascular endothelial cell growth factor show promise in inhibiting tumor growth in experimental models (8–11). Also, antisense strategies targeting basic fibroblast growth factor and its receptor have demonstrated antitumor effects (2). Recently, AS[3] and endostatin, enzymatic cleavage products of plasminogen and collagen type XVIII, respectively, have been isolated from tumor-bearing mice (12, 13). AS is generated from plasminogen by enzymatic activity derived from the tumor itself (14–16) or from host macrophages infiltrating the tumor (17). Treatment with AS or endostatin causes significant tumor regression and can cause tumor dormancy in mouse tumor model systems (18, 19). Recently, it has been reported that gene transfer of a cDNA encoding the AS peptide in a viral vector can inhibit tumor growth (20, 21). Importantly, these anti-angiogenic proteins exhibit no detectable toxicity in experimental animals (12, 13).

Anti-angiogenic proteins, although effective at shrinking tumors, are not tumoricidal. Tumor regrowth frequently occurs once treatment with the angiogenesis inhibitor is terminated (18, 19). One strategy to overcome this therapeutic limitation is to combine angiogenesis inhibitors with cytotoxic therapies. In this context, we recently combined AS with IR and demonstrated a marked increase in antitumor effects (22). Here, we report that there is a temporal interaction between AS and IR. AS delivered concomitantly with IR for 2 days is as effective at suppressing primary tumor growth as a 14-day course of AS administration combined with an identical course of IR. By contrast, AS is not as effective if delivered after IR. Taken together with previous data demonstrating that AS and IR fail to exhibit an interactive killing effect in tumor cells (22), these data suggest that AS and IR interact primarily on the tumor microvessels. This finding is especially important in that adequate supplies of AS are not yet available for prolonged human administration.

Materials and Methods

Cell Lines and Cell Culture. LLC cells (low metastatic strain, LM), a gift of J. Folkman (Dept. of Surgery, Children's Hospital, Harvard Univ. Medical School, Boston, MA; Ref. 12), were grown at 37°C in 7% CO_2 in DMEM with 10% heat-inactivated (56°C for 20 min) fetal bovine serum. Cells were subcultured no more than ten times before being used in animal experiments.

Animals and Tumor Model. Eight-week-old female C57BL/6 mice (Frederick Cancer Research Institute, Frederick, MD) were housed in accordance with the University of Chicago's institutional guidelines. Depending on the experimental protocol, 5×10^5 to 2×10^6 cells suspended in PBS were injected s.c. into the right hind limb. Tumors were allowed to attain a volume of approximately 500 mm^3 when treatment with either AS, IR, or a combination of the two was begun. All of the experiments were replicated a minimum of two times.

Received 9/1/98; accepted 10/27/98.

The costs of publication of this article were defrayed in part by the payment of page charges. This article must therefore be hereby marked *advertisement* in accordance with 18 U.S.C. Section 1734 solely to indicate this fact.

[1] Supported in part by National Cancer Institute Grant CA42596.

[2] To whom requests for reprints should be addressed, at Department of Radiation and Cellular Oncology, University of Chicago, 5841 South Maryland Avenue, Chicago, IL 60637. Phone: (773) 702-0817; Fax: (773) 834-7233; E-mail: rrw@rover.uchicago.edu.

[3] The abbreviations used are: AS, angiostatin; IR, ionizing radiation; LLC, Lewis lung carcinoma.

Tumor volume was estimated by direct measurement and then calculated using the formula for the volume of an ellipsoid, as described previously (22). Measurements were made three times a week for the duration of the experiments. Depending on the experiment, five to eight mice were assigned to each experimental group on day 0. Because of tumor burden, usually three to five mice per group remained at the conclusion. At various time points, mice were anesthetized using Metafane inhalation and killed by cervical dislocation to obtain tissue for histology.

Tumor Irradiation. Mice were irradiated using a GE Maxitron X-ray generator operating at 150 kV, 30 mA, using a 1-mm aluminum filter at a dose rate of 188 cGy/min. Mice were shielded with lead except for the tumor-bearing right hind limb. The specific dosage and schedule for IR exposure is described when that experiment is discussed.

AS Production and Dosage. Human AS was generated from human plasminogen as described previously (15). AS was suspended in PBS and administered as i.p. injections twice daily at a total dose of 25 mg/kg/day (0.5 mg/day per mouse) or 50 mg/kg/day (1 mg/day per mouse). The duration of AS treatment and its administration relative to radiation therapy is described for each individual experiment.

Data Analysis. Mean tumor volumes for each experimental group ± the SE were calculated. Differences between treatment groups were determined by a one-way ANOVA using the SigmaStat 2.0 statistics software package (Jandel Scientific). Differences between individual pairs of treatment groups were determined using Student's *t* test. Differences between treatment groups were considered statistically significant when $P = 0.05$.

Results and Discussion

Effect of AS Dose on LLC Growth. To characterize the effects of human AS alone on LLC, we tested two different doses, 25 mg/kg/day and 50 mg/kg/day, divided twice daily (Fig. 1). Untreated controls received PBS. Neither of the two doses caused shrinkage or growth arrest of these primary tumors, which are large compared to the tumors used in earlier investigations of the effects of AS on LLC growth (12, 18, 19). By day 9, the difference between tumor volumes in the untreated control group and the group receiving 25 mg/kg/d of AS was statistically significant ($P = 0.033$), as was the difference between untreated controls and those receiving 50 mg/kg/d of AS group ($P = 0.002$). There was no significant difference in tumor volume between the two groups receiving different doses of AS.

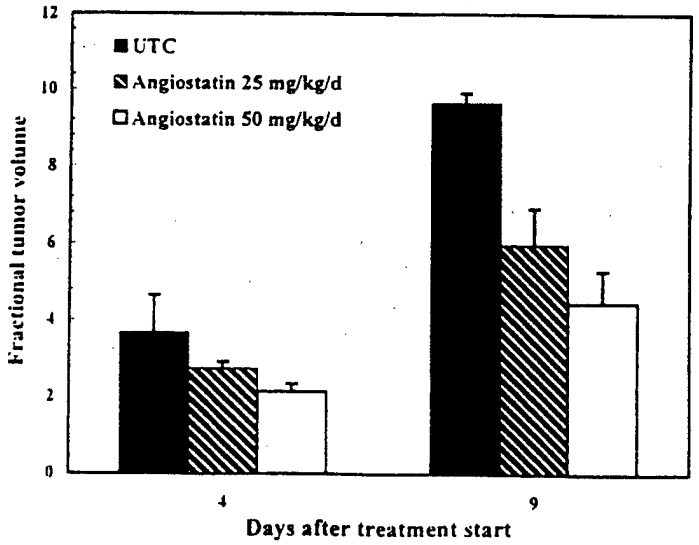

Fig. 1. The effect of different doses of AS on the growth of LLCs implanted in the hind limbs of mice. Mice bearing LLCs in their right hind limb (mean volume = 499 ± 188 mm^3) were treated with AS at a dose of either 25 mg/kg/day or 50 mg/kg/day, and the growth of the tumors was measured relative to their initial volumes at days 4 and 9 after treatment began. At day 9, the difference between tumor volumes in the untreated control group and the group receiving AS at 25 mg/kg/day was statistically significant ($P = 0.033$), as was the difference between tumor volumes in the untreated controls and the group receiving AS at 50 mg/kg/day ($P = 0.002$), but in these experiments, AS at 50 mg/kg/day did not produce statistically significantly more tumor volume reduction than AS at 25 mg/kg/day ($P = 0.27$).

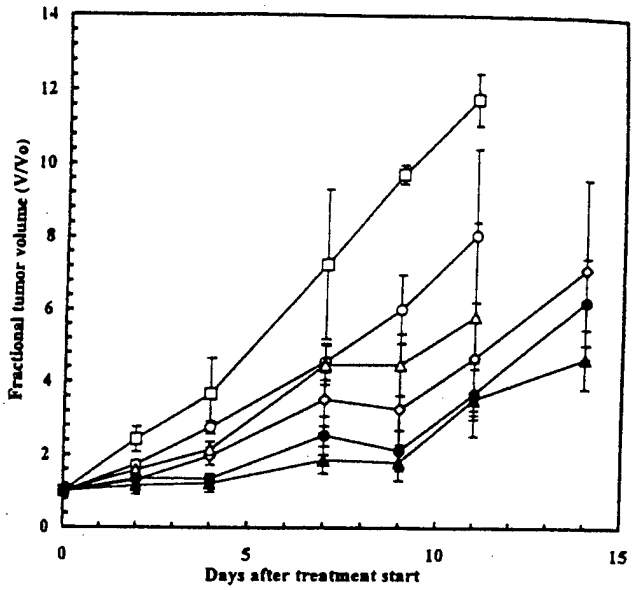

Fig. 2. The effect on tumor growth of differing AS dosages combined with IR. Mice bearing LLCs in their hind limbs were treated with varying combinations of IR and AS. IR was administered as two doses of 20 Gy on days 0 and 1. AS was administered at a dose of either 25 mg/kg/day or 50 mg/kg/day on days 0 through 13. Mean tumor volume on day 0 was 499 ± 188 mm^3. □, untreated controls; ◇, IR alone; ○, AS at 25 mg/kg/d; ●, IR + AS at 25 mg/kg/d; △, AS at 50 mg/kg/d; ▲, IR + AS at 50 mg/kg/d.

Effect of Combined Therapy with IR and AS on LLC Growth. Next we investigated the effect of combining IR with these two different doses of AS. In initial studies, we treated LLC tumors with differing dose schedules of IR to define a regimen that produced growth delay (data not shown). Because the LLC is a rapidly growing tumor that can increase in volume 10-fold within 14 days, we chose a regimen with two IR fractions consisting of 20 Gy given on each of the first 2 days of the experiment. Mice were treated either with AS alone at doses of 25 or 50 mg/kg/d for the duration of the experiment or with IR alone at a dose of 40 Gy given as two 20 Gy doses on consecutive days. (Fig. 2.) The combination of AS and IR was more effective as an antitumor therapy than either of the therapies alone, although there was no significant difference between IR plus 25 mg/kg/day AS and IR plus 50 mg/kg/day AS. For experiments investigating the temporal interaction of IR and AS, we, therefore, used the lower dose, 25 mg/kg/day.

IR Plus a 2-Day Course of AS Is as Effective as IR Plus a 14-Day Course of AS. To determine whether the interactive effect of AS and IR on tumor growth inhibition could be achieved with a short concomitant course of AS, we asked which temporal sequence of AS relative to IR is most effective: (*a*) IR and AS administered concomitantly; (*b*) AS administered after IR is completed; or (*c*) IR and AS delivered concomitantly, with AS continued after IR is completed. We hypothesized that, if the interaction of AS with IR requires the presence of AS at the time of IR administration, then there should be a superior antitumor effect when AS is administered concomitantly with IR than when AS is administered after the completion of the course of IR.

Mice bearing LLC tumors in their hind limbs were treated with combinations of IR and AS at a dose of 25 mg/kg/day according to the following: (*a*) IR (20 Gy × 2 doses administered on day 0 and 1) plus a long course of AS, which was administered for the duration of the experiment (days 0 through 13); (*b*) IR (20 Gy × 2 doses administered on day 0 and 1) plus a short course of AS, which was administered only during the 2 days when the IR was administered (days 0 and 1);

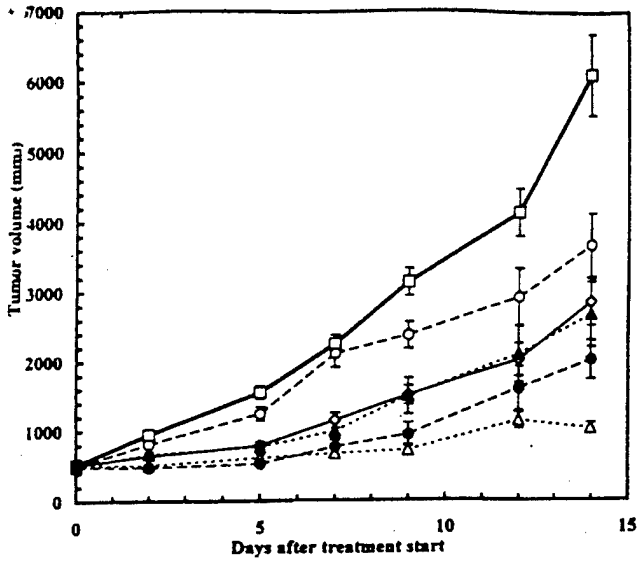

Fig. 3. The effect on tumor growth of varying the timing of AS doses relative to treatment with IR. Mice bearing LLCs in their hind limbs were treated with varying combinations of IR and AS. IR and AS were administered either alone or in combination. IR (20 Gy) was administered on days 0 and 1 for a total of 40 Gy. AS was administered at a dose of 25 mg/kg/day in all of the groups receiving AS. Mean tumor volume on day 0 was 510 ± 151 mm^3. See text for further comments. □, untreated controls; ◇, radiation (20 Gy on days 0 and 1, total = 40 Gy); ○, AS for 14 days (day 0 through 13); △, radiation (20 Gy on days 0 and 1, total = 40 Gy) administered concurrently with AS for two days (day 0 and 1); ●, radiation (20 Gy on days 0 and 1, total = 40 Gy) administered with AS, with the AS continued on days 2 through 13 for a total of 14 days of AS (days 0 through 13); ▲, radiation (20 Gy on days 0 and 1, total = 40 Gy) followed by AS beginning on the day after IR is completed (day 2) and continued through day 13.

and (*c*) IR (20 Gy × 2 doses administered on day 0 and 1) followed by AS beginning on the day after IR and continuing for the duration of the experiment (days 2 through 13). These experimental groups were compared with mice treated with either IR alone or AS alone and to untreated controls (Fig. 3.)

By day 9, from an initial volume of 510 ± 151 mm^3, tumors in the untreated control mice had grown to 3123 ± 195 mm^3; in the IR-alone group to 1491 ± 135 mm^3 ($P < 0.05$ relative to untreated control); and in the AS-alone group to 2357 ± 194 mm^3 ($P > 0.05$ relative to untreated control). By day 9 of treatment, in the combined-treatment groups, tumors treated with IR plus continuous AS reached a volume of 932 ± 165 mm^3 ($P < 0.05$ relative to IR alone); in the group receiving IR followed by days 2 through 13 of AS, 1480 ± 259 mm^3 ($P > 0.05$ relative to IR alone, not significant); and in the group receiving IR plus 2 days of AS, 705 ± 81 mm^3 ($P < 0.001$ relative to IR alone). By day 14, the tumors in the untreated control group had achieved a mean volume of 6110 ± 582 mm^3; IR alone, 2854 ± 338 mm^3 ($P < 0.05$ relative to untreated control); AS alone, 3666 ± 453 mm^3 ($P < 0.05$ relative to untreated control); IR plus short-course AS, 1032 ± 78 mm^3 ($P < 0.001$ relative to IR alone); IR plus long-course AS, 2022 ± 282 mm^3 ($P = 0.036$ relative to IR alone); and IR followed by AS, 2677 ± 469 mm^3 ($P > 0.05$ relative to IR alone).

There is a trend toward increased tumor regression in all of the experiments in the IR-plus-short-course-AS group, even when compared with mice receiving IR plus long-course AS, although the difference is not statistically significant. The observations that IR combined with a short concomitant course of AS is more effective in causing tumor regression than a longer course of AS administered after IR and that further AS administered after IR combined with concomitant AS does not improve tumor shrinkage (Fig. 3) demonstrate a temporal requirement for the interaction of AS and IR.

Inhibition of tumor angiogenesis provides a therapy directed at a target common to the growth and metastasis of all tumors, regardless of histological type (3, 7). Studies of endogenous inhibitors of angiogenesis such as AS and endostatin demonstrate potent antitumor effects in murine tumor models (12, 13, 18, 19). Because these agents are not tumoricidal, primary treatment of malignancies with anti-angiogenic agents may require lifelong therapy. We previously reported that such limitations might be overcome by a strategy of combining AS with a cytotoxic agent (22). Although the combination of IR and AS produced more tumor volume reduction in the combined-treatment group, the dosing schedule we tested required relatively large quantities of AS.

Our results support an interaction between IR and AS in tumor growth inhibition that occurs only during IR treatment and is dependent upon the action of AS on tumor blood vessel endothelium at the time IR is administered. This interaction does not occur unless AS is present at the time of IR administration, and tumor volume shrinkage is not increased by the continuation of AS treatment after IR has been completed (Fig. 3). AS does not affect the exponential growth of LLC *in vitro* (data not shown). Also, AS does not increase the killing of LLCs by IR in clonogenic killing assays but does enhance vascular endothelial cell killing by IR (22). These observations, when combined with the present study demonstrating a distinct temporal interaction between IR and AS, suggest that the combination of AS and IR does not target the tumor itself but, instead, targets the tumor blood vessels. Furthermore, the observation that additional treatment with AS beyond a brief, concomitant exposure of the tumor to AS and a cytotoxic agent such as IR produces no additional benefit in tumor regression is important because it suggests that limited AS supplies may be most effectively and efficiently used in combination with cytotoxic therapies such as IR, rather than as a primary therapy. These results suggest a new approach in the design of clinical trials with AS and other anti-angiogenic agents.

References

1. Thomas, K. A. Vascular endothelial growth factor, a potent and selective angiogenic agent. J. Biol. Chem., *271:* 603–606, 1996.
2. Wang, Y., and Becker, D. Antisense targeting of basic fibroblast growth factor and fibroblast growth factor receptor-1 in human melanomas blocks intratumoral angiogenesis and tumor growth. Nat. Med., *3:* 887–893, 1997.
3. Hanahan, D., and Folkman, J. Patterns and emerging mechanisms of the angiogenic switch during tumorigenesis. Cell, *86:* 353–364, 1996.
4. Folkman, J. Angiogenesis in cancer, vascular, rheumatoid and other disease. Nat. Med., *1:* 27–31, 1995.
5. Hanahan, D., Christofori, G., Naik, P., and Arbeit, J. Transgenic mouse models of tumour angiogenesis: the angiogenic switch, its molecular controls, and prospects for preclinical therapeutic models. Eur. J. Cancer, *32A:* 2386–2393, 1996.
6. Weidner, N., Semple, J. P., Welch, W. R., and Folkman, J. Tumor angiogenesis and metastasis: correlation in invasive breast carcinoma. N. Engl. J. Med., *324:* 1–8, 1991.
7. Fidler, I. J., and Ellis, L. M. The implications of angiogenesis for the biology and therapy of cancer metastasis. Cell, *79:* 185–188, 1994.
8. Asano, M., Yukita, A., Matsumoto, T., Kondo, S., and Suzuki, H. Inhibition of tumor growth and metastasis by an immunoneutralizing monoclonal antibody to human vascular endothelial growth factor/vascular permeability factor$_{121}$. Cancer Res., *55:* 5296–5301, 1995.
9. Goldman, C. K., Kendall, R. L., Cabrera, G., Soroceanu, L., Heike, Y., Gillespie, G. Y., Siegal, G. P., Mao, X., Bett, A. J., Huckle, W. R., Thomas, K. A., and Curiel, D. T. Paracrine expression of a native soluble vascular endothelial growth factor receptor inhibits tumor growth, metastasis, and mortality rate. Proc. Natl. Acad. Sci. USA, *95:* 8795–8800, 1998.
10. Lin, P., Sankar, S., Shan, S., Dewhirst, M. W., Polverini, P. J., Quinn, T. Q., and Peters, K. G. Inhibition of tumor growth by targeting tumor endothelium using a soluble vascular endothelial growth factor receptor. Cell Growth Differ., *9:* 49–58, 1998.
11. Lin, P., Buxton, J. A., Acheson, A., Radziejewski, C., Maisonpierre, P. C., Yancopoulos, G. D., Channon, K. M., Hale, L. P., Dewhirst, M. W., George, S. E., and Peters, K. G. Antiangiogenic gene therapy targeting the endothelium-specific receptor tyrosine kinase Tie2. Proc. Natl. Acad. Sci. USA, *95:* 8829–8834, 1998.
12. O'Reilly, M. S., Holmgren, L., Shing, Y., Chen, C., Rosenthal, R. A., Moses, M., Lane, W. S., Cao, Y., Sage, E. H., and Folkman, J. Angiostatin: a novel angiogenesis inhibitor that mediates the suppression of metastases by a Lewis lung carcinoma. Cell, *79:* 315–328, 1994.
13. O'Reilly, M. S., Boehm, T., Shing, Y., Fukai, N., Vasios, G., Lane, W. S., Flynn, E., Birkhead, J. R., Olsen, B. R., and Folkman, J. Endostatin: an endogenous inhibitor of angiogenesis and tumor growth. Cell, *88:* 277–285, 1997.

14. Gately, S., Twardowski, P., Stack, M. S., Patrick, M., Boggio, L., Cundiff, D. L., Schnaper, H. W., Madison, L., Volpert, O., Bouck, N., Enghild, J., Kwaan, H. C., and Soff, G. A. Human prostate carcinoma cells express enzymatic activity that converts human plasminogen to the angiogenesis inhibitor, angiostatin. Cancer Res., *56:* 4887–4890, 1996.
15. Gately, S., Twardowski, P., Stack, M. S., Cundiff, D. L., Grella, D., Castellino, F. J., Enghild, J., Kwaan, H. C., Lee, F., Kramer, R. A., Volpert, O., Bouck, N., and Soff, G. A. The mechanism of cancer-mediated conversion of plasminogen to angiogenesis inhibitor angiostatin. Proc. Natl. Acad. Sci. USA, *94:* 10868–10872, 1997.
16. Stathakis, P., Fitzgerald, M., Matthias, L. J., Chesterman, C. N., and Hogg, P. J. Generation of angiostatin by reduction and proteolysis of plasmin: catalysis by a plasmin reductase secreted by cultured cells. J. Biol. Chem., *272:* 20641–20645, 1997.
17. Dong, Z., Kumar, R., Yang, X., and Fidler, I. J. Macrophage-derived metalloelastase is responsible for the generation of angiostatin in Lewis lung carcinoma. Cell, *88:* 801–810, 1997.
18. Boehm, T., Folkman, J., Browder, T., and O'Reilly, M. S. Antiangiogenic therapy of experimental cancer does not induce acquired drug resistance. Nature (Lond.), *390:* 404–407, 1997.
19. O'Reilly, M. S., Holmgren, L., Chen, C., and Folkman, J. Angiostatin induces and sustains dormancy of human primary tumors in mice. Nat. Med., *2:* 689–692, 1996.
20. Griscelli, F., Li, H., Bennaceur-Griscelli, A., Soria, J., Opolon, P., Soria, C., Perricaudet, M., Yeh, P., and Lu, H. Angiostatin gene transfer: inhibition of tumor growth *in vivo* by blockage of endothelial cell proliferation associated with a mitosis arrest. Proc. Natl. Acad. Sci. USA, *95:* 6367–6372, 1998.
21. Tanaka, T., Cao, Y., Folkman, J., and Fine, H. A. Viral vector-targeted antiangiogenic gene therapy utilizing an angiostatin complementary DNA. Cancer Res., *58:* 3362–3369, 1998.
22. Mauceri, H., Hanna, N., Beckett, M., Gorski, D. H., Staba, M. J., Stellato, K. A., Bigelow, K., Heimann, R., Gately, S., Dhanabal, M., Soff, G., Sukhatme, V. P., Kufe, D., and Weichselbaum, R. R. Interaction of angiostatin and ionizing radiation in anti-tumour therapy. Nature (Lond.), *394:* 287–291, 1998.

CANCER RESEARCH (Advances in Brief)

Blockade of the Vascular Endothelial Growth Factor Stress Response Increases the Antitumor Effects of Ionizing Radiation[1]

David H. Gorski, Michael A. Beckett, Nora T. Jaskowiak, Douglas P. Calvin, Helena J. Mauceri, Rabih M. Salloum, Saraswathy Seetharam, Ann Koons, Danielle M. Hari, Donald W. Kufe, and Ralph R. Weichselbaum[2]

Departments of Radiation and Cellular Oncology [D. H. G., M. A. B., D. P. C., H. J. M., S. S., A. K., D. M. H., R. R. W.] and Surgery [N. T. J., R. M. S.], University of Chicago, Chicago, Illinois 60637, and Dana Farber Cancer Institute, Harvard Medical School, Boston, Massachusetts 02115 [D. W. K.]

Abstract

The family of vascular endothelial growth factor (VEGF) proteins include potent and specific mitogens for vascular endothelial cells that function in the regulation of angiogenesis. Inhibition of VEGF-induced angiogenesis, either by neutralizing antibodies or a dominant-negative soluble receptor, blocks the growth of primary and metastatic experimental tumors. Here we report that VEGF expression is induced in Lewis lung carcinomas (LLCs) both *in vitro* and *in vivo* after exposure to ionizing radiation (IR) and in human tumor cell lines (Seg-1 esophageal adenocarcinoma, SQ20B squamous cell carcinoma, T98 and U87 glioblastomas, and U1 melanoma) *in vitro*. The biological significance of IR-induced VEGF production is supported by our finding that treatment of tumor-bearing mice (LLC, Seg-1, SQ20B, and U87) with a neutralizing antibody to VEGF-165 before irradiation is associated with a greater than additive antitumor effect. *In vitro*, the addition of VEGF decreases IR-induced killing of human umbilical vein endothelial cells, and the anti-VEGF treatment potentiates IR-induced lethality of human umbilical vein endothelial cells. Neither recombinant VEGF protein nor neutralizing antibody to VEGF affects the radiosensitivity of tumor cells. These findings support a model in which induction of VEGF by IR contributes to the protection of tumor blood vessels from radiation-mediated cytotoxicity and thereby to tumor radioresistance.

Introduction

Tumors influence the surrounding host stroma by inducing angiogenesis to supply their oxygen and nutrient needs. In normal tissues, angiogenesis is tightly regulated by the balance between angiogenic and antiangiogenic factors (1). One of the most important angiogenic proteins, VEGF,[3] is expressed by diverse human tumors (2–4). Evidence for the importance of VEGF-induced angiogenesis in tumor growth includes the observation that inhibition of VEGF action by neutralizing antibodies or a dominant-negative soluble receptor blocks the growth of primary and metastatic experimental tumors (5–9) and that, in a mouse fibrosarcoma model, disruption of tumor-specific VEGF expression results in decreased tumor growth and vascularity, as well as increased tumor cell apoptosis (10). Moreover, it has been observed that serum VEGF levels are elevated in certain patients with malignant tumors after radiation therapy (11). These observations suggest that the paracrine relationship between the tumor and its vasculature represents a potential target for a strategy to enhance IR-induced antitumor activity.

In the present study, we demonstrate that exposure of LLC and human tumor xenografts to IR is associated with induction of VEGF expression. We also show that blocking the action of this IR-mediated increase in VEGF using neutralizing anti-VEGF antibodies results in increased endothelial cell killing by IR and produces greater than additive antitumor effects in murine tumor model systems. These findings support a model in which induction of VEGF by IR contributes to the protection of tumor blood vessels from radiation-mediated cytotoxicity and thereby to tumor radioresistance, suggesting that an effective use of anti-VEGF antibodies in clinical antitumor therapy is in combination with a cytotoxic therapy such as IR.

Materials and Methods

Cell Culture. LLC cells (a gift of J. Folkman) and SQ20B cells were maintained as described previously (12, 13). HUVECs were maintained in EGM-2 medium (Clonetics). U87 and T98 human glioblastoma cells were maintained in RPMI 1640 (Life Technologies, Inc.) + 10% FBS (Intergen); U1 melanoma cells, DMEM (75%) + F12 (25%) + 10% FBS; Seg-1 esophageal adenocarcinoma cells (a gift of D. Beer; Ref. 14), DMEM + 10% FBS.

Tumor Models and Administration of IR. To establish tumors, LLC cells were injected s.c. into the right hind limb (1×10^6 cells in PBS) of C57BL/6 female mice (Frederick Cancer Research Institute). To establish human tumor xenografts, SQ20B human squamous cell carcinoma cells (Ref. 15; 5×10^6), Seg-1 esophageal adenocarcinoma cells (Ref. 14; 3×10^6), and U87 glioblastoma cells (3×10^6) were injected s.c. into the hind limb of female athymic nude mice (Frederick Cancer Research Institute). Tumor volume was determined by direct measurement with calipers and calculated by the formula (length × width × depth/2) and reported as the mean volume ± SE, as described previously (12, 13). Tumors were allowed to attain a mean size between 350–450 mm^3 (LLC, 442 ± 14 mm^3; SQ20B, 372 ± 16 mm^3; Seg-1, 407 ± 20 mm^3; U87, 453 ± 32 mm^3), after which mice were divided into experimental groups and treated. Tumors were irradiated using a GE Maxitron X-ray generator operating at 150 kV, 30 mA, using a 1-mm aluminum filter at a dose rate of 188 cGy/min. LLC tumors received 40 Gy (20 Gy on days 0 and 1); SQ20B, 40 Gy (10 Gy on days 0, 1, 2, and 3); Seg-1, 20 Gy (5 Gy on days 0, 1, 2, and 3); and U87, 40 Gy (5 Gy on days 0, 1, 4, 5, 7, 8, 11, and 12). Mice were shielded with lead except for the tumor-bearing right hindlimb. The care and treatment of animals were in accordance with institutional guidelines.

Neutralizing Antibodies against VEGF. For experiments with LLC tumors, neutralizing polyclonal goat antibody (IgG) against recombinant mouse VEGF-164 (R & D Systems) was suspended in PBS and administered via i.p. injection (10 μg/mouse, 3 h before each IR fraction). For experiments with human tumor xenografts, a neutralizing monoclonal antibody to recombinant human VEGF-165 (R & D Systems) was used (10 μg/mouse, 3 h before each IR fraction). Control mice in experiments with LLC and human tumor xenografts received nonimmune goat IgG (Sigma) or mouse IgG (Sigma), respectively. Monoclonal anti-VEGF antibody was used for most *in vitro* experiments with HUVECs, but in some *in vitro* experiments, a polyclonal goat anti-human VEGF-165 neutralizing antibody (R & D Systems) was used.

Received 4/14/99; accepted 6/1/99.

The costs of publication of this article were defrayed in part by the payment of page charges. This article must therefore be hereby marked *advertisement* in accordance with 18 U.S.C. Section 1734 solely to indicate this fact.

[1] This work was supported by National Cancer Institute Grants CA42596 and CA41068, as well as Grant DE/CA11921 from the Chicago Oral Cancer Center and a grant from the Lederer Foundation. Dr. Calvin is supported in part by National Cancer Institute Training Grant T32CA09675. We also acknowledge support from the Center for Radiation Therapy, The Chicago Tumor Institute, and the Geraldi-Norton Foundation.

[2] To whom requests for reprints should be addressed, at Department of Radiation and Cellular Oncology, University of Chicago, 5841 South Maryland Avenue, Chicago, IL 60637. Phone: (773) 702-0817; Fax: (773) 834-7233; E-mail: rrw@rover.uchicago.edu.

[3] The abbreviations used are: VEGF, vascular endothelial growth factor; LLC, Lewis lung carcinoma; IR, ionizing radiation; HUVEC, human umbilical vein endothelial cell; MTT, 3-(4, 5-dimethylthiazol-2yl)-2, 5-diphenyltetrazolium bromide.

Table 1 *VEGF levels in Lewis lung carcinoma tumors after exposure to 40 Gy*

	Untreated controls		Ionizing radiation (40 Gy)	
Day	Mean tumor volume (mm^3 ± SE)	VEGF (pg VEGF/mg total protein)	Mean tumor volume (mm^3 ± SE)	VEGF (pg VEGF/mg total protein)
2	947 ± 43	69 ± 21	641 ± 22	234 ± 79[a]
5	1545 ± 93	46 ± 18	786 ± 52	135 ± 32[a]
14	6110 ± 582	90 ± 23	2854 ± 338	194 ± 47[a]

[a] $P < 0.05$ relative to VEGF levels in untreated controls.

Measurement of VEGF Levels in Tumor Extracts and Conditioned Media. Tumor extracts were prepared by homogenizing tumors in a buffer containing 150 mM NaCl, 10 mM Tris, 5 mM EDTA, 0.5% Triton X-100, and 1 μM dithiothreitol (pH 7.5), 50 μM PMSF, 1 μg/ml leupeptin, and 2 μg/ml aprotinin. The homogenate was subjected to three freeze-thaw cycles in liquid nitrogen to lyse cells and then spun at 5000 × *g* at 4°C to pellet debris. VEGF levels were measured in tumor extract supernatants by ELISA (R & D Systems). VEGF levels were normalized to total extract protein concentration as measured by Lowry assay and expressed as pg VEGF/mg total extract protein. For *in vitro* studies, cells were plated in six-well plates, allowed to attach overnight, and exposed to IR. At various time points, VEGF levels in conditioned media were measured by ELISA and normalized to cell number in each well.

Northern Blots. Total RNA was isolated from cultured cells and tumor tissue by the guanidine thiocyanate method (16) using Trizol LS (Life Sciences, Inc.). Twenty-five μg of total RNA was fractionated on 1.2% agarose gels containing formaldehyde and blotted onto nylon membranes, then hybridized with a ^{32}P-labeled cDNA probe encoding human VEGF (17). Hybridizations were carried out at 60°C in 0.5 M sodium phosphate (pH 7.0), 7% sodium dodecyl sulfate, 1 mM EDTA, and 1% bovine serum albumin (18), and blots were washed to a stringency of 0.2× SSC. After autoradiography, blots were stripped of probe and rehybridized to a labeled cDNA encoding rat glyceraldehyde-3-phosphate dehydrogenase to demonstrate message integrity.

MTT Assays. HUVECs were plated (1×10^3 cells/well in 96 well plates) in EGM-2 media (Clonetics) containing 2% fetal calf serum and allowed to attach overnight. Medium was replaced with EGM-2 plus 2% fetal calf serum containing different concentrations of recombinant human VEGF-165 (R & D Systems). In other experiments, the concentration of VEGF-165 was kept constant (10 ng/ml), and either a neutralizing polyclonal or monoclonal anti-human VEGF-165 antibody (R & D Systems) was added before treatment with IR. Ninety-six h after IR, cells were pulsed with MTT (Sigma; Ref. 19) at 0.5 mg/ml culture volume for 4 h, after which the medium was removed, and the dye was solubilized in dimethyl sulfoxide. Except where otherwise noted, the dose of IR used was 10 Gy. Absorbance was measured at 515 nm and normalized to untreated control cells by the following equation:

$$P = \frac{A - A_0}{A_{control} - A_0}$$

where P is the proliferation relative to control, A is absorbance at 515 nm (A_{515}), $A_0 = A_{515}$ at $T = 0$ h, and $A_{control} = A_{515}$ for control cells (unirradiated, grown in 10 ng/ml VEGF-165).

Clonogenic Assays. Clonogenic assays were performed as described previously (13). Briefly, HUVECs and LLCs were plated in EGM-2 medium. Eighteen h after plating, HUVEC medium was replaced with serum-free medium containing no bFGF, to which a defined amount (0–100 ng/ml) of recombinant VEGF-165 (R & D Systems) had been added. Four h later, cells were irradiated with doses of 0–1000 cGy using a cobalt source. Cells were incubated for 48 h, after which medium was replaced with complete EGM-2 containing 10 ng/ml VEGF. After 14–17 days, cells were stained with crystal violet. Colonies were counted, and surviving fractions were determined. Colonies containing >50 cells were scored as positive.

Data Analysis. Statistical significance was determined using one-way ANOVA or Student's *t* test, as appropriate.

Results and Discussion

We examined the production of VEGF by LLC tumors *in vivo* after exposure to IR. LLC tumors were established in the hindlimbs

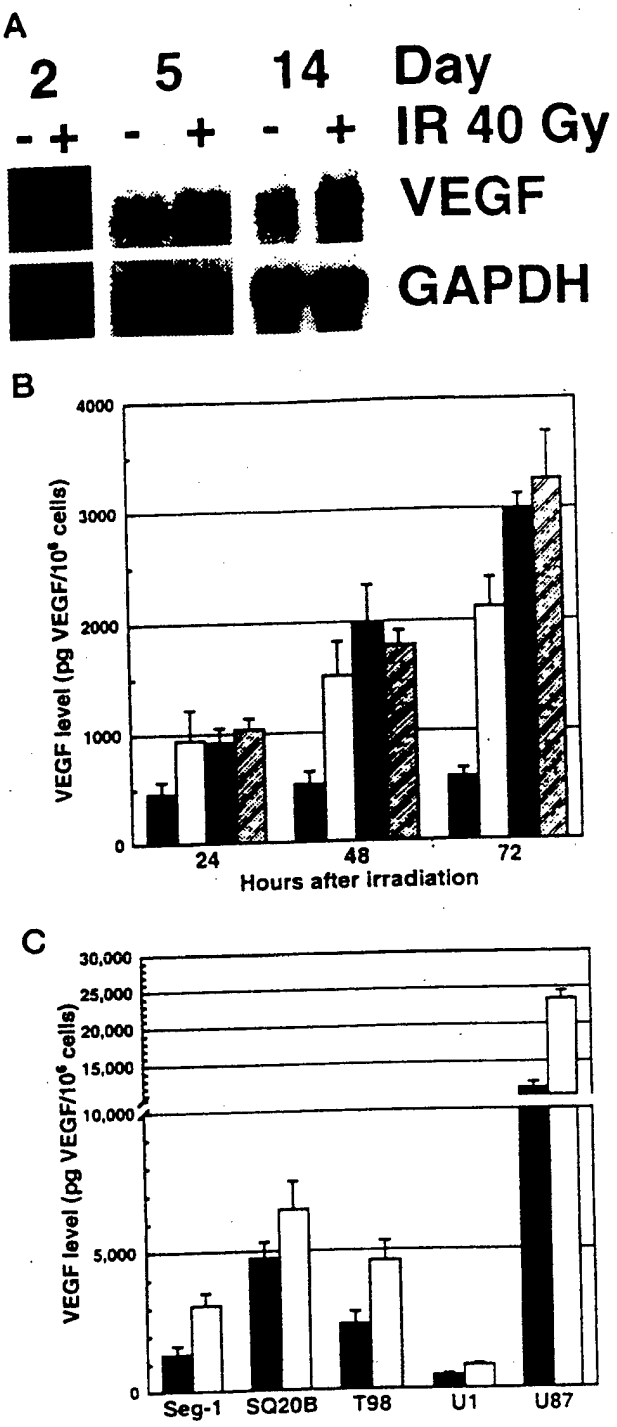

Fig. 1. VEGF levels in LLC and human tumor xenografts. *A*, VEGF mRNA levels in LLC tumors after IR exposure. LLC tumors were exposed to 40 Gy (two 20-Gy fractions). Total RNA was isolated from irradiated tumors and probed with a cDNA encoding human VEGF-165, after which they were stripped of probe and reprobed with a cDNA to glyceraldehyde-3-phosphate dehydrogenase to demonstrate message integrity. Blots from a representative experiment are displayed. *B*, VEGF protein levels in LLC conditioned medium after IR exposure. LLCs were plated in six-well plates at 25% confluence, allowed to attach overnight, and then irradiated with 0, 5, 10, or 20 Gy. Conditioned medium was collected every 24 h, and VEGF levels were normalized to cell number. A dose-dependent increase in VEGF secretion was observed for all doses of IR ($P < 0.05$). ■, 0 cGy; □, 500 cGy; ■, 1000 cGy; ■, 2000 cGy. Data are presented as means; *bars*, SE. *C*, VEGF expression in human tumor cell lines. Subconfluent human tumor cells (Seg-1 esophageal adenocarcinoma, SQ20B squamous cell carcinoma, U1 melanoma, and U87 and T98 glioblastoma) were exposed to 10 Gy. Conditioned medium from radiated and unirradiated cells was collected 24 h later. VEGF levels in conditioned media were measured by ELISA and normalized to cell number. An IR-dependent increase in VEGF secretion was observed in each cell line: Seg-1 ($P = 0.02$), SQ20B ($P = 0.08$), T98 ($P = 0.02$), U1 ($P = 0.009$), and U87 ($P = 0.0009$). No VEGF was detectable in medium unconditioned by cells. ■, no IR; □, 1000 cGy. Data are presented as means; *bars*, SE.

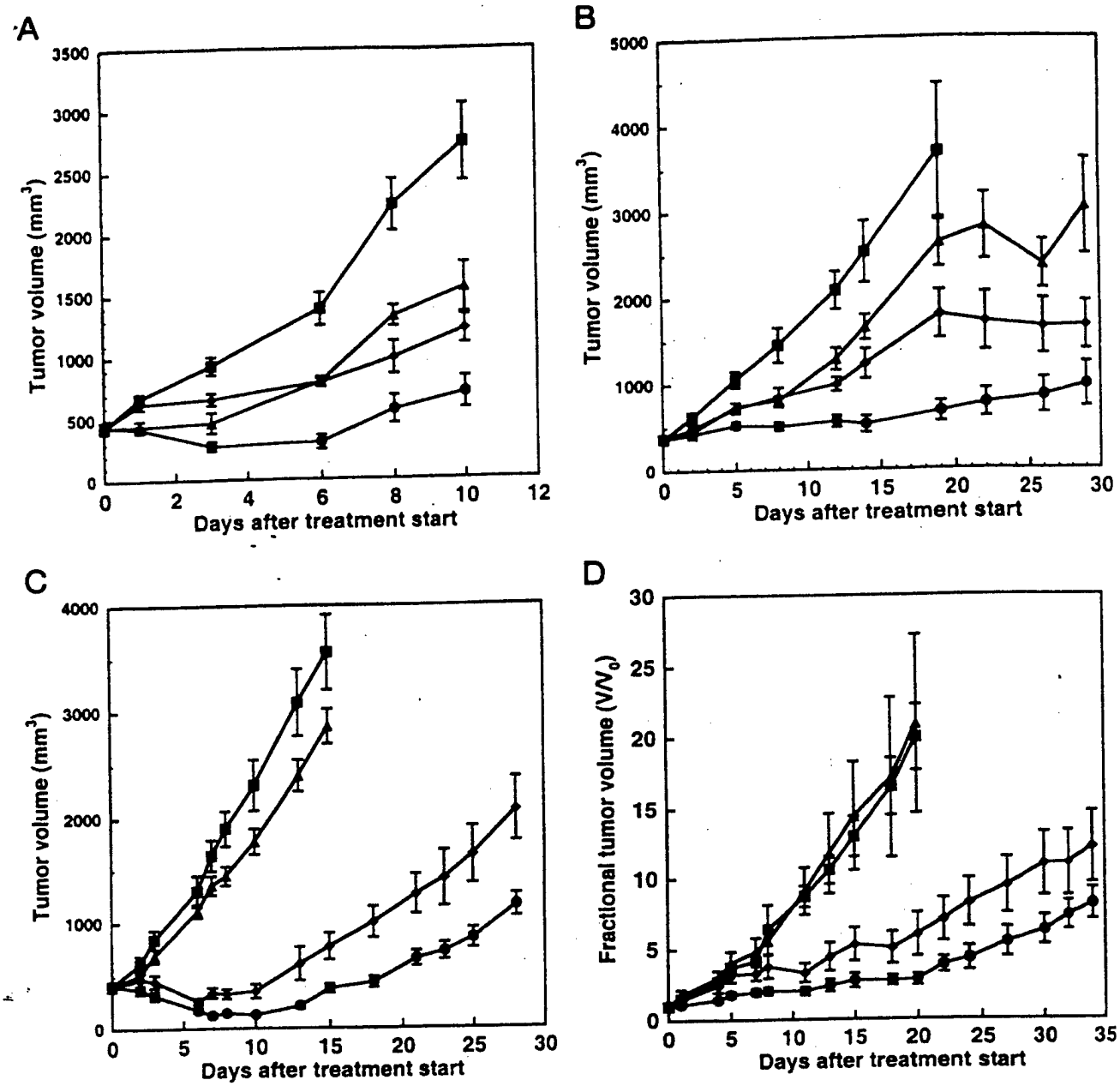

Fig. 2. Effect of VEGF blockade before treatment with IR in murine tumors and human xenografts. Tumor-bearing mice were treated with neutralizing anti-VEGF antibody, IR, or a combination of the two, and tumor volumes were measured (see "Materials and Methods"). ■, control; ◆, IR alone; ▲, anti-VEGF antibody alone; ●, IR combined with anti-VEGF antibody. Data are presented as the means; *bars*, SE; *Ps* are for combined therapy relative to IR alone. *A*, LLC. Mice were divided into experimental groups (n = 5/group) and treated with: 40 Gy administered as two 20-Gy fractions on days 0 and 1; 40 Gy plus polyclonal goat anti-mouse VEGF-164 antibody administered 3 h before each fraction; or goat anti-mouse VEGF-164 antibody alone The experiment was repeated three times. There was a statistically significant difference between the IR alone and combined treatment groups for all days after day 3 ($P < 0.02$ for all days). *B*, SQ20B squamous cell carcinoma xenografts. Mice were divided into experimental groups (n = 6–8/group) and treated as follows: 40 Gy administered as four 10-Gy fractions on days 0, 1, 2, and 3; 40 Gy plus monoclonal anti-human VEGF-165 antibody administered 3 h before each fraction; or monoclonal anti-human VEGF-165 antibody alone. There was a statistically significant difference between the IR alone and combined treatment groups for all days after day 5 ($P < 0.03$ for all days). *C*, Seg-1 esophageal adenocarcinoma xenografts. Mice were divided into experimental groups (n = 8/group) and treated as follows: 20 Gy administered as four 5-Gy fractions on days 0, 1, 2, and 3; 20 Gy plus monoclonal anti-human VEGF-165 antibody administered 3 h before each fraction; or monoclonal anti-human VEGF-165 antibody alone administered identically to the combined treatment group. There was a statistically significant difference between the IR alone and combined treatment groups for all days after day 6 ($P < 0.02$ for all days). *D*, U87 glioblastoma xenografts. Mice were divided into experimental groups (n = 6/group) and treated as follows: 40 Gy administered as eight 5-Gy doses on days 0, 1, 4, 5, 7, 8, 11, and 12; 40 Gy plus monoclonal anti-human VEGF-165 antibody administered 3 h before each dose of IR; or monoclonal anti-human VEGF-165 antibody alone. Results are reported as fractional tumor volumes, with an initial tumor volume of 453 ± 32 mm³. There was a statistically significant difference between the IR alone and combined treatment groups for all days after day 11 ($P < 0.05$ for all days).

of female C57BL/6 mice and allowed to grow to a volume of 510 ± 11 mm³ (2.5% body weight). They were then irradiated with 20 Gy on days 0 and 1 and harvested at days 2, 5, or 14. VEGF levels in extracts from control tumors remained relatively constant (46–90 pg/mg total protein) for 14 days (Table 1). By contrast, on day 2, the mean VEGF level in irradiated tumors was increased more than 3-fold compared with that in unirradiated tumors (234 ± 79 pg/mg total protein, $P = 0.032$). The mean VEGF level in irradiated tumors remained 2.2-fold higher than that in unirradiated tumors at day 14 (194 ± 47 pg/mg total protein, $P = 0.027$). Plasma VEGF levels remained low or undetectable in both control and irradiated animals (data not shown). To confirm the effects of IR, VEGF mRNA levels were assessed in the same tumors by Northern blot analysis. VEGF transcripts were induced 3-fold 2

Table 2 *Effect of combining anti-VEGF antibody and ionizing radiation*

Tumor	Day[b]	Fractional tumor volume relative to untreated controls[a]				
		Ionizing radiation	Anti-VEGF antibody	Combined (expected)[c]	Combined (observed)	Observed/ expected[d]
LLC	6	0.570	0.574	0.327	0.220	0.673
Seg-1	13	0.198	0.778	0.154	0.069	0.448
SQ20B	19	0.512	0.715	0.366	0.182	0.497
U87	18	0.302	1.000	0.302	0.166	0.550

[a] Obtained by dividing the mean volume of treated tumors by that of untreated controls.
[b] The day at which tumors treated with both anti-VEGF and IR demonstrated the most pronounced greater than additive growth inhibition.
[c] Obtained by multiplying the fractional tumor volumes obtained by each treatment modality individually to yield the fractional tumor volume expected if the effects of each treatment modality were additive.
[d] Obtained by dividing the observed fractional tumor volume by the expected fractional tumor volume. A ratio <1 indicates a greater than additive effect, and a ratio >1 indicates a less than additive effect. Effects were greater than additive for LLC beginning on day 3; for Seg-1, day 6; for SQ20B, day 12; and for U87, day 3.

days after exposure to IR and remained elevated for 14 days (Fig. 1*A*).

To determine whether IR induces VEGF in tumor cells, subconfluent LLC cells were exposed to different doses of IR. Conditioned medium was harvested at various intervals for measurement of VEGF levels by ELISA. VEGF levels in LLC-conditioned media exhibited an IR dose-dependent increase within 24 h. By 72 h, VEGF levels were elevated 6-fold over control in media from LLC irradiated with 20 Gy (Fig. 1*B*). VEGF expression *in vitro* was also measured in irradiated human tumor cell lines: Seg-1 (esophageal adenocarcinoma; Ref. 14); SQ20B (a radioresistant squamous cell carcinoma line; Ref. 15); U1 (melanoma); and T98 and U87 (glioblastoma). Under basal conditions, these tumor cell lines secreted widely differing quantities of VEGF, but all demonstrated an IR-dependent increase in VEGF production within 24 h of treatment with 10 Gy (Fig. 1*C*). These findings demonstrate that IR induces VEGF expression in diverse tumor cell types.

To determine whether induction of tumor VEGF secretion by IR affects the antitumor response, we treated LLC tumors with neutralizing antibodies against murine VEGF-164 before IR exposure. Female C57BL/6 mice bearing LLC tumors were divided into experimental groups and treated as follows: IR alone, 20 Gy on consecutive days (40 Gy total); anti-VEGF (10 μg 3 h before each fraction); and IR plus anti-VEGF (Fig. 2*A*). By day 6, consistent with previous observations (5, 6, 8, 9), treatment with anti-VEGF alone produced a 42.6% reduction in tumor volume (796 $\pm$ 41 mm^3; $P = 0.004$). IR alone produced 43.0% reduction (792 $\pm$ 30 mm^3; $P = 0.006$). However, the combination of IR and anti-VEGF resulted in a 78.0% reduction (305 $\pm$ 58 mm^3; $P = 0.001$ relative to IR alone), a greater than additive effect.

To extend these findings to other tumor models, we combined neutralizing anti-VEGF antibody with IR in human squamous cell carcinoma and esophageal adenocarcinoma xenografts. Athymic nude mice bearing radioresistant human head and neck squamous cell carcinoma xenografts (SQ20B; Ref. 15) were treated with IR and a monoclonal neutralizing antibody against human VEGF-165. SQ20B xenografts were treated with IR alone (40 Gy administered as four 10-Gy fractions), anti-VEGF alone (10 μg i.p. 3 h before each fraction), or combined IR and anti-VEGF (10 μg administered 3 h before treatment with IR). As observed for LLC, VEGF blockade markedly increased the efficacy of IR in inhibiting tumor growth (Fig. 2*B*). Next, we examined a xenograft model for a human esophageal adenocarcinoma. Female athymic nude mice bearing Seg-1 xenografts (14) were treated with IR alone (20 Gy in four 5-Gy fractions), anti-VEGF (10 μg administered 3 h before each fraction), or combined therapy. Again, the antitumor effect of IR was enhanced by anti-VEGF (Fig. 2*C*). As shown for LLC, the antitumor effects of combined therapy were greater than additive in both human xenografts (Table 2).

Finally, to determine whether this combined approach is effective against a tumor that secretes large quantities of basal and IR-stimulated VEGF, we treated athymic mice bearing U87 glioblastoma xenografts with combined IR (eight 5-Gy fractions, see "Materials and Methods") and anti-VEGF therapy (10 μg administered 3 h before each IR fraction). By day 18, anti-VEGF produced no detectable tumor growth inhibition, and IR alone inhibited tumor growth by 68.8% relative to untreated controls (Fig. 2*D*). Combined therapy, however, produced an 83.4% inhibition ($P = 0.046$), also a greater than additive effect.

We examined tumor volume data for all tumors on the day of maximum tumor regression in the combined treatment group relative to the tumor regression observed on the same day for groups treated with each therapy alone. In each tumor type, the effect of combined therapy was greater than additive (Table 2) beginning early in treatment (for LLC, day 3; Seg-1, day 6; SQ20B, day 12; and U87, day 2) and continued for the course of the experiment. We also examined the growth data in terms of number of days for tumors to regrow to twice the original volume. The time for untreated LLC tumors to grow to twice their initial volume was 2.6 $\pm$ 0.5 days. IR alone produced a growth delay of 4.0 $\pm$ 1.0 days, whereas anti-VEGF delayed growth to twice initial volume by 3.4 $\pm$ 0.7 days. However, combined treatment produced a greater than additive growth delay (9.2 $\pm$ 1.4 days, $P = 0.02$). Even greater combined effects were observed for tumor xenografts. For U87 xenografts, time to tumor volume doubling was 2.4 $\pm$ 0.6 days and was delayed 1.1 $\pm$ 0.3 days by IR and only 0.3 $\pm$ 0.1 days by anti-VEGF alone. However, combined treatment produced a growth delay of 9.0 $\pm$ 4.3 days ($P = 0.03$). Of note, of the tumors we examined, U87 glioblastoma produced the most VEGF *in vitro*. Similar greater than additive effects of a magnitude between that observed for LLC and U87 were observed for SQ20B ($P = 0.003$) and Seg-1 xenografts ($P = 0.001$; data not shown). These findings demonstrate that blocking the effects of VEGF enhances the tumoricidal effects of IR in diverse tumor models of human malignancies for which IR is a major therapeutic modality, an observation that may have implications for human therapy. Importantly, this effect was observed using a dose of anti-VEGF that by itself had little to no effect on tumor growth, indicating that even a slight inhibition of VEGF action can result in a marked increase in the antitumor effect of IR.

To investigate the mechanism of the effects observed *in vivo* and assess the effects of VEGF on IR-mediated killing of tumor cells and endothelial cells *in vitro*, we measured the survival of HUVECs after exposure to IR. The effect of exogenous VEGF protein on IR-mediated cell killing of HUVECs was assessed by MTT proliferation assay (19) and clonogenic assay (13; Fig. 3). As measured by MTT assay, pretreatment with VEGF protected HUVECs against the cytotoxic effects of 10 Gy in a dose-dependent fashion (Fig. 3*A*). Clonogenic survival after IR was also increased in a dose-dependent fashion

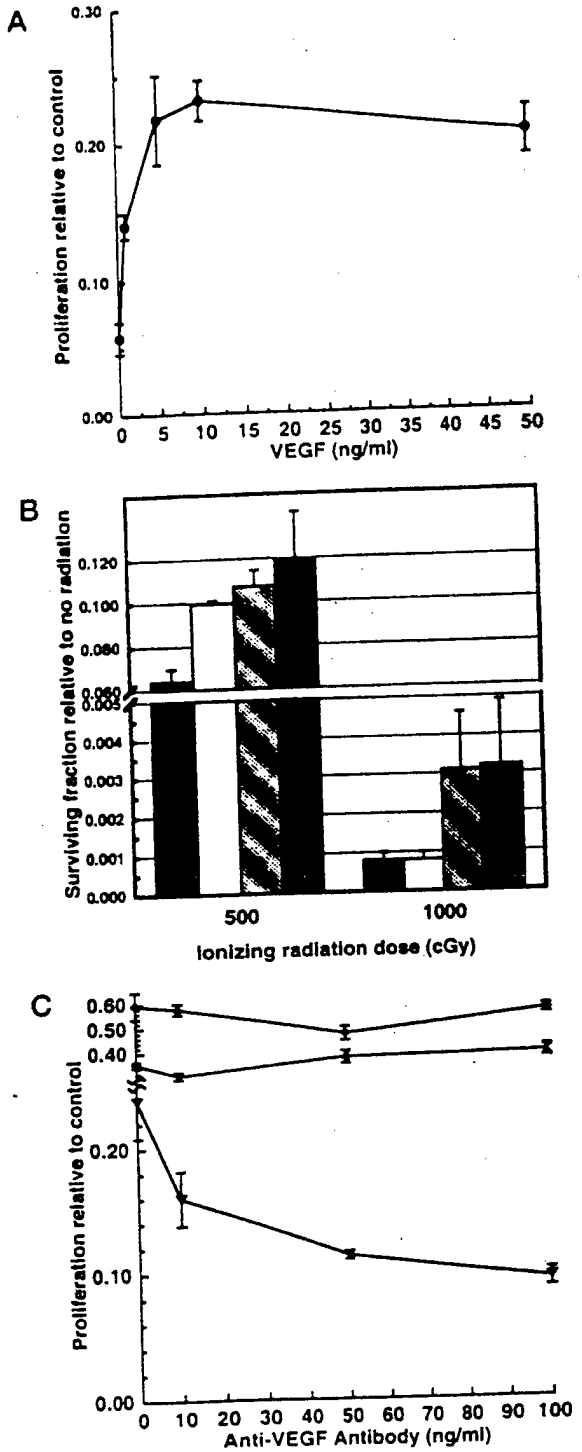

Fig. 3. Effect of manipulating VEGF levels on IR-mediated vascular endothelial cell killing *in vitro*. For MTT assays, HUVECs were plated in 96-well plates at 1×10^3 cells/well and treated with either differing concentrations of recombinant human VEGF-165 or monoclonal anti-human VEGF-165 antibody before exposure to IR, and absorbance readings measured 96 h after IR were done (see "Materials and Methods"). For clonogenic survival assays, HUVECs were treated with different concentrations of VEGF 4 h before irradiation (see "Materials and Methods"). *A*, MTT assay for HUVECs pretreated with varying concentrations of recombinant human VEGF-165 4 h before IR treatment. Absorbance measurements are normalized to those obtained under standard conditions (no IR treatment and VEGF = 10 ng/ml). *B*, clonogenic survival assay for HUVECs pretreated with 0, 1, 10, or 100 ng/ml VEGF-165 ± 500 and 1000 cGy. Surviving fraction is normalized to plating efficiency for unirradiated cells. VEGF protected HUVECs from IR-mediated killing at 500 cGy ($P < 0.05$ for all doses of VEGF) and 1000 cGy (10 ng/ml VEGF, $P = 0.06$; 100 ng/ml VEGF, $P = 0.07$). ■, 0 ng/ml VEGF; ▨, 1 ng/ml; ▧, 10 ng/ml; ■, 100 ng/ml. *C*, MTT assay for HUVECs and SQ20B cells pretreated with monoclonal anti-VEGF-165 antibody 4 h before treatment with 1000 cGy. Absorbance measurements were taken at 96 h after IR and normalized to those obtained with no pretreatment with antibody. VEGF = 10 ng/ml for both cell types. ◆, SQ20B. X, LLC. ▼, HUVECs.

when VEGF was added to the HUVEC culture medium (Fig. 3*B*). By contrast, adding anti-VEGF to the culture medium before IR exposure decreased HUVEC proliferation in a dose-dependent fashion (Fig. 3*C*). Neither SQ20B nor LLC proliferation was affected by VEGF or anti-VEGF (Fig. 3*C* and data not shown). These results demonstrate that IR-induced VEGF production by tumors specifically inhibits the lethal effects of IR on endothelial cells, and that blocking VEGF action increases endothelial cell killing by IR. The effect of manipulating VEGF levels on the radiosensitivity of vascular endothelial cells *in vitro* is on the order of 3–4-fold and therefore relatively modest (Fig. 3). However, the observation that pretreatment of tumor-bearing animals with neutralizing antibody against VEGF at doses that alone are insufficient to cause significant tumor growth inhibition before exposing tumors to IR suggests that this effect is biologically significant *in vivo*.

IR is a major therapeutic modality that is primarily effective in the treatment of relatively small tumors, whereas large tumors respond only with considerable toxicity to normal tissues. Our findings demonstrate that IR can induce VEGF expression by experimental tumors, and that this VEGF induction may represent a tumor response to radiation stress. Importantly, blocking the effects of VEGF production by irradiated LLC and human tumor xenografts results in greater than additive antitumor effects *in vivo* for very large experimental tumors (Fig. 2 and Table 2). In addition, VEGF abrogates the killing of endothelial cells by IR, whereas blocking the action of VEGF increases IR-induced killing. These findings support a model in which the disruption of the paracrine relationship between tumor and endothelium enhances the efficacy of IR in killing tumor cells. Our present results, combined with previous results showing that angiostatin and IR also produce greater than additive antitumor effects (12, 13), emphasize the potential importance of combining irradiation with an angiogenesis inhibitor because the tumor cells, tumor stroma, and their interactions are targeted by this combined therapy. Depriving the tumor endothelium of VEGF may thus represent an important strategy to increase the antitumor effects of IR and may indicate that the best use of antiangiogenic therapy is in combination with cytotoxic antitumor therapies such as IR.

Acknowledgments

We thank Drs. Judah Folkman and David Beer for supplying tumor cell lines and Drs. Samuel Hellman, Daniel Haraf, and Mitchell Posner for their support.

References

1. Hanahan, D., and Folkman, J. Patterns and emerging mechanisms of the angiogenic switch during tumorigenesis. Cell, *86:* 353–364, 1996.
2. Ferrara, N., and Davis-Smyth, T. The biology of vascular endothelial growth factor. Endocr. Rev., *18:* 4–25, 1997.
3. Neufeld, G., Cohen, T., Gengrinovitch, S., and Poltorak, Z. Vascular endothelial growth factor (VEGF) and its receptors. FASEB J., *13:* 9–22, 1999.
4. Thomas, K. A. Vascular endothelial growth factor, a potent and selective angiogenic agent. J. Biol. Chem., *271:* 603–606, 1996.
5. Asano, M., Yukita, A., Matsumoto, T., Kondo, S., and Suzuki, H. Inhibition of tumor growth and metastasis by an immunoneutralizing monoclonal antibody to human vascular endothelial growth factor/vascular permeability factor-121. Cancer Res., *55:* 5296–5301, 1995.
6. Borgstrom, P., Hillan, K. J., Sriramarao, P., and Ferrara, N. Complete inhibition of angiogenesis and growth of microtumors by anti-vascular endothelial growth factor neutralizing antibody: novel concepts of angiostatic therapy from intravital videomicroscopy. Cancer Res., *56:* 4032–4039, 1996.
7. Goldman, C. K., Kendall, R. L., Cabrera, G., Soroceanu, L., Heike, Y., Gillespie, G. Y., Siegal, G. P., Mao, X., Bett, A. J., Huckle, W. R., Thomas, K. A., and Curiel, D. T. Paracrine expression of a native soluble vascular endothelial growth factor receptor inhibits tumor growth, metastasis, and mortality rate. Proc. Natl. Acad. Sci. USA, *95:* 8795–8800, 1998.
8. Kanai, T., Konno, H., Tanaka, T., Baba, M., Matsumoto, K., Nakamura, S., Yukita, A., Asano, M., Suzuki, H., and Baba, S. Anti-tumor and anti-metastatic effects of human-vascular-endothelial-growth-factor-neutralizing antibody on human colon and gastric carcinoma xenotransplanted orthotopically into nude mice. Int. J. Cancer, *77:* 933–936, 1998.

9. Kim, K. J., Li, B., Winer, J., Armanini, M., Gillett, N., Phillips, H. S., and Ferrara, N. Inhibition of vascular endothelial growth-factor-induced angiogenesis suppresses tumour growth *in vivo*. Nature (Lond.), *362:* 841–844, 1993.
10. Grunstein, J., Roberts, W. G., Mathieu-Costello, O., Hanahan, D., and Johnson, R. S. Tumor-derived expression of vascular endothelial growth factor is a critical factor in tumor expansion and vascular function. Cancer Res., *59:* 1592–1598, 1999.
11. Gridley, D. S., Loredo, L. N., Slater, J. D., Archambeau, J. O., Bedros, A. A., Andres, M. L., and Slater, J. M. Pilot evaluation of cytokine levels in patients undergoing radiotherapy for brain tumor. Cancer Detect. Prev., *22:* 20–29, 1998.
12. Gorski, D. H., Mauceri, H. J., Salloum, R. M., Gately, S., Hellman, S., Beckett, M. A., Sukhatme, V. P., Soff, G. A., Kufe, D. W., and Weichselbaum, R. R. Potentiation of the antitumor effect of ionizing radiation by brief concomitant exposures to angiostatin. Cancer Res., *58:* 5686–5689, 1998.
13. Mauceri, H., Hanna, N., Beckett, M., Gorski, D. H., Staba, M. J., Stellato, K. A., Bigelow, K., Heimann, R., Gately, S., Dhanabal, M., Soff, G., Sukhatme, V. P., Kufe, D., and Weichselbaum, R. R. Interaction of angiostatin and ionizing radiation in anti-tumour therapy. Nature (Lond.), *394:* 287–291, 1998.
14. Hughes, S. J., Nambu, Y., Soldes, O. S., Hamstra, D., Rehemtulla, A., Iannettoni, M. D., Orringer, M. B., and Beer, D. G. Fas/APO-1 (CD95) is not translocated to the cell membrane in esophageal adenocarcinoma. Cancer Res., *57:* 5571–5578, 1997.
15. Weichselbaum, R. R., Dahlberg, W., and Little, J. B. Inherently radioresistant cells exist in some human tumors. Proc. Natl. Acad. Sci. USA, *82:* 4732–4735, 1985.
16. Chomczynski, P., and Sacchi, N. Single-step method of RNA isolation by acid guanidinium thiocyanate- phenol-chloroform extraction. Anal. Biochem., *162:* 156–159, 1987.
17. Mukhopadhyay, D., Knebelmann, B., Cohen, H. T., Ananth, S., and Sukhatme, V. P. The von Hippel-Lindau tumor suppressor gene product interacts with Sp1 to repress vascular endothelial growth factor promoter activity. Mol. Cell. Biol., *17:* 5629–5639, 1997.
18. Church, G. M., and Gilbert, W. Genomic sequencing. Proc. Natl. Acad. Sci. USA, *81:* 1991–1995, 1984.
19. Carmichael, J., DeGraff, W. G., Gazdar, A. F., Minna, J. D., and Mitchell, J. B. Evaluation of a tetrazolium-based semiautomated colorimetric assay: assessment of radiosensitivity. Cancer Res., *47:* 943–946, 1987.

Gene Therapy Targeted by Ionising Radiation Targets Both Tumour Cells and Tumour Vasculature

Helena J. Mauceri,[a] Michael A. Beckett,[a] Saraswathy Seetharem,[a] Donald W. Kufe[b] and Ralph R. Weichselbaum[a]

[a]Department of Radiation and Cellular Oncology, University of Chicago, Chicago, Illinois 60637 USA; and [b]Dana Farber Cancer Institute and Harvard Medical School, Boston, Massachusetts 02115 USA

The Molecular Basis for Radiation-Inducible Gene Therapy

Genetic radiotherapy, or gene therapy targeted by ionising radiation, is a concept whereby the cDNA encoding a cytotoxin is ligated downstream from a radiation-inducible promoter. Transcription of the gene encoding the cytotoxin is induced after ionising radiation exposure. The early growth response 1 gene (*EGR1*) encodes a zinc-finger transcription factor which binds to the DNA sequence CGCCCGC (1, 2). We reported that *EGR1* is transcriptionally induced after exposure to ionising radiation (3). Promoter deletion analysis of the EGR1 promoter elements demonstrated that the first three 5 CarG boxes are the most important, thereby permitting spatial and temporal regulation of cytotoxic gene expression after exposure to ionising radiation (4).

Tumour necrosis factor α (TNF) is a multifunctional cytokine produced principally by activated macrophages and lymphocytes that mediate the cellular immune response (5). TNF also has important roles in mediating endotoxic shock, inflammation and haemorrhagic necrosis of transplanted tumours (6). TNF enhances the cell killing produced by ionising radiation in tumour cells both in vitro and in vivo (7–9). A clinical study that combined systemically administered TNF and therapeutic radiation demonstrated promising results for local tumour control. However, systemic toxicity limited the therapeutic efficacy of this treatment combination (7, 10). We therefore proposed that localising TNF within the tumour volume, using gene therapy combined with radiotherapy, might eliminate systemic toxicity (11).

To demonstrate the feasibility of this gene therapy approach, the radiation-responsive DNA sequences of the EGR1 promoter were ligated upstream to the cDNA of human TNF. As a proof of principle, the EGR-TNF construct was transfected into HL525 human leukaemia cells. When SQ-20B human xenografts growing in athymic nude mice were directly injected with HL525.EGR-TNF cells and exposed to ionising radiation, significant tumour regression and cures were observed (12).

Adenoviral Gene Therapy

We selected an adenovirus type 5 as a gene delivery vector for the EGR-TNF construct. Adenoviruses are capable of transferring genes to nondividing and dividing cells, rarely integrate DNA into the genome of cells, and can be produced in high titers (13, 14). The EGR-TNF construct was inserted in place of the Ad1 early genes and most of the Ad3 gene to create the Ad.EGR-TNF vector. This vector was directly injected into SQ-20B xenografts. Treatment with Ad.EGR-TNF alone (2×10^8 PFU, twice weekly for two weeks) or ionising radiation alone (five 10-Gy fractions for 2.5 weeks to a total dose of 50 Gy) produced tumour regression to a mean of 30% (day 28) or 51% (day 25) of the original volume, respectively. By contrast, the mean

tumour volume of xenografts treated with Ad.EGR-TNF plus 50 Gy was reduced to 16% of original volume (day 38, $P < 0.05$). By day 60, mean tumour volume was reduced by 90% in 12 of 16 tumours in the combined treatment group (Ad.EGR-TNF + 50 Gy) compared with ionising radiation alone (10 of 23 tumours), or Ad.EGR-TNF alone (5 of 16 tumours, $P < 0.04$). No regression was observed in tumours treated with Ad.null (an adenovirus lacking the TNF gene) with or without ionising radiation. No human TNF was detected in the serum of animals treated with Ad.EGR-TNF and no animal demonstrated TNF associated cachexia. A slight increase in oedema and fibrosis were observed in hind limbs treated with combined therapy, but no loss of mobility or skin desquamation was observed (15).

Histopathology of Xenografts Treated with Adenoviral Gene Therapy

We performed microscopic analysis of SQ-20B xenografts treated with Ad.EGR-TNF (1×10^7 and 1×10^7 PFU) and ionising radiation (20 Gy, delivered as four 5 Gy fractions). Xenografts growing in nude mice and treated with Ad.EGR-TNF or Ad.null virus with and without ionising radiation. Tumours were excised on day 7 and scored for percentage thrombosis/high-power field. A significant increase in intratumoural vascular thrombosis and tumour necrosis was seen in xenografts treated with Ad.EGR-TNF and ionising radiation, but not in xenografts treated with Ad.EGR-TNF alone or ionising radiation alone ($P = 0.0001$). We also examined if combined treatment produced thrombosis that was selective for tumour vessels or whether the restriction of thrombosis was due to spatial confinement of TNF to the tumour volume. Skeletal muscle in the hind limbs of non-tumour-bearing nude mice were injected with 1×10^9 PFU Ad.EGR-TNF and treated with 20 Gy (four 5-Gy fractions). Despite high levels of TNF (determined by ELISA) no vascular thrombosis was observed in skeletal muscle tissue sections (16).

Mice Treated with Anticoagulants and Adenoviral Gene Therapy

To determine if intratumoural coagulation and thrombosis were essential components of the antitumour effects after combined treatment with Ad.EGR-TNF and ionising radiation, SQ-20B tumour-bearing mice were treated with anticoagulants throughout treatment. SQ-20B tumour-bearing mice were treated with ancrod (thrombin-like enzyme from the venom of the Malayan pit viper, Calloselasma rhodostoma) diluted in saline. Mice were injected intraperitoneally at a dose of 3 U/kg, twice weekly for two weeks to coincide with Ad.EGR-TNF injections. A second group of SQ-20B tumour-bearing mice were treated with coumadin (Warfarin Sodium for Injection, USP, DuPont Pharm, Manati, Puerto Rico). Coumadin was diluted in saline and administered by gavage at a dose of 1.0 mg/kg, twice weekly for 2 weeks. Prothrombin times were monitored in a separate group of mice. Xenografts were injected with Ad.EGR-TNF and irradiated with 50 Gy as in previous experiments.

The pattern of tumour regression observed in animals treated with anticoagulants was similar to that reported previously. Furthermore, in animals treated with anticoagulants, combined treatment with Ad.EGR-TNF + ionising radiation produced a 50% reduction in mean tumour volume 9 days earlier than in our previously published studies in which animals were not treated with anticoagulants. These findings demonstrated that systemic treatment with anticoagulants did not reverse the

antitumour effects after treatment with Ad.EGR-TNF and ionising radiation. We concluded that TNF-mediated thrombosis of the tumour vasculature was not the major antitumour effect of combined treatment with Ad.EGR-TNF and ionising radiation.

Treatment with Adenoviral Gene Therapy Is Associated with a Decrease in Tumor Microvascular Density

Because vascular thrombosis was not directly related to the antitumour effects observed after combined treatment with Ad.EGR-TNF and ionising radiation, we evaluated the effects of treatment on the tumour neovasculature. Immunohistochemical analyses were performed using an antibody to PECAM-1 (CD31), a protein which is constitutively expressed on the surface of endothelial cells. We examined representative tissue sections from SQ-20B tumours treated with Ad.EGR-TNF alone, ionising radiation alone, or the combination of Ad.EGR-TNF and ionising radiation. Ten high-power fields (400×) were counted at the growing edge of the tumour immediately adjacent to the skeletal muscle and skin. When we examined tumours from animals treated with Ad.EGR-TNF and ionising radiation, we found a marked reduction in the total number of tumour vessels when compared with either treatment alone. The observation of a marked decrease in vascular density is similar to that described after treatment with angiogenesis inhibitors (17, 18). These findings led to the hypothesis that combined treatment with Ad.EGR-TNF and ionising radiation alters tumour angiogenesis, in part, due to the production of antiangiogenic factors.

Treatment with Adenoviral Gene Therapy Is Associated with and Elevations in Plasma Angiostatin Levels

Angiostatin, a cleavage product of plasminogen, was first isolated from the blood and urine of C57BL mice bearing Lewis lung carcinoma tumours by O'Reilly and colleagues (19). It has been demonstrated that angiostatin inhibits the growth and migration of endothelial cells in vitro and the growth of primary and metastatic tumour in mice (19–21). We examined if TNF adenoviral gene therapy was associated with angiostatin production by conducting a preliminary study. Nude mice bearing SQ-20B xenografts were treated with Ad.EGR-TNF alone (2×10^8 PFU, twice weekly for 2 weeks), ionising radiation alone (five 10-Gy fractions for 2.5 weeks to a total dose of 50 Gy), the combination of Ad.EGR-TNF and ionising radiation, or untreated (controls). At day 22, mice were sacrificed, blood was collected, and plasma was separated for Western analysis. We found that mice receiving combined treatment (Ad.EGR-TNF and ionising radiation) exhibited elevated plasma angiostatin levels compared with animals treated with Ad.EGR-TNF alone and ionising radiation alone. These data suggest that our gene therapy approach target both the tumour cells and the tumour vasculature possibly mediated by the production of angiostatin. Our recently published data suggest a cytotoxic interaction between ionising radiation and angiostatin on the tumour vasculature (22).

Summary

Radiation-inducible *TNF* gene therapy attacks the tumour cells as well as the tumour microvasculature, thereby expanding the therapeutic target of ionising radiation. The spatial and temporal control of gene therapy by ionising radiation avoids systemic toxicity by limiting *TNF* induction to the tumour bed. Investigation of

highly radiation-inducible promoters linked to therapeutic agents may enhance the therapeutic ratio of ionising radiation.

Acknowledgements

This research was supported by Grant CA-41068 from The National Cancer Institute, The Chicago Tumor Institute at The University of Chicago and The Center for Radiation Therapy.

References

1. X. M. Cao, Mol. Cell Biol. 10, 1931–1939 (1990).
2. B. Christy, D. Nathans, Proc. Natl. Acad. Sci. USA 86, 8737–8741 (1989).
3. D. E. Hallahan, Proc. Natl. Acad. Sci. USA 88, 2156–2160 (1991).
4. R. Datta, Proc. Natl. Acad. Sci. USA 89, 10149–10153 (1992).
5. W. Fiers, FEBS Lett. 285, 199–212 (1991).
6. S. T. Malik, F. R. Balkwill, Immunol. Ser. 56, 239–268 (1992).
7. D. E. Hallahan, Cancer J. Sci. Am. 1, 204 (1995).
8. G. Sersa, V. Willingham, L. Milas, Int. J. Cancer 42, 129–134 (1988).
9. G. H. Wong, T. McHugh, R. Weber, D. V. Goeddel, Proc. Natl. Acad. Sci. USA 88, 4372–4376 (1991).
10. D. E. Hallahan, M. A. Beckett, D. Kufe, R. R. Weichselbaum, Int. J. Radiat. Oncol. Biol. Phys. 19, 69–74 (1990).
11. R. R. Weichselbaum, D. E. Hallahan, V. P. Sukhatme, D. W. Kufe, Int. J. Radiat. Oncol. Biol. Phys. 24, 565–567 (1992).
12. R. R. Weichselbaum, Cancer Res. 54, 4266–4269 (1994).
13. R. R. Weichselbaum, D. Kufe, Lancet 349 (Suppl.), SII10–12 (1997).
14. B. Avalosse, F. Dupont, A. Burny, Curr. Opin. Oncol. 7, 94–100 (1995).
15. D. E. Hallahan, Nat. Med. 1, 786–791 (1995).
16. H. J. Mauceri, Cancer Res. 56, 4311–4314 (1996).
17. B. A. Teicher, Y. Emi, Y. Kakeji, D. Northey, Eur. J. Cancer 32A, 2461–2466 (1996).
18. L. Holmgren, M. S, O'Reilly, J. Folkman, Nat. Med. 1, 149–153 (1995).
19. M. O'Reilly, Cancer Res. 54, 6083–6086 (1994).
20. B. K. Sim, Cancer Res. 57, 1329–1334 (1997).
21. Y. Cao, J. Biol. Chem. 271, 29461–29467 (1996).
22. H. J. Mauceri, Nature 394, 287–291 (1998).

Enhanced eradication of local and distant tumors by genetically produced interleukin-12 and radiation

SARASWATHY SEETHARAM[1], MARY-JANE STABA[2], L. PHILIP SCHUMM[3], KARIN SCHREIBER[4], HANS SCHREIBER[4], DONALD W. KUFE[5] and RALPH R. WEICHSELBAUM[1]

Departments of [1]Radiation and Cellular Oncology, [2]Pediatrics, [3]Health Studies, [4]Pathology, University of Chicago, Chicago, IL 60637; [5]Cancer Pharmacology, Dana Farber Cancer Institute, Harvard Medical School, Boston, MA 02115, USA

Received July 19, 1999; Accepted August 10, 1999

Abstract. Ionizing radiation (IR) is frequently unsuccessful in the treatment of cancer because of local failure or distant metastases. The efficacy of systemically administered cytokines for cancer therapy is often limited by toxicity. We report that intratumoral injection of an adenoviral vector with interleukin-12 (IL-12) enhances local anti-tumor effects of irradiation (IR). We demonstrate that microscopic tumor growth at a distant site is suppressed following treatment of the primary tumor with adeno-murine IL-12 (Adm.IL-12). The results support a model in which the anti-angiogenic effects of IL-12 contribute to the local anti-tumor effects of radiation, while IL-12 induced immunity suppresses growth of microscopic tumors distant from the primary irradiated site. These data suggest that combining radiotherapy with IL-12 improves both local and distant tumor control compared to either treatment alone. Immunoradiotherapy may be employed in addition to or in place of current conventional therapies to increase local control and decrease distant tumor growth.

Introduction

Radiation therapy, an important method of treating localized human cancer, is frequently unsuccessful because of large tumor cell burden, micro-environmental factors and/or intrinsic cellular mechanisms that contribute to radioresistance (1,2). Physical modification in radiotherapy delivery or combination with chemotherapeutic agents are current modalities under clinical investigation to treat radioresistant tumors (1,3). Limitations of conventional treatment modifications include increases in toxicity with relatively small increments in tumor control. By contrast, recent studies have demonstrated that anti-angiogenic strategies combined with radiotherapy increase tumor cell kill without increasing toxicity (4,5).

Adjuvant chemotherapy is delivered before the development of clinically evident metastases. This approach has proven effective in the treatment of different pediatric tumors (6) and in the management of certain adult tumors (7). However, resistant histologies or large subclinical tumor burdens limit the efficacy of adjuvant chemotherapy. Therefore, improvements in adjuvant therapy are needed.

Immunization against putative tumor associated antigens is under development for the treatment of micrometastasis. One method of immunization is local intratumoral delivery of genes encoding cytokines or costimulatory molecules to induce specific anti-tumor immunity and circumvent systemic toxicity (8). IL-12 is a heterodimeric cytokine (9) that is produced primarily by antigen presenting cells (APCs) and plays an important role in mediating immune response (10). Mechanisms of action of IL-12 include stimulation of $CD4^+$, $CD8^+$ and natural killer cells. IL-12 also increases the production of IFN-γ by natural killer and T cells (11). Studies in animals and the results of human clinical trials suggest that IL-12 activated $CD8^+$ T cells play a crucial role in anti-tumor immunity (12,13). IL-12 is also reported to possess anti-angiogenic activity mediated by induction of IFN-γ (14). However, human trials administering IL-12 alone as an anti-tumor agent have to date been unsuccessful.

We reasoned that IL-12 might enhance the local anti-tumor effects of IR as a consequence of anti-angiogenic effects. IL-12 could also suppress tumors distant from the irradiated primary site by inducing the anti-tumor immunity. To test these hypotheses, we used as a model the poorly immunogenic syngeneic mouse tumor AG104A (15) and administered fractionated radiotherapy and an adenoviral expression vector (Ad.mIL-12) that can infect host tumor cells and provide high concentrations of IL-12 following local delivery.

Materials and methods

Cell culture. Spontaneously appearing murine fibrosarcoma cells (15), (AG104A of C3H/HeN (MTV) origin from Dr Hans Schreiber) were maintained without passage in Dulbecco's

Correspondence to: Professor Ralph R. Weichselbaum, Department of Radiation and Cellular Oncology, University of Chicago, Chicago, IL 60637, USA

Key words: fibrosarcoma, gene therapy, cytokines, anti-angiogenic

modified Eagle medium (Gibco), 10% fetal calf serum (Intergen) and 1% penicillin/streptomycin (Gibco).

Adenoviral vector. Construction and characterization of a recombinant type 5 adenoviral vector (Ad5) expressing murine IL-12 (Dr Donald Kufe) have been previously described (13). The E1a region was replaced with a bicistronic expression cassette consisting of the murine cDNAs for the p35 and p40 subunits of IL-12. Expression was driven by an internal ribosomal entry site sequence from the encephalomyocarditis virus and the SV40 polyadenylation signal under the control of cytomegalovirus immediate early promoter and enhancer. Ad.mIL-12 vector was propagated on 293 cells and purified (16).

Growth of AG104A tumors and treatment. AG104A cells ($5x10^6$ cells in 100 µl PBS) were injected subcutaneously (s.c.) into the right hind limbs of female C3H/HeN (MTV) mice (Frederick Cancer Research Institute). Tumor volume was measured directly with calipers and calculated biweekly from the formula (length x width x height/2) and reported as fractional tumor volume ± SEM. When the tumors reached an average volume of 217 mm^3 (SD = 102) treatment was initiated. Animals were divided into the following treatment groups so that the mean tumor volumes were roughly equivalent: control (untreated), IR alone, Ad.mIL-12 alone, Ad.null with IR and Ad.mIL-12 with IR. Mice were injected intratumorally with $5x10^9$ plaque forming units (PFU) of Ad.mIL-12 or Ad5 (Ad.null) virus on day 0, 4 h before radiation. Tumors were radiated with 5 Gy/day, for 5 days to a total of 25 Gy using a Maxitron generator, 150 kV, 30 mA at 1.88 Gy/min. The care and treatment of all experimental animals was in accordance with institutional guidelines.

Immunohistochemistry. At days 3, 7 and 21 tumors from untreated and treated animals were excised and fixed in 10% neutral formalin. After embedding in paraffin, 5 µm sections were cut and mounted. Briefly, sections were dried, deparaffinized and rehydrated. After quenching endogenous peroxidase activity and blocking with bovine serum albumin, slides were incubated at 4°C overnight with a 1:50 dilution of rat anti-mouse $CD31^+$ monoclonal antibody (Pharmingen) and were incubated for 1 h with biotinylated rabbit anti-rat immunoglobulin (Vector Laboratories).

Blood vessels were visualized using the Vectastain elite ABC kit, Vector PK-6100 (Vector). Slides were dipped in 0.125% osmium tetroxide (Sigma) to enhance positivity and counterstained with 1% methyl green (Trevigen). Ten high power fields (x400) were examined using a Nikon Microphot-FX microscope equipped with a Sony digital camera. Vessels were counted using Macintosh Image Pro-Plus Imaging software.

Bilateral AG104A tumor studies. A subset of the animals described above were also injected with AG104 A cells ($5x10^6$ cells in 100 µl) into the left hind limbs concurrently on the first day of treatment administered to the right limb. Left limb tumor volumes were measured for 35 days. Tumor induction rates were defined as the number of measurable left limb

Rechallenge studies. AG104A right limb tumor bearing mice were treated as described above. Two different rechallenge studies were performed. i) Sixty days after complete regression of primary right limb tumors mice were injected with $5x10^6$ AG104A cells in 100 µl PBS in the opposite limb. Mice were observed for tumor regrowth and survival for 160 days. ii) To determine whether $CD8^+$ lymphocytes mediated the anti-tumor immunity, mice successfully treated with Ad.mIL-12 and radiation were depleted of $CD8^+$ T cells. The anti-$CD8^+$ (anti-lyt.2) producing hybridoma YTS 169.4 (17) (from Dr Hans Schreiber) was used to deplete $CD8^+$ lymphocytes. Twenty-five days after complete regression of the primary tumor mice were injected intraperitoneally (i.p.) with 0.2 ml conditioned medium from cultured hybridoma (n=3). On day 4, mice were injected with $1x10^5$ AG104A cells in their left hind limbs. An additional dose of 0.2 ml conditioned medium was injected i.p. on day 7. Control mice were treated with control antibody (n=3). Mice were observed for tumor regrowth for 30 days.

Data analysis. Right limb tumor volumes were converted to fractional tumor volumes (volume/volume at start of treatment) and plotted as mean ± SEM for each treatment group. Comparisons between groups were performed on day 21 using Wilcoxon's rank sum test since untreated control animals were killed after day 21. In addition, complete regression rates (defined as zero volume) on day 60 were compared between groups using Fisher's exact test. Average vessel counts were transformed using natural logarithms and analyzed using ANOVA, including treatment group and day as covariates. For the bilateral studies a linear regression model was fit to the data starting on day 10, permitting both the day 10 volume and the rate of change thereafter to vary depending upon the treatment administered to the tumor in the right limb. The model was fit using the Generalized Estimating Equations Approach (18). The correlation between measurements on the same animal was assumed to be that of a first order autoregressive process, however standard errors were estimated using the sandwich estimator and are therefore valid even if the true correlation structure deviates from this assumption. Induction rates (defined as the proportion of animals with non-zero volumes) on day 35 were analyzed using logistic regression (19), using radiation and Ad.mIL-12 as binary covariates. Estimates are presented as odds [p/(1-p)] ratios. All p-values reported are two sided.

Results

To determine whether concurrent delivery of Ad.mIL-12 with radiation increases local anti-tumor effects, we treated mouse hind limb AG104A tumors with intratumoral injection of Ad.mIL-12 and fractionated radiation. Mice were sacrificed at 60 days after starting treatment and/or when hind limb tumor volumes measured greater than 2500 mm^3. Untreated control tumors grew to a mean volume of 2500 mm^3 by day 21. No spontaneous tumor regressions were observed. Ad.mIL-12 inhibited tumor growth both when administered alone ($p<0.001$ on day 21) and when administered in conjunction with IR ($p<0.001$ on day 21), whereas the addition of IR to Ad.null

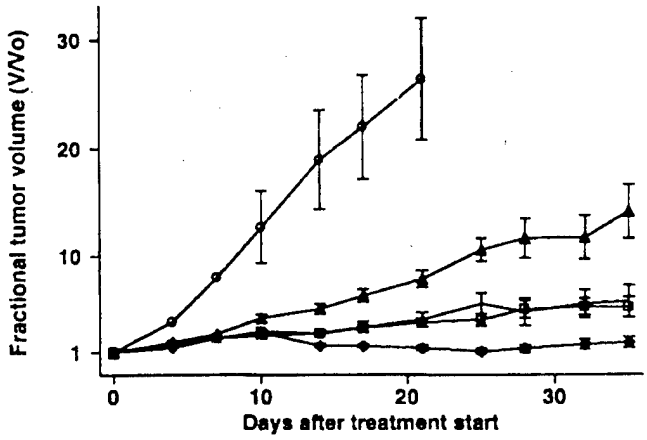

Figure 1. Antitumor activity of Ad.mIL-12 on AG104A tumors. AG104A ($5x10^6$ cells in 100 µl PBS) were injected subcutaneously into the right hind limbs of female C3H/HeN(MTV) mice. Tumor volumes were measured biweekly throughout the study. Tumors were treated with IR alone, Adm.IL-12 alone, Ad.null plus IR or Ad.mIL-12 plus IR. Mean fractional tumor volume ± SEM is reported. Untreated control, circle; IR alone, square; Adm.IL-12 alone, triangle; Ad.null plus IR, no symbol; Adm.IL-12 plus IR, diamond. Controls were sacrificed after day 21. The proportion of mice remaining on day 35 was 0.86, IR alone; 0.66, Adm.IL-12 alone; 0.93, Ad.null plus IR; 0.96, Adm.IL-12 plus IR.

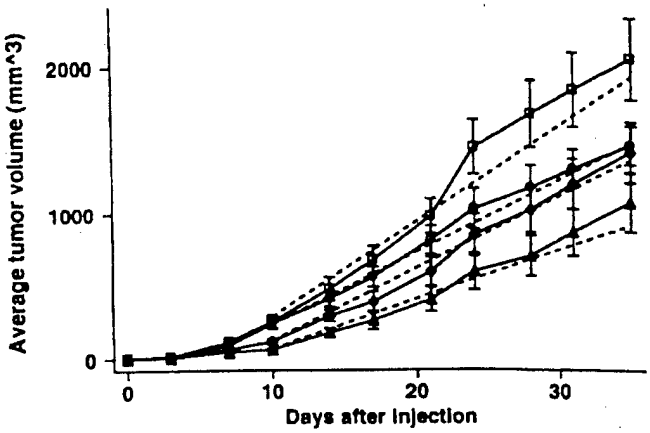

Figure 2. Distant tumor control by Ad.mIL-12. Mice were injected with AG104A cells into the left hind limbs concurrently on the first day of treatment administered to the right limb. Bilateral tumor volumes were measured for 35 days and calculated as described in Materials and methods. Mean tumor volume ± SEM in left limb is reported. Dashed lines indicate fitted values from linear regression model. Control, circle; IR alone, square; Adm.IL-12 alone, triangle; Adm.IL-12 plus IR, diamond.

Table I. Tumor regression and induction rates.

Treatment group	Day 60 Right limb Regression rate	Day 35 Left limb Induction rate
Control	0/39	19/19
Ad.mIL-12	11/51	14/21
IR	14/53	19/21
Ad.null plus IR	3/14	
Ad.mIL-12 plus IR	26/44	16/21

Right limb tumors were grown and treated as described in Materials and methods. Tumors were measured biweekly throughout the study. Complete regression rates (defined as zero volume) on day 60 were computed including the number of tumors with volume equal to zero divided by the number of mice in each group. Induction rates for the untreated left limb tumors were calculated by dividing the number of measurable left limb tumors by the number of mice in each group on day 35.

are presented in Table I. The addition of Ad.mIL-12 increased the regression rate compared to that of IR alone (p=0.002). The rate for Ad.mIL-12 plus radiation was higher than that of Ad.null plus IR (p=0.029). Taken together, these data indicate that the anti-tumor effects of Ad.mIL-12 increase the efficacy of IR in achieving local tumor control.

To study the mechanistic basis for the effects of IL-12 and radiation, we assessed the effects on angiogenesis with anti-CD31 staining of AG104A tumor sections. Histopathology of tumor sections at days 3, 7 and 21 (Table II) revealed a decrease in the vascularity of tumors treated with Ad.mIL-12 as compared to control ($p<0.001$) and those treated with Ad.mIL-12 and IR as compared to IR alone (p=0.001). These results suggest that Ad.mIL-12 inhibits angiogenesis and thereby contributes to significant tumor regression.

Because IL-12 stimulates immune responses, we determined if injection of Ad.mIL-12 into AG104A tumors induces a therapeutic effect against microscopic tumors at distant sites. A subset of animals were concurrently injected with $5x10^6$ AG104A cells into the left limb as described above. Mice were sacrificed when either hind limb tumor volume measured greater than 2500 mm^3. Table I shows the number of animals in each group that developed detectable left hind limb tumors by day 35. Based on a logistic regression model, Ad.mIL-12 reduced the odds of tumor induction by 87% (p=0.011) whereas IR had no effect (p=0.975).

A linear regression was fit to the mean tumor volume starting on day 10 (Fig. 2). Based on this model, Ad.mIL-12 reduced the average day 10 volume by 165 mm^3 ($p<0.001$), and reduced the growth rate thereafter by 16 mm^3/day (p=0.030). These results suggest that the extent of IL-12 production in the treated tumor is a determinant for suppression of distant tumor growth.

To determine whether successfully cured mice develop long-term immunity, we rechallenged tumor-free mice with $5x10^6$ AG104A cells into the opposite limb 60 days after complete primary tumor regression. Mice were observed for tumor growth for an average of 160 days. None of the 9 (0%) animals treated with Ad.mIL-12 alone and only 4 of 15 (27%) animals treated with Ad.mIL-12 plus radiation demonstrated tumor growth by day 29. By contrast, tumors were induced in

Table II. Effect of combining Ad.mIL-12 with IR on tumor vasculature.

Treatment group	Days after start of treatment 3	7	21
Control	6.5	7.3	7.9
	(1.6)	(6.8)	(3.5)
Adm.IL-12	8.2	5.0	3.7
	(0.5)	(1.9)	(0.9)
IR	4.1	6.0	7.0
	(1.1)	(0.5)	(1.2)
Ad.null[a] plus IR	5.9	4.8	4.2
Adm.IL-12 plus IR	3.2	5.1	2.3
	(0.6)	(1.7)	(0.3)

Representative tumor sections from 3 mice/treatment/day were processed and visualized as described in Materials and methods. Ten high power fields were counted and average number of vessels per field is reported. Numbers in parentheses indicate standard deviation (n=3). [a]Only one animal/treatment/day was examined.

6 of 6 (100%) animals that had irradiated primary tumors, and 3 of 3 (100%) animals with tumors treated with Ad.null plus radiation. These findings support the establishment of anti-tumor immunity as a consequence of local Ad.mIL-12 treatment.

To further assess whether the tumor rejection following treatment with Ad.mIL-12 results in a $CD8^+$ T cell mediated immune response, we depleted $CD8^+$ lymphocytes in 3 mice that had been successfully treated with Ad.mIL-12 plus radiation. Tumors developed in all $CD8^+$ depleted animals 7 days after inoculation of $1x10^5$ AG104A cells, while mice injected with control antibody failed to develop tumors. Our results demonstrate that IL-12 induces a potent local and distant anti-tumor effects through $CD8^+$ dependent immunity.

Discussion

The present results suggest that Ad.mIL-12 enhances anti-tumor effects of IR by suppression of tumor angiogenesis. Considering that IL-12 is anti-angiogenic (14) and IR alone does not target the tumor vasculature (4,20) the study supports a model whereby IL-12 targets the tumor vessels through the production of IFN-γ and IR targets the tumor cells. Induction of anti-tumor immunity as demonstrated by tumor rechallenge studies suggest that IL-12 may also increase the local anti-tumor effects of IR by an immune response. The enhanced activates T and NK cells it could also induce macrophage activation through the induction of IFN-γ. Local endogenous production of mIL-12 by activated macrophages may act as a feedback mechanism on tumor associated NK and T cells to promote increased cell killing which would be enhanced by IR induced cell injury (21). The potent anti-tumor interaction of IL-12 and IR when delivered by an adenoviral vector is achieved with no increase in toxicity compared with IR alone. In contrast, clinical trials in humans have demonstrated substantial toxicity with systemically administered IL-12. These data are of importance since 20-30% of all cancer patients die of local failure as well as experience substantial morbidity (22).

Data demonstrating minimal tumor regrowth in animals cured following treatment with Ad.mIL-12 alone or with IR and tumor regrowth following $CD8^+$ depletion strongly support the induction of anti-tumor immunity in animals treated with Ad.mIL-12. These data are consistent with the finding that greater production of IL-12 confers more effective anti-tumor activity against tumor growth in the contralateral limb. Our data, therefore, provide support for a strategy of tumor vaccination whereby both local control and microscopic distant tumor growth are suppressed, without increases in host toxicity by transduction of tumor cells with Ad.mIL-12. Our results support a paradigm shift for the use of immuno-therapy and radiation therapy whereby genetic constructs are introduced into primary tumors in patients undergoing therapeutic radiation. This model for adjuvant immuno-radiotherapy may provide improvements in control of both local and micrometastatic tumors compared to conventional treatments.

Acknowledgments

This work was supported by NCI grant CA 41068-10, as well as grant from Varian Inc., California and a gift from the Passis family. SS, MJS and RRW thank Dr S. Hellman for helpful discussions.

References

1. Hellman S: Principles of cancer management: radiation therapy. In: Cancer, Principles and Practice of Oncology. 5th edition. DeVita VT Jr, Hellman SA and Rosenberg SA (eds). Lippincott-Raven Publ., New York, pp307-332, 1997.
2. Weichselbaum RR, Dahlberg W and Little JB: Inherently radioresistant cells exist in some human tumors. Proc Natl Acad Sci USA 82: 4732-4735, 1985.
3. Tannock IF: Conventional cancer therapy: promise broken or promise delayed? Lancet 351: SII 9-16, 1998.
4. Mauceri HJ, Hanna NN, Beckett MA, Gorski DH, Staba MJ, Stellato KA, Bigelow K, Heimann R, Gately S, Dhanabal M, Soff GA, Sukhatme VP, Kufe DW and Weichselbaum RR: Combined effects of angiostatin and ionizing radiation in antitumour therapy. Nature 394: 287-291, 1998.
5. Teicher BA, Sotomayor EA and Huang ZD: Antiangiogenic agents potentiate cytotoxic cancer therapies against primary and metastatic disease. Cancer Res 52: 6702-6704, 1992.
6. Meyers PA, Gorlick R, Heller G, Casper E, Lane J, Huvos AG and Healey JH: Intensification of preoperative chemotherapy for osteogenic sarcoma: results of the Memorial Sloan-Kettering (T12) protocol. J Clin Oncol 16: 2452-2458, 1998.
7. Bonadonna G, Brusamolino E, Valagussa P, Rossi A, Brugnatelli L, Brambilla C, De Lena M, Tancini G, Bajetta E, Musumeci R and Veronesi U: Combination chemotherapy as an

8. Pardoll DM: Paracrine cytokine adjuvants in cancer immunotherapy. Annu Rev Immunol 13: 399-415, 1995.
9. Kobayashi M, Fitz L, Ryan M, Hewick RM, Clark SC, Chan S, Loudon R, Sherman F, Perussia B and Trinchieri G: Identification and purification of natural killer cell stimulatory factor (NKSF), a cytokine with multiple biologic effects on human lymphocytes. J Exp Med 170: 827-845, 1989.
10. Trinchieri G: Interleukin-12 and its role in the generation of TH1 cells. Immunol Today 14: 335-338, 1993.
11. Trinchieri G: Interleukin-12 and interferon-gamma. Do they always go together? Am J Pathol 147: 1534-1538, 1995.
12. Brunda MJ, Luistro L, Warrier RR, Wright RB, Hubbard BR, Murphy M, Wolf SF and Gately MK: Antitumor and antimetastatic activity of interleukin 12 against murine tumors. J Exp Med 178: 1223-1230, 1993.
13. Chen L, Chen D, Block E, O'Donnel M, Kufe DW and Clinton SK: Eradication of murine bladder carcinoma by intratumor injection of a bicistronic adenoviral vector carrying cDNAs for the IL-12 heterodimer and its inhibition by the IL-12 p40 subunit homodimer. J Immunol 159: 351-359, 1997.
14. Voest EE, Kenyon BM, O'Reily MS, Truitt G, D'Amato RJ and Folkman J: Inhibition of angiogenesis *in vivo* by interleukin 12. J Natl Cancer Inst 87: 581-587, 1995.
15. Ward PL, Koeppen H, Hurteau T and Schreiber H: Tumor antigens defined by cloned immunological probes are highly polymorphic and are not detected on autologous normal cells. J Exp Med 170: 217-232, 1989.
16. Hitt M, Bett AJ, Prevec L and Graham FL: Construction and Propagation of Human Adenovirus Vectors. Academic Press, San Diego, pp479-490, 1994.
17. Cobbold SP, Jayasuriya A, Nash A, Prospero TD and Waldmann H: Therapy with monoclonal antibodies by elimination of T cell subsets *in vivo*. Nature 312: 548-550, 1984.
18. Liang KY and Zeger SL: Longitudinal data analysis using generalized linear models. Biometrika 73: 13-22, 1986.
19. Cox DR and Snell EJ: Analysis of Binary Data. 2nd edition. Chapman and Hall, New York, 1989.
20. Budach W, Taghian A, Freeman J, Gioioso D and Suit HD: Impact of stromal sensitivity on radiation response of tumors. J Natl Cancer Inst 85: 988-993, 1993.
21. Teicher BA, Ara G, Buxton D, Leonard J and Schaub RG: Optimal scheduling of interleukin-12 and fractionated radiation therapy in the murine Lewis lung carcinoma. Radiat Oncol Investig 6: 71-80, 1998.
22. Perez CA and Brady LW: Principles and Practice of Oncology. 3rd edition. Lippincott-Raven Publ., New York, 1998.

[CANCER RESEARCH 60, 2520–2526, May 1, 2000]

Anti-angiogenic Cues from Vascular Basement Membrane Collagen[1]

Pablo C. Colorado, Adriana Torre, George Kamphaus, Yohei Maeshima, Helmut Hopfer, Keiko Takahashi, Ruediger Volk, Eric D. Zamborsky, Seth Herman, Pradip K. Sarkar, Mark B. Ericksen, Mohanraj Dhanabal, Michael Simons, Mark Post, Donald W. Kufe, Ralph R. Weichselbaum, Vikas P. Sukhatme, and Raghu Kalluri[2]

Department of Medicine and the Cancer Center, Beth Israel Deaconess Medical Center and Harvard Medical School [P. C. C., A. T., G. K., Y. M., H. H., K. T., R. V., E. D. Z., S. H., P. K. S., M. B. E., M. D., M. S., M. P., V. P. S., R. K.], and Dana Farber Cancer Institute and Harvard Medical School [D. W. K.], Boston, Massachusetts 02215, and Department of Radiation and Cellular Oncology, University of Chicago, Chicago, Illinois 60637 [R. R. W.]

ABSTRACT

Vascular basement membrane is an important structural component of blood vessels and has been shown to interact with and modulate vascular endothelial behavior during angiogenesis. During the inductive phase of tumor angiogenesis, this membrane undergoes many degradative and structural changes and reorganizes to a native state around newly formed capillaries in the resolution phase. Such matrix changes are potentially associated with molecular modifications that include expression of matrix gene products coupled with conformational changes, which expose cryptic protein modules for interaction with the vascular endothelium. We speculate that these interactions provide important endogenous angiogenic and anti-angiogenic cues. In this report, we identify an important anti-angiogenic vascular basement membrane-associated protein, the 26-kDa NC1 domain of the α_1 chain of type IV collagen, termed arresten. Arresten was isolated from human placenta and produced as a recombinant molecule in *Escherichia coli* and 293 embryonic kidney cells. We demonstrate that arresten functions as an anti-angiogenic molecule by inhibiting endothelial cell proliferation, migration, tube formation, and Matrigel neovascularization. Arresten inhibits the growth of two human xenograft tumors in nude mice and the development of tumor metastases. Additionally, we show that the anti-angiogenic activity of arresten is potentially mediated via mechanisms involving cell surface proteoglycans and the $\alpha_1\beta_1$ integrin on endothelial cells. Collectively, our results suggest that arresten is a potent inhibitor of angiogenesis with a potential for therapeutic use.

INTRODUCTION

The development of new blood vessels from preexisting ones is generally referred to as angiogenesis (1). In the adult, new blood vessels arise via angiogenesis, a process critical for normal physiological events such as wound repair, the menstrual cycle, and endometrium remodeling (2). In the last three decades, considerable research has been conducted documenting that tumor growth and metastasis require angiogenesis (3). This process is pivotal to the survival and subsequent growth of solid tumors beyond a few cubic millimeters in size (4). Vascular basement membrane constitutes an insoluble structural wall of newly formed capillaries and undergoes several changes during tumor-induced angiogenesis (5). Initially, the membrane is degraded and disassembled but is finally reorganized to a native state around a newly formed capillary (5). Such vascular matrix changes during angiogenesis are associated with the expression of matrix proteins that can interact with vascular endothelium and provide endogenous angiogenic and anti-angiogenic signals (5). Basement membranes are composed of macromolecules such as type IV collagen, laminin, HSPGs,[3] fibronectin, and entactin (6). Type IV collagen is composed of six genetically distinct gene products, namely, α_1–α_6 (7). The α_1 and α_2 isoforms are ubiquitously present in human basement membranes (8). The other four isoforms exhibit restricted distributions (9). Type IV collagen promotes cell adhesion, migration, differentiation, and growth (8). It is thought to play a crucial role in endothelial cell proliferation and behavior during the angiogenic process (5). Several studies have shown the anti-angiogenic properties associated with inhibitors of collagen metabolism, supporting the notion that basement membrane collagen synthesis and deposition are crucial for blood vessel formation and survival (10). Additionally, the COOH-terminal globular NC1 domain of type IV collagen is speculated to play an important role in the assembly of type IV collagen suprastructure, basement membrane organization, and modulation of cell behavior (11, 12). Recently, the NC1 domain of the α_2 chain of type IV collagen (canstatin) was identified as an angiogenesis inhibitor (13) In the present study, we demonstrate the pivotal role of arresten, the NC1 domain of the α_1 chain of type IV collagen, in modulating the function of capillary endothelial cells and blood vessel formation using *in vitro* and *in vivo* models of angiogenesis and tumor growth.

MATERIALS AND METHODS

Recombinant Production of Arresten in *Escherichia coli*. The sequence encoding arresten was amplified by PCR from the α_1 NC1 (IV)/pDS vector (14) using a forward primer (5′-CGGGATCCTTCTGTTGATCACGGCTTC-3′) and a reverse primer (5′-CCCAAGCTTTGTTCTTCTCATACAGAC-3′). The resulting cDNA fragment was digested with *Bam*HI and *Hind* III and ligated into predigested pET22b(+) (Novagen, Madison, WI). This placed arresten downstream of and in frame with the pelB leader sequence, allowing for periplasmic localization and expression of soluble protein. Additional vector sequence was added to the protein encoding amino acids MDIGINSD. The 3′ end of the sequence was ligated in frame with the polyhistidine tag sequence. Additional vector sequence between the 3′ end of the cDNA and the his tag encoded the amino acids KLAAALE. Positive clones were sequenced on both strands.

Plasmid constructs encoding arresten were first transformed into *E. coli* HMS174 (Novagen) and then transformed into BL21 for expression (Novagen). Overnight bacterial culture was used to inoculate a 500-ml culture in Luria-Bertani medium. This culture was grown for ~4 h until the cells reached an A_{600} of 0.6. Then, protein expression was induced by addition of isopropyl-1-thio-β-D-galactopyranoside to a final concentration of 1–2 mM. After a 2-h induction, cells were harvested by centrifugation at 5,000 × *g* and lysed by resuspension in 6 M guanidine, 0.1 M NaH_2PO_4, and 0.01 M Tris-HCl (pH 8.0). Resuspended cells were sonicated briefly, and centrifuged at 12,000 × *g* for 30

Received 12/22/99; accepted 3/1/00.

The costs of publication of this article were defrayed in part by the payment of page charges. This article must therefore be hereby marked *advertisement* in accordance with 18 U.S.C. Section 1734 solely to indicate this fact.

[1] Supported in part by NIH Grants DK-51711 and DK-55001 (to R. K.) and R01-CA-42596-12 (to R. W.), Deutsche Forschungsgemeinschaft Grant HO 2138/1-1 (to H. H.), a 1998 Hershey Prostate Cancer Research Award (to R. K.), a 1998 American Society of Nephrology Carl Gottschalk Research Award (to R. K.), a 1998 National Kidney Foundation Murray award (to R. K.). a 1998 Beth Israel Deaconess Medical Center Enterprise Award (to R. K.), and research funds from the Beth Israel Deaconess Medical Center. M. D., G. K., R. R. W., D. W. K., V. P. S., and R. K. have an equity position with Ilex Oncology, a company that is clinically developing arresten.

[2] To whom requests for reprints should be addressed, at Nephrology Division, Department of Medicine, RW 563a, Beth Israel Deaconess Medical Center, 330 Brookline Avenue, Boston, MA 02215. Phone: (617) 667-0445; Fax: (617) 975-5663; E-mail: rkalluri@caregroup.harvard.edu.

[3] The abbreviations used are: HSPG, heparan sulfate proteoglycan; HPLC, high-performance liquid chromatography; HPEC, human prostate epithelial cell; bFGF, basic fibroblast growth factor; VEGF, vascular endothelial growth factor; PCNA, proliferating cell nuclear antigen; HUVEC, human umbilical vein endothelial cell; CPAE, calf pulmonary arterial endothelial.

min. The supernatant fraction was passed over a 5-ml Ni-nitrilotriacetic acid-agarose column (Qiagen, Chatsworth, CA) four to six times at a speed of 2 ml/min. Nonspecifically bound protein was removed by washing with both 10 and 25 mM imidazole in 8 M urea, 0.1 M NaH_2PO_4, and 0.01 M Tris-HCl (pH 8.0). Arresten protein was eluted from the column with increasing concentrations of imidazole (50, 125, and 250 mM) in 8 M urea, 0.1 M NaH_2PO_4, and 0.01 M Tris-HCl (pH 8.0). The eluted protein was dialyzed twice against PBS at 4°C. A minor portion of the total protein precipitated during dialysis. Dialyzed protein was collected and centrifuged at ~3,500 × *g* and separated into pellet and supernatant fractions. Protein concentration in each fraction was determined by the bicinchoninic acid assay (Pierce, Rockford, IL) and quantitative SDS-PAGE analysis. The fraction of total protein in the pellet was ~22%, with the remaining 78% recovered as a soluble protein. The total yield of protein was approximately 10 mg/liter.

Recombinant Production of Endostatin in Yeast. Mouse endostatin was produced in *Picchia pastoris* and purified as described previously (15).

Expression of Arresten in 293 Embryonic Kidney Cells. We used the pDS plasmid containing α_1(IV)NC1 (14) to PCR amplify arresten in a way that it would add a leader signal sequence in frame into the pcDNA 3.1 (Invitrogen, Carlsbad, CA) eukaryotic expression vector. The leader sequence from the 5′ end of the full-length α_1(IV) chain was cloned 5′ to the NC1 domain to enable protein secretion into the culture medium. The arresten-containing recombinant vectors were sequenced using flanking primers. Error-free cDNA clones were further purified and used for *in vitro* translation studies to confirm protein expression (data not shown). The arresten-containing plasmid and control plasmid were used to transfect 293 cells using the calcium chloride method. Transfected clones were selected by Geneticin (Life Technologies, Inc., Gaithersburg, MD) antibiotic treatment. The cells were passed for 3 weeks in the presence of the antibiotic until no cell death was evident. Clones were expanded into T-225 flasks and grown until confluent. Then, the supernatant was collected and concentrated using an Amicon (Beverly, MA) concentrator. The concentrated supernatant was analyzed by SDS-PAGE, immunoblotting, and ELISA for arresten expression. Strong binding in the supernatant was detected by ELISA (data not shown). The arresten-containing supernatant was subjected to affinity chromatography using arresten-specific antibodies (14). Arresten antibody was generated to a purified protein as described previously (14). This antibody recognized only the α_1 NC1 domain (14). A major peak was identified, containing a monomer of ~30 kDa that was immunoreactive with arresten antibodies.

Isolation of Native Arresten. Native arresten from human placenta was isolated using bacterial collagenase, anion exchange chromatography, gel filtration chromatography, HPLC, and affinity chromatography (6, 14). Type IV collagen monomers isolated from human placenta were HPLC purified using a C-18 hydrophobic column.

Inhibition of Endothelial Cell Proliferation. CPAE cells were grown to confluence in DMEM with 10% FCS and kept contact inhibited for 48 h. Human renal cell carcinoma cells (786-0; data not shown), PC-3 cells (human prostate adenocarcinoma), HPECs, and A-498 (renal carcinoma) cells (data not shown) were used as controls in this experiment. Cells were harvested by trypsinization (Life Technologies) at 37°C for 5 min. A suspension of 12,500 cells in DMEM with 1% FCS was added to each well of a 24-well plate coated with 10 μg/ml fibronectin. The cells were incubated for 24 h at 37°C with 5% CO_2 and 95% humidity. The medium was removed and replaced with DMEM containing 0.5% FCS and 3 ng/ml bFGF (R&D Systems, Inc., Minneapolis, MN). Unstimulated controls received no bFGF. Cells were treated with concentrations of arresten or endostatin ranging from 0.01 to 50 μg/ml. All wells received 1 μCi of [^{3}H]thymidine at the time of treatment. After 24 h the medium was removed, and the wells were washed with PBS. Cells were extracted with 1 N NaOH and added to a scintillation vial containing 4 ml of ScintiVerse II (Fisher Scientific, Springfield, NJ) solution. Thymidine incorporation was measured using a scintillation counter. All groups represent triplicate samples.

Cell Cycle Analysis. Cell cycle analysis was performed as reported previously (16). Briefly, CPAE cells were grown to confluence in DMEM containing 10% FBS and growth arrested by contact inhibition for 48 h. A suspension of 500,000 cells was seeded in each well of a six-well plate in DMEM containing 1% FBS and 5 ng/ml VEGF. Different doses of arresten were added, and the cells were harvested 18 h after treatment. Cells were fixed in ice-cold 95% ethanol and rehydrated 3 h later at room temperature for 30 min in rehydration buffer (2% FBS and 0.1% Tween 20 in PBS). Next, the cells were centrifuged at 1,200 rpm for 10 min and resuspended in 0.5 ml of rehydration buffer. RNase was added at 5 μg/ml and allowed to incubate for 1 h at 37°C, followed by staining with propidium iodide at 5 μg/ml. The data were analyzed using a Becton Dickinson (San Jose, CA) FACStar plus flow cytometer. The percentage of cells in S phase was calculated using ModFit software.

Endothelial Tube Assay. Matrigel (Collaborative Biomolecules, Bedford, MA) was added (320 μl) to each well of a 24-well plate and allowed to polymerize (17). A suspension of 25,000 mouse aortic endothelial cells in EGM-2 (Clonetics, Inc., Walkersfield, MD) medium without antibiotic was passed into each well coated with Matrigel. The cells were treated with arresten, BSA, sterile PBS, or 7S domain in increasing concentrations. All assays were performed in triplicate. Cells were incubated for 24–48 h at 37°C and viewed using an Olympus Optical (Tokyo, Japan) CK2 microscope (3.3 ocular, 10× objective). The cells were then photographed using 400 DK-coated TMAX film (Eastman Kodak, Rochester, NY). Cells were stained with Diff-Quik fixative (Sigma Chemical Co., St. Louis, MO) and photographed again (17). Ten fields were viewed, and tubes were counted and averaged.

Matrigel Assay. Matrigel was thawed overnight at 4°C. Before injection into C57BL/6 mice it was mixed with 20 units/ml heparin (Pierce), 150 ng/ml bFGF (R&D Systems), and either 1 μg/ml arresten or 10 μg/ml endostatin. Control groups received no angiogenic inhibitor. The Matrigel mixture was injected s.c. using a 21-gauge needle. After 14 days, mice were sacrificed, and the Matrigel plugs were removed. Matrigel plugs were fixed in 4% paraformaldehyde (in PBS) for 4 h at room temperature and then switched to PBS for 24 h. The plugs were embedded in paraffin, sectioned, and H&E stained. Sections were examined by light microscopy, and the number of blood vessels from 10 high-power fields was counted and averaged.

Inhibition of Tumor Metastases. C57BL/6 mice were i.v. injected with 1 million MC38/MUC1 cells. Controls (five mice) received sterile PBS, and the experimental group (six mice) received 4 mg/kg arresten every other day for 26 days. Pulmonary tumor nodules were counted for each mouse in both groups and averaged after 26 days of treatment. Two deaths were recorded in each group.

***In Vivo* Tumor Studies.** Human renal cell carcinoma cells (786-0) were maintained in DMEM with 10% FCS until confluent. The cells were harvested, and 2 million were injected into 7- to 9-week-old athymic nude mice. The tumors were allowed to grow to ~700 or 100 mm^3. Arresten was injected i.p. daily at a dosage of 10 or 20 mg/kg. Control groups received either BSA or the PBS vehicle daily. Human prostate adenocarcinoma cells (PC-3) were maintained in F12K medium with 10% FCS until confluent. The cells were harvested, and 5 million were injected into 7- to 9-week-old male athymic nude mice. The tumors grew to ~60 or 200 mm^3. The mice were injected daily with 10 or 4 mg/kg arresten or 20 mg/kg endostatin. Control groups received daily injections of PBS. In both experiments tumor volume was measured using the standard formula length × width^2 × 0.52 (18). Each group contained five or six mice.

Immunohistochemistry. Mice were sacrificed after 10–20 days of arresten treatment. Tumors were excised and fixed in 4% paraformaldehyde. Tissues were paraffin embedded, and 3-μm sections were cut and mounted on glass slides. Sections were deparaffinized, rehydrated, and treated with 300 mg/ml protease XXIV (Sigma) at 37°C for 5 min. Digestion was stopped with 100% ethanol, and sections were air dried and blocked with 10% rabbit serum. Then, slides were incubated at 4°C overnight with a 1:50 dilution of rat anti-mouse CD-31 monoclonal antibody (PharMingen, San Diego, CA), followed by two successive 30-min incubations at 37°C of 1:50 dilutions of rabbit anti-rat immunoglobulin and rat alkaline phosphatase anti-alkaline phosphatase (DAKO, Carpinteria, CA). The color reaction was performed with new fuchsin, and sections were counterstained with hematoxylin. Finally, blood vessels in 15 fields were counted, averaged, divided by the tumor volume, and plotted. For PCNA staining, tissue sections were incubated for 60 min at room temperature with a 1:200 dilutions of anti-PCNA antibody (Signet Laboratories, Inc., Dedham, MA). Detection was carried out according to the manufacturer's recommendations using the USA horseradish peroxidase system (Signet). Finally, the slides were counterstained with hematoxylin. Staining for fibronectin and type IV collagen was performed using polyclonal anti-fibronectin (Sigma) at a dilution of 1:500 and anti-type IV collagen (ICN, Costa Mesa, CA) at a dilution of 1:100. The Vectastain Elite ABC kit (Vector

Laboratories, Burlingame, CA) was used for detection according to the manufacturer's recommendations.

Scatchard Analysis. Scatchard analysis was performed as described previously (19). Briefly, CPAE cells were plated on a 96-well plate (10,000 cells per well) in DMEM with 10% FCS and grown to confluence. The cells were then washed with ice-cold PBS and incubated with 180 pmol of ^{125}I-arresten with and without increasing concentrations of unlabeled arresten ranging from 150 pmol to 100 nmol comprising a total of 27 data points. The cells were incubated with this mixture for 2 h at 4°C. Then, the cells were washed with ice-cold PBS and extracted with 1 N NaOH, and radioactivity was measured in a scintillation counter.

ELISA for HSPG. Direct ELISA was performed as described previously (9). HSPG (100 ng; Sigma) was coated on a 96-well plate in triplicate in a 2-fold molar excess of binding proteins arresten, bFGF, and BSA. Binding was established with antibodies to bFGF, arresten, and BSA. The ELISA was developed with an alkaline phosphatase secondary antibody and read in a plate reader at absorbance of 405 nm.

Cell Adhesion Assay. Ninety-six-well plates were coated with human arresten or human type IV collagen (Collaborative Biomolecules, Bedford, MA) at a concentration of 10 μg/ml or human vitronectin at 0.5 μg/ml overnight at 37°C. The remaining protein binding sites were blocked with 10% BSA (Sigma) in PBS for 2 h at 37°C. HUVECs were grown to subconfluence (70–80%) in EGM-2 MV medium (Clonetics). The cells were gently trypsinized and resuspended in serum-free medium (1.5×10^5 cells/ml). The cells were then mixed with 10 μg/ml antibody and incubated for 15 min with gentle agitation at room temperature. Next, 100 μl of the cell suspension were added to each well, and the plate was incubated for 45 min at 37°C with 5% CO_2. Unattached cells were removed by washing with serum-free medium, and attached cells were counted. Control mouse IgG and mouse monoclonal antibody to the human β_1 integrin subunit (clone P4C10) were purchased from Life Technologies. Monoclonal antibodies to the α_1 integrin subunit (clone CD49a), the α_6 subunit, the α_v subunit, and $\alpha_v\beta_3$ (LM609) were purchased from Chemicon International (Temecula, CA).

RESULTS

Human arresten was produced in *E. coli* using a bacterial expression plasmid, pET-22b (capable of periplasmic transport, thus resulting in soluble protein) as a fusion protein with a COOH-terminal 6-histidine tag. The *E. coli*-expressed protein was isolated predominantly as a soluble protein, and SDS-PAGE analysis revealed a monomeric band at 29 kDa. The additional 3 kDa arise from polylinker and histidine tag sequences and were immunodetected by both arresten and 6-histidine tag antibodies (Fig. 1, *a* and *b*). Human arresten was also produced as a secreted soluble protein in 293

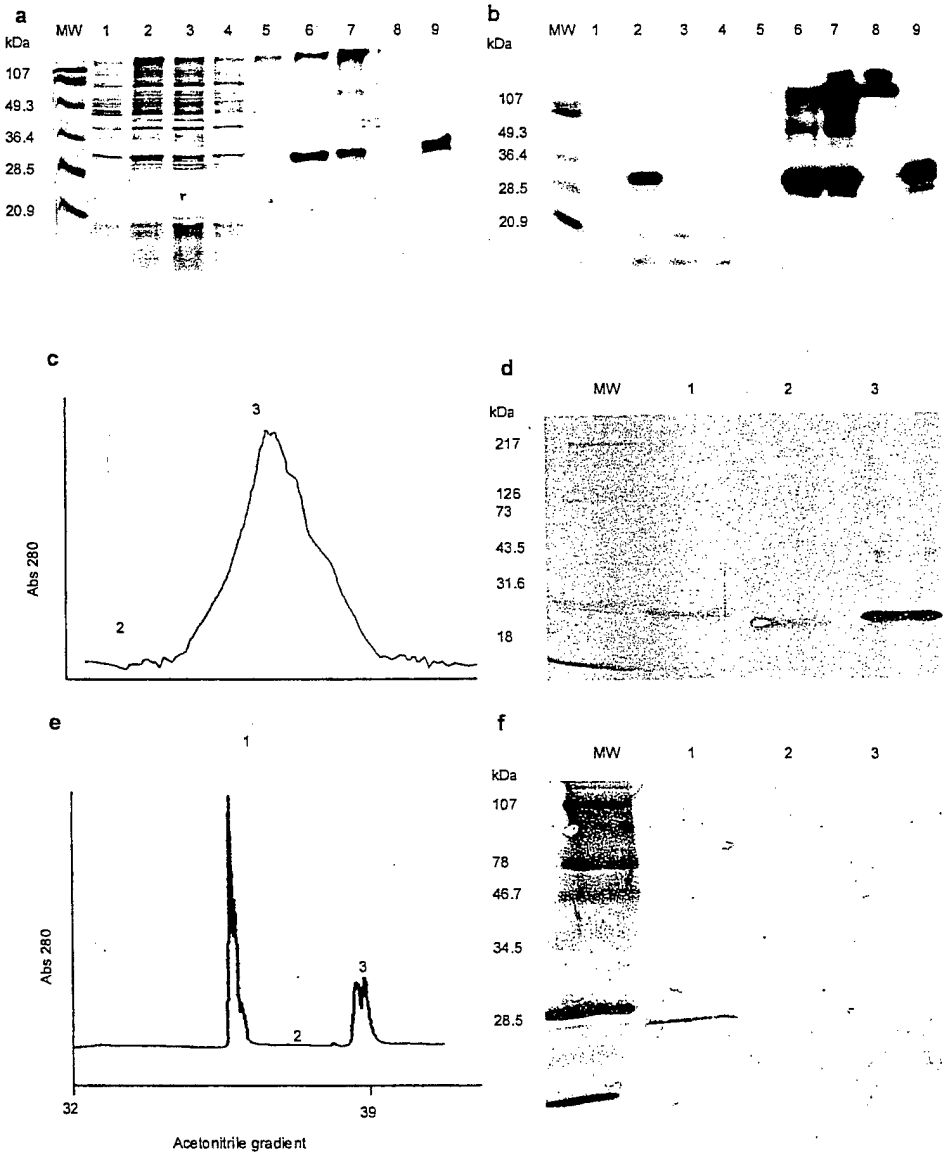

Fig. 1. Recombinant production of arresten in *E. coli*: expression in pET22b(+) bacterial plasmid. *a*, SDS-PAGE Coomassie Blue staining; *b*, immunoblot analysis; *MW*, molecular weight marker; *Lane 1*, uninduced cells; *Lane 2*, induced cells; *Lane 3*, unbound fraction; *Lane 4*, 10 mM imidazole wash; *Lane 5*, 25 mM imidazole wash; *Lane 6*, 50 mM imidazole eluted protein; *Lane 7*, 125 mM imidazole eluted protein; *Lane 8*, 250 mM imidazole eluted protein; *Lane 9*, reducing conditions (10% β-mercaptoethanol). Five micrograms of protein were loaded in each lane. Embryonic kidney cells (293) that expressed arresten-containing supernatant were subjected to affinity chromatography using arresten-specific antibodies (14). A major peak was identified, containing a monomer of ~30 kDa that was immunoreactive with arresten antibodies (*c* and *d*). *d*, *MW*, molecular weight marker; *Lane 1*, unconcentrated supernatant; *Lane 2*, minor peaks from region 2 in *C*; *Lane 3*, major peak 3. SDS-PAGE analysis revealed a single major band at ~30 kDa (data not shown). We were able to generate 1–2 mg of recombinant human arresten in 1 liter of culture fluid. Arresten isolated from human placenta is shown as a representative reverse phase profile (*e*). One major peak and a second peak with shoulders were observed when constituent proteins were resolved using an acetonitrile gradient (32–39%). SDS-PAGE analysis revealed two bands in the first peak and no detectable proteins in the second peak (data not shown). Immunoblotting identified arresten in peak 1; however, no immunodetectable protein was observed in area 2 or peak 3 (*e* and *f*). *f*, *MW*, molecular weight marker; *Lane 1*, peak 1; *Lane 2*, peak 2; *Lane 3*, peak 3.

embryonic kidney cells using the pcDNA 3.1 eukaryotic vector. This recombinant protein (without any purification or detection tags) was isolated using affinity chromatography, and a pure monomeric form was detected in the major peak by SDS-PAGE and immunoblot analyses (Fig. 1, *c* and *d*). In addition, human arresten was isolated from human placenta by gel filtration, HPLC, and affinity chromatography techniques; a 26-kDa molecule was detected by SDS-PAGE and immunoblot analyses (Fig. 1, *e* and *f*).

In assays of endothelial cell proliferation, a dose-dependent inhibition of bFGF-stimulated endothelial cells was detected, with an ED_{50} value of 0.25 μg/ml (Fig. 2*a*) using *E. coli*-produced soluble protein. These results support earlier observations that α_1 and α_2 type IV collagen isolated from the Engelbreth-Holm-Swarm mouse sarcoma tumor may be inhibitory to capillary endothelial cells (5). No significant effect was observed on the proliferation of renal carcinoma cells (786-0; data not shown), prostate cancer cells (PC-3) or HPECs, even at arresten doses of up to 50 μg/ml (Fig. 2, *c* and *d*). In contrast, endostatin inhibited CPAE cell proliferation with an ED_{50} value of 0.75 μg/ml, 3-fold higher than arresten, and did not inhibit A-498 cancer cells (data not shown; Ref. 15). Cell cycle analysis was also performed using FACScan technology to assess the antiproliferative properties of arresten in the presence of VEGF. We observed a decrease in the number of CPAE cells in S-phase in the presence of arresten. These results correlate with thymidine incorporation proliferation assays described above (Fig. 2*b*).

When mouse aortic endothelial cells are cultured on Matrigel, a solid gel of mouse basement membrane proteins, they rapidly align and form hollow tube-like structures (20). Arresten, produced in 293 cells, selectively inhibited endothelial tube formation in a dose-dependent manner (Fig. 2, *f* and *h*). Similar results were also obtained using *E. coli*-produced arresten (data not shown). The 7S domain of

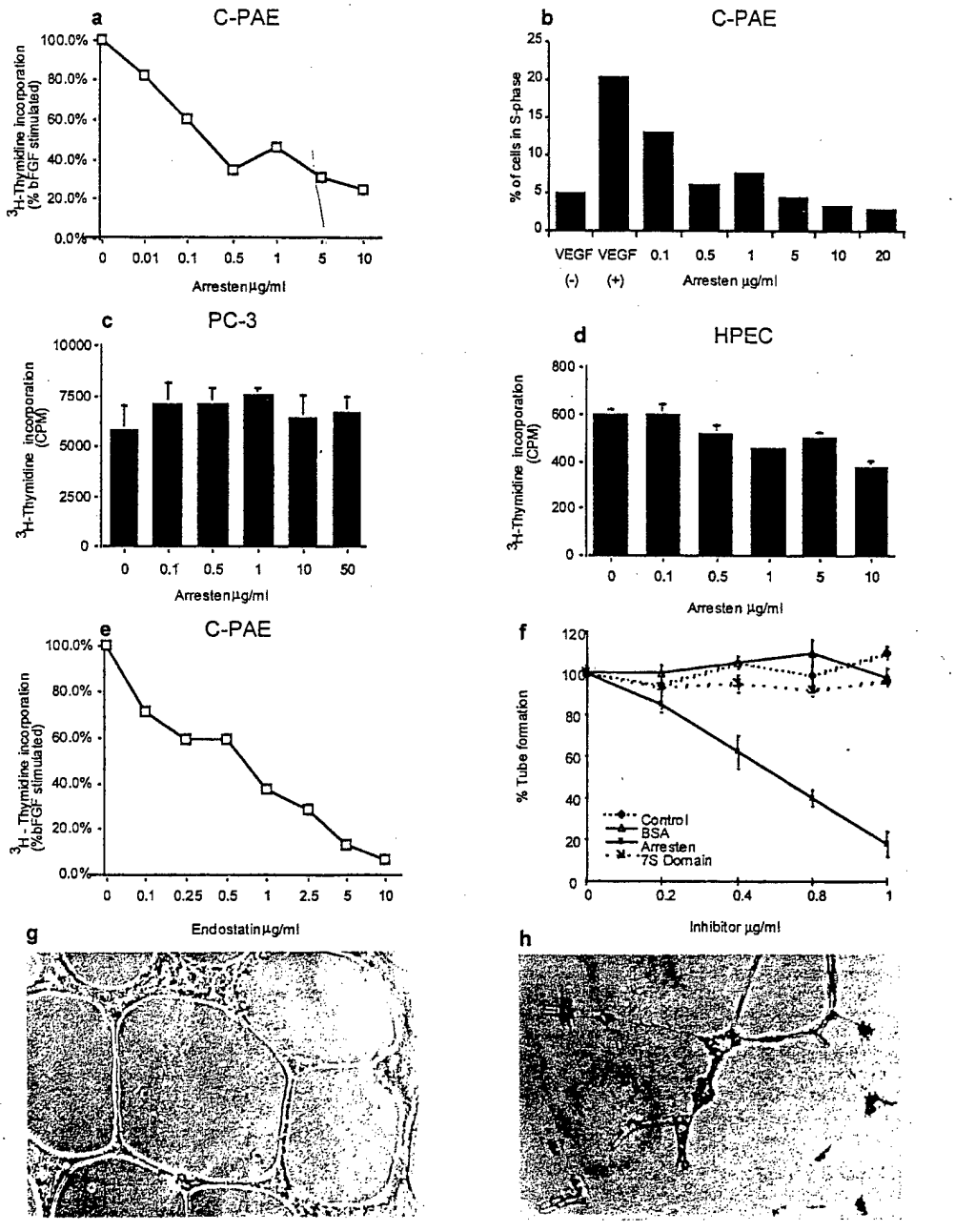

Fig. 2. Inhibition of endothelial cell proliferation. CPAE (*a* and *e*) cells and control nonendothelial cells, PC-3 cells (*c*) and HPECs (*d*), were treated with concentrations of arresten or endostatin ranging from 0.01 to 50 μg/ml. All wells received 1 μCi of [^{3}H]thymidine at the time of treatment. Thymidine incorporation was measured using a scintillation counter. All groups represent triplicate samples. *b*, cell cycle analysis. Growth-arrested CPAE cells were treated with concentrations of arresten ranging from 0.1 to 20 μg/ml. The cells were stimulated with 5 ng/ml VEGF, trypsinized, and harvested after 18 h. The *VEGF* (−) value is the percentage of cells in S-phase at the beginning of the experiment. *f–h*, endothelial tube assay with mouse aortic endothelial cells. Ten fields were viewed, and tubes were counted and averaged (*f*). Well-formed tubes can be observed in *g* treated with 7S domain control (magnification, ×100). Arresten-treated (0.8 μg/ml) mouse aortic endothelial cells (magnification, ×100) are shown in *h*.

type IV collagen (NH_2-terminal noncollagenous domain) had no effect on endothelial tube formation (Fig. 2*g*). Maximum inhibition with arresten was attained between 0.8 and 1 μg/ml (Fig. 2*f*).

To test the *in vivo* effect of arresten on the formation of new capillaries, we performed a Matrigel plug assay in mice (21). Matrigel was placed in the presence of bFGF, with or without increasing concentrations of arresten. A 50% reduction in the number of blood vessels was observed at 1 μg/ml arresten and 10 μg/ml endostatin (Fig. 3*a*). Collectively, these results suggest that arresten affects the formation of new blood vessels by inhibiting more than one step in the angiogenic process.

To assess the effect of arresten on metastasis, 1×10^6 MC38/MUC1 cancer cells were administered by tail vein to C57BL/6 mice (22). Treatment with 5 mg/kg arresten (i.p.) was initiated the following day and continued every other day for 26 days. The results show a significant reduction of pulmonary nodules in arresten-treated mice compared with the control group (Fig. 3*b*).

Next, we tested the effect of arresten on established primary tumors in mice. Arresten, *E. coli* produced, inhibited the growth of large (Fig. 3*c*) and small (Fig. 3*d*) renal cell carcinoma tumors. In experiments performed with PC-3 human prostate tumors in mice, arresten at 10 mg/kg inhibited tumor growth similar to endostatin at 20 mg/kg (Fig. 3*e*). A similar degree of inhibition was observed with arresten administered at 4 mg/kg, and this inhibition continued for 12 days after arresten treatment was stopped (Fig. 3*f*). After 12 days, the tumors escaped the effect of arresten and began growing at the same rate as the controls (data not shown). A CD-31 staining pattern of treated (Fig. 3*h*) *versus* control (Fig. 3*g*) mice is shown. Blood vessels in 15 high-magnification fields were counted and averaged. This number was divided by the volume of the tumor and averaged (18.7 ± 6.2 control *versus* 10.5 ± 7.2 treated; Fig. 3*l*). Finally, tumor sections were stained for PCNA, fibronectin, and type IV collagen. We found no difference in tumor cell proliferation or in type IV collagen and fibronectin content surrounding tumor cells in the treated and untreated mice, again demonstrating the endothelial cell specificity of arresten (Fig. 3, *j–l*, representative arresten-treated sections).

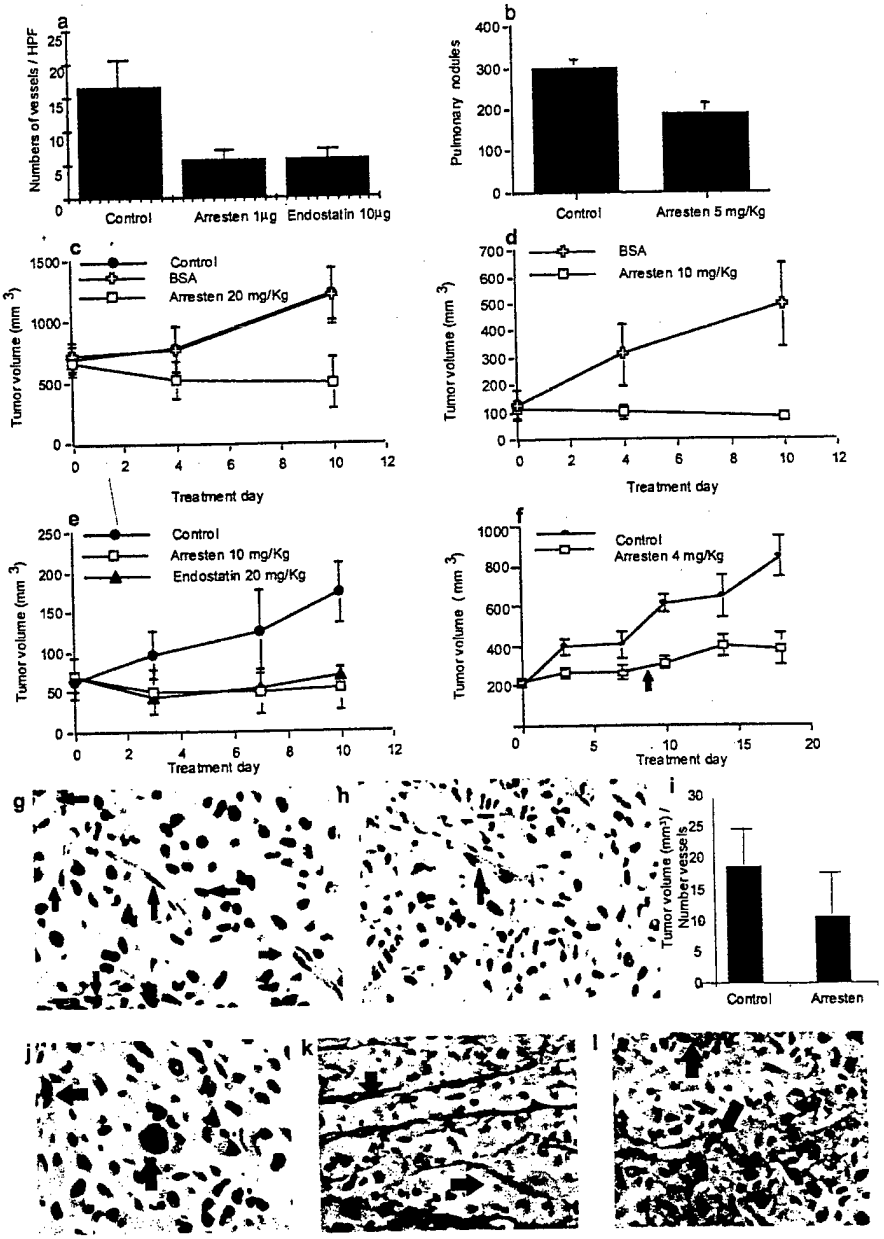

Fig. 3. Matrigel plug assay. Before injection into C57BL/6 mice, Matrigel (Collaborative Biomolecules) was mixed with 20 units/ml heparin (Pierce), 150 ng/ml bFGF (R&D Systems), and either 1 μg/ml arresten or 10 μg/ml endostatin. Control groups received no angiogenic inhibitor. After 14 days, plugs were removed, sectioned, and H&E stained. *a*, sections were examined by light microscopy and the number of blood vessels from 10 high-power fields was counted and averaged. *b*, inhibition of tumor metastases. C57BL/6 mice were injected i.v. with 1 million MC38/MUC1 cells. Controls (five mice) received sterile PBS, and the experimental group (six mice) received 4 mg/kg arresten every other day for 26 days. Pulmonary tumor nodules were counted for each mouse in both groups and averaged after 26 days of treatment. *c–f, in vivo* tumor studies. 786-0 cells (2 million cells) were injected s.c. into 7- to 9-week-old male athymic nude mice. The tumors were allowed to grow to ~700 mm^3 (*c*) or ~100 mm^3 (*d*; each group contained six mice). Arresten was injected i.p. daily (10 or 20 mg/kg) for 10 days in sterile PBS. The control group received either BSA or the PBS vehicle. *e*, human prostate adenocarcinoma cells (PC-3) were harvested and injected s.c. (5×10^6 cells) into 7- to 9-week-old male athymic nude mice. Experimental groups were injected i.p. daily with arresten (10 mg/kg) or endostatin (20 mg/kg) protein. The control group received PBS each day. *f*, this experiment was identical to the above PC-3 model, except the arresten dosage was reduced to only 4 mg/kg/day. The treatment was stopped after 8 days (*arrow*); however, significant inhibition continued for 12 more days with no additional arresten treatment. At this point, tumors escaped the effect of arresten (data not shown). *g–l*, immunohistochemistry. Mice were sacrificed after 10–20 days of arresten treatment. Tumors were excised, and 3 μm-sections were mounted on glass slides. CD-31 staining of blood vessels is shown in a control mouse (*g*) and an arresten-treated mouse (*h*). *i*, CD-31 blood vessel quantification for arresten-treated and control-treated tumors. For PCNA staining, tissue sections were incubated for 60 min at room temperature with a 1:200 dilution of anti-PCNA antibody. Detection was carried out according to the manufacturer's recommendations using the USA horseradish peroxidase system. The PCNA staining is shown in *j* (*arrows*). Staining for fibronectin and type IV collagen was performed using polyclonal anti-fibronectin at a dilution of 1:500 and anti-type IV collagen at a dilution of 1:100. The Vectastain Elite ABC kit was used for detection according to the manufacturer's recommendations. Fibronectin staining is shown in *k* (*arrows*), and type IV collagen staining is shown in *l* (*arrows*).

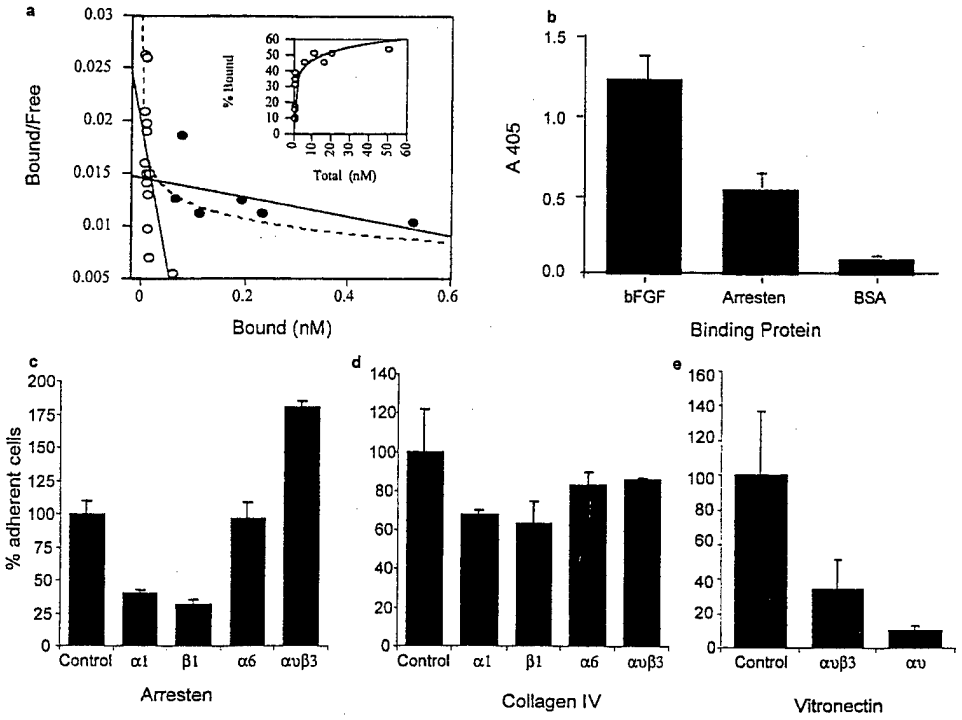

Fig. 4. Scatchard analysis. *a*, binding analysis of arresten to endothelial (CPAE) cells. There are two curves represented showing high- and low-affinity arresten receptors. *b*, HSPG direct ELISA. HSPG was coated on a 96-well plate, and binding to bFGF, arresten, or BSA was assessed as described in "MATERIALS AND METHODS." *c–e*, cell adhesion assay. HUVECs were preincubated with an integrin antibody and plated on arresten-coated (*c*), collagen type IV-coated (*d*), or vitronectin-coated (*e*) plates. The amount of cell binding was compared with the control (*c*), which is HUVECs incubated with a control mouse IgG. We observed an inhibition of 60% in cell adhesion for the α_1 subunit and a 70% inhibition for the β_1 subunit (*c* and *d*).

To gain further insight into the anti-angiogenic mechanism of action of arresten, we studied its binding to endothelial cells. Iodinated human placenta arresten was incubated with CPAE cells, and a Scatchard analysis was performed (19). Our data revealed two different binding sites (Fig. 4*a*). The high-affinity, low-capacity binding site has a K_{d_1} value of 8.5×10^{-11} M and a maximum number of binding sites of 3×10^6 sites per cell. The other low-affinity, high-capacity binding site has a K_{d_2} value of 4.6×10^{-8} M and a maximum number of binding sites of 6×10^7 sites per cell. It has been shown that HSPG binds the α_1 NC1 domain of type IV collagen (23). Also, recent studies have speculated that $\alpha_1\beta_1$ and $\alpha_2\beta_1$ integrins bind to type IV collagen isolated from the Engelbreth-Holm-Swarm mouse sarcoma tumor (24).

We assessed the capacity of arresten to mediate endothelial cell binding via $\alpha_1\beta_1$ and $\alpha_2\beta_1$ integrins. Our results show that functionally blocking α_1 and β_1 integrin subunit antibodies significantly diminish the binding of HUVECs to arresten-coated culture wells (Fig. 4*c*). We found an inhibition of endothelial cell attachment to arresten-coated plates of 60% with α_1 antibody and 70% with β_1 integrin antibody. The control α_6 integrin antibody showed no binding inhibition to arresten. The $\alpha_V\beta_3$ antibody did not inhibit endothelial cell binding to arresten but increased binding (Fig. 4*c*). On the other hand, with type IV collagen-coated plates, we observed an inhibition of 30% with α_1, 40% with β_1, and 15% with $\alpha_v\beta_3$ neutralizing antibodies (Fig. 4*d*). Again, the α_6 neutralizing antibody had no effect on binding. We speculate that the difference in cell adhesion between arresten and type IV collagen-coated plates in the presence of α_1 and β_1 integrin antibodies is due to additional integrin binding sites on the entire type IV collagen molecule in comparison with arresten, which may contain a single integrin binding site (Fig. 4, *c* and *d*). To demonstrate the efficiency of the $\alpha_V\beta_3$ neutralizing antibody, we performed a control adhesion experiment with its ligand, vitronectin (Fig. 4*e*). The neutralizing $\alpha_V\beta_3$ and α_V antibodies were able to inhibit endothelial cell binding to vitronectin by 60 and 90%, respectively.

HSPG binding to arresten was assessed by ELISA. ELISA plates were coated with HSPG and incubated with arresten, bFGF, or BSA. Our results show that HSPG binds both arresten and bFGF as reported earlier (Ref. 23; Fig. 4*b*). Taken together in conjunction with earlier reports (23), these results suggest that arresten may be binding HSPG on the cell surface (Fig. 4, *a* and *b*).

DISCUSSION

We propose that the molecular mechanism associated with the tumor-suppressing activity of arresten as well as the specific inhibition of endothelial cell proliferation and migration by arresten may be mediated by the $\alpha_1\beta_1$ integrin. These results suggest that binding of arresten to $\alpha_1\beta_1$ may down-regulate VEGF-induced proliferation and migration of endothelial cells, as suggested previously by VEGF-induced expression of $\alpha_1\beta_1$ integrin on endothelial cells (25).

In support of our findings, it has been shown that α_1 integrin neutralizing antibodies can suppress angiogenesis *in vivo* (24). Among the collagen integrins, $\alpha_1\beta_1$ activates the Ras-Shc-mitogen-activated protein kinase pathway, promoting cell proliferation (26). Our studies suggest that arresten may be antagonizing this effect in endothelial cells. In addition, Pozzi *et al.* (27) recently described decreased angiogenesis in tumor-bearing α_1 integrin-deficient mice.

Whether arresten functions by suppressing the activity of VEGF and/or bFGF directly remains to be elucidated. Future comparative studies with other recently discovered inhibitors such as restin, troponin 1, kringle 5, pigment epithelium-derived factor, and vasostatin will also be very insightful in establishing the unique anti-angiogenic property of arresten (28–30).

ACKNOWLEDGMENTS

We thank Dr. Donald Senger for helpful discussion regarding integrin adhesion assays.

REFERENCES

1. Kumar, R., Kuniyasu, H., Bucana, C. D., Wilson, M. R., and Fidler, I. J. Spatial and temporal expression of angiogenic molecules during tumor growth and progression. Oncol. Res., *10:* 301–311, 1998.

2. Folkman, J. Angiogenesis in cancer, vascular, rheumatoid and other disease. Nat. Med., *1:* 27–31, 1995.
3. Holash, J., Wiegand, S. J., and Yancopoulos, G. D. New model of tumor angiogenesis: dynamic balance between vessel regression and growth mediated by angiopoietins and VEGF. Oncogene, *18:* 5356–5362, 1999.
4. Okada, F., Rak, J. W., Croix, B. S., Lieubeau, B., Kaya, M., Roncari, L., Shirasawa, S., Sasazuki, T., and Kerbel, R. S. Impact of oncogenes in tumor angiogenesis: mutant K-ras up-regulation of vascular endothelial growth factor/vascular permeability factor is necessary, but not sufficient for tumorigenicity of human colorectal carcinoma cells. Proc. Natl. Acad. Sci. USA, *95:* 3609–3614, 1998.
5. Madri, J. A. Extracellular matrix modulation of vascular cell behaviour. Transpl. Immunol., *5:* 179–183, 1997.
6. Timpl, R. Macromolecular organization of basement membranes. Curr Opin Cell Biol., *8:* 618–624, 1996.
7. Prockop, D. J., and Kivirikko, K. I. Collagens: molecular biology, diseases, and potentials for therapy. Annu. Rev. Biochem., *64:* 403–434, 1995.
8. Paulsson, M. Basement membrane proteins: structure, assembly, and cellular interactions. Crit. Rev. Biochem. Mol. Biol., *27:* 93–127, 1992.
9. Kalluri, R., Shield, C. F., Todd, P., Hudson, B. G., and Neilson, E. G. Isoform switching of type IV collagen is developmentally arrested in X-linked Alport syndrome leading to increased susceptibility of renal basement membranes to endoproteolysis. J. Clin. Invest., *99:* 2470–2478, 1997.
10. Maragoudakis, M. E., Missirlis, E., Karakiulakis, G. D., Sarmonica, M., Bastakis, M., and Tsopanoglou, N. Basement membrane biosynthesis as a target for developing inhibitors of angiogenesis with anti-tumor properties. Kidney Int., *43:* 147–150, 1993.
11. Zhang, X., Hudson, B. G., and Sarras, M. P., Jr. Hydra cell aggregate development is blocked by selective fragments of fibronectin and type IV collagen. Dev. Biol., *164:* 10–23, 1994.
12. Tsilibary, E. C., Reger, L. A., Vogel, A. M., Koliakos, G. G., Anderson, S. S., Charonis, A. S., Alegre, J. N., and Furcht, L. T. Identification of a multifunctional, cell-binding peptide sequence from the a1(NC1) of type IV collagen. J. Cell Biol., *111:* 1583–1591, 1990.
13. Kamphaus, G. D., Colorado, P. C., Panka, D. J., Hopfer, H., Ramchandran, R., Torre, A., Maeshima, Y., Mier, J. W., Sukhatme, V. P., and Kalluri, R. Canstatin, a novel matrix-derived inhibitor of angiogenesis and tumor growth. J Biol Chem., *275:* 1209–1215, 2000.
14. Neilson, E. G., Kalluri, R., Sun, M. J., Gunwar, S., Danoff, T., Mariyama, M., Myers, J. C., Reeders, S. T., and Hudson, B. G. Specificity of Goodpasture autoantibodies for the recombinant noncollagenous domains of human type IV collagen. J. Biol. Chem., *268:* 8402–8405, 1993.
15. Dhanabal, M., Ramchandran, R., Volk, R., Stillman, I. E., Lombardo, M., Iruela-Arispe, M. L., Simons, M., and Sukhatme, V. P. Endostatin: yeast production, mutants, and antitumor effect in renal cell carcinoma. Cancer Res., *59:* 189–197, 1999.
16. Dhanabal, M., Volk, R., Ramchandran, R., Simons, M., and Sukhatme, V. P. Cloning, expression, and in vitro activity of human endostatin. Biochem. Biophys. Res. Commun., *258:* 345–352, 1999.
17. Grant, D. S., Kibbey, M. C., Kinsella, J. L., Cid, M. C., and Kleinman, H. K. The role of basement membrane in angiogenesis and tumor growth. Pathol. Res. Pract., *190:* 854–863, 1994.
18. O'Reilly, M. S., Boehm, T., Shing, Y., Fukai, N., Vasios, G., Lane, W. S., Flynn, E., Birkhead, J. R., Olsen, B. R., and Folkman, J. Endostatin: an endogenous inhibitor of angiogenesis and tumor growth. Cell, *88:* 277–285, 1997.
19. Sarkar, P. K., and Ray, A. K. Specific binding of L-triiodothyronine modulates Na(+)-K(+)-ATPase activity in adult rat cerebrocortical synaptosomes. Neuroreport, *9:* 1149–1152, 1998.
20. Haralabopoulos, G. C., Grant, D. S., Kleinman, H. K., Lelkes, P. I., Papaioannou, S. P., and Maragoudakis, M. E. Inhibitors of basement membrane collagen synthesis prevent endothelial cell alignment in matrigel in vitro and angiogenesis in vivo. Lab. Invest., *71:* 575–582, 1994.
21. Passaniti, A., Taylor, R. M., Pili, R., Guo, Y., Long, P. V., Haney, J. A., Pauly, R. R., Grant, D. S., and Martin, G. R. A simple, quantitative method for assessing angiogenesis and anti-angiogenic agents using reconstituted basement membrane, heparin, and fibroblast growth factor. Lab. Invest., *67:* 519–528, 1992.
22. Gong, J., Chen, D., Kashiwaba, M., and Kufe, D. Induction of antitumor activity by immunization with fusions of dendritic and carcinoma cells. Nat. Med., *3:* 558–561, 1997.
23. Keller, K. M., Keller, J. M., and Kuhn, K. The C-terminus of type I collagen is a major binding site for heparin. Biochim. Biophys. Acta, *882:* 1–5, 1986.
24. Senger, D. R., Claffey, K. P., Benes, J. E., Perruzzi, C. A., Sergiou, A. P., and Detmar, M. Angiogenesis promoted by vascular endothelial growth factor: regulation through alpha1beta1 and alpha2beta1 integrins. Proc. Natl. Acad. Sci. USA, *94:* 13612–13617, 1997.
25. Bloch, W., Forsberg, E., Lentini, S., Brakebusch, C., Martin, K., Krell, H. W., Weidle, U. H., Addicks, K., and Fassler, R. Beta 1 integrin is essential for teratoma growth and angiogenesis. J. Cell Biol., *139:* 265–278, 1997.
26. Pozzi, A., Wary, K. K., Giancotti, F. G., and Gardner, H. A. Integrin alpha1beta1 mediates a unique collagen-dependent proliferation pathway in vivo. J. Cell Biol., *142:* 587–594, 1998.
27. Pozzi, A., Moberg, P., Miles, L., Wagner, S., Soloway, P., and Gardner, H. Elevated matrix metalloprotease and angiostatin levels in integrin $\alpha 1$ knockout mice cause reduced tumor vascularization, Proc. Natl. Acad. Sci. USA, *97:* 2202–2207, 2000.
28. Moses, M. A., Wiederschain, D., Wu, I., Fernandez, C. A., Ghazizadeh, V., Lane, W. S., Flynn, E., Sytkowski, A., Tao, T., and Langer, R. Troponin I is present in human cartilage and inhibits angiogenesis. Proc. Natl. Acad. Sci. USA, *96:* 2645–2650, 1999.
29. Pike, S. E., Yao, L., Jones, K. D., Cherney, B., Appella, E., Sakaguchi, K., Nakhasi, H., Teruya-Feldstein, J., Wirth, P., Gupta, G., and Tosato, G. Vasostatin, a calreticulin fragment, inhibits angiogenesis and suppresses tumor growth. J. Exp. Med., *188:* 2349–2356, 1998.
30. Dawson, D. W., Volpert, O. V., Gillis, P., Crawford, S. E., Xu, H., Benedict, W., and Bouck, N. P. Pigment epithelium-derived factor: a potent inhibitor of angiogenesis. Science (Washington DC), *285:* 245–248, 1999.

Molecular Cell Biology Research Communications 3, 277–282 (2000)
doi:10.1006/mcbr.2000.0222, available online at http://www.idealibrary.com on IDEAL®

Angiostatin Induces Mitotic Cell Death of Proliferating Endothelial Cells

Danielle Hari,*,[1] Michael A. Beckett,*,[1] Vikas P. Sukhatme,† Mohanraj Dhanabal,† Edwardine Nodzenski,* Hua Lu,† Helena J. Mauceri,* Donald W. Kufe,‡ and Ralph R. Weichselbaum*

*Department of Radiation and Cellular Oncology, University of Chicago, Chicago, Illinois 60637; †Department of Medicine, Beth Israel Deaconess Medical Center, Boston, Massachusetts; and ‡Division of Pharmacology, Dana Farber Cancer Institute, Boston, Massachusetts

Received June 12, 2000

Angiostatin is an inhibitor of tumor angiogenesis that induces regression of experimental tumors and enhances the antitumor effects of radiation therapy. We report that the cytotoxic effects of angiostatin are restricted to the proliferating endothelial cell population. In addition, angiostatin and ionizing radiation (IR) interact by inducing death of dividing endothelial cells. We also show that angiostatin and IR interact to inhibit endothelial cell migration. These findings demonstrate that angiostatin targets the proliferating tumor vasculature and provide a mechanistic basis for the cytotoxic interaction of angiostatin and IR. © 2000 Academic Press

Angiogenesis is an important component of normal physiological processes such as wound healing and development, and is a key regulator of chronic inflammation and tumorigenesis (1, 2). Tumor angiogenesis has recently received much attention as a potential therapeutic focus in cancer treatment (3, 4). Tumors can usually achieve a size of only 1–2 mm before angiogenesis is required. Also, tumor vessels are derived from normal endothelial cells that are genetically stable and are unlikely to become resistant to agents employed in cancer therapy (5, 6). Therefore, inhibition of angiogenesis is hypothesized to be important in the treatment of both primary tumors and metastases.

Several naturally occurring proteins produced by neoplasms regulate tumor blood vessel growth as positive and negative regulators of angiogenesis. Angiostatin, the first of the naturally occurring antiangiogenic molecules described, is a cleavage product that includes the first four-kringle domains of plasminogen (7, 8). Angiostatin derived from mice bearing Lewis lung carcinoma tumors (LLC) has been shown to suppress the growth of both primary and metastatic tumors (9, 10). More recently, recombinant angiostatin and angiostatin delivered as gene therapy have been shown to inhibit primary and metastatic tumor growth in a variety of models (11–13). However, experiments to date have yielded little insight into the mechanism of action of angiostatin. *In vitro* studies examining the effects of angiostatin on endothelial cells demonstrate inhibition of endothelial cell growth and migration. One report indicated that angiostatin binds ATP synthetase (14), while other reports suggest that induction of cell cycle arrest and apoptosis are responsible for the effects of angiostatin on endothelial cells (13, 15, 16). Angiostatin has also been reported to interact with ionizing radiation (IR) to induce greater antitumor effects than either treatment alone and without added toxicity (17).

Here we report that angiostatin induces clonogenic death in endothelial cell lines from different species by a mitotic rather than apoptotic mode of cell death. We demonstrate that angiostatin is preferentially cytotoxic to proliferating endothelial cells and exhibits a cytotoxic interaction with IR in the proliferating endothelial cell population. We also report that angiostatin interacts with IR to inhibit endothelial cell migration.

MATERIALS AND METHODS

Cell culture. Human umbilical vein endothelial cells (HUVEC), human aortic endothelial cells (HAEC), and EGM-2 growth medium were purchased from Clonetics Corporation (BioWhittaker, Walkersville, MD). Bovine aortic endothelial cells (BAEC) and growth medium were purchased from Cell Applications, Inc. (San Diego, CA). The plating and passaging of cells was performed using the manufacturer's instructions. The endothelial cells used for experimentation were from passage 4 to 9.

[1] Contributed equally to this work.

1522-4724/00 $35.00

Angiostatin production. Murine angiostatin was cloned and expressed using a yeast expression system. Briefly, a cDNA encoding mouse plasminogen, obtained from ATCC, was amplified using Vent DNA polymerase. The primers employed were designed with the appropriate restriction sites to permit cloning directly into the yeast shuttle plasmid pPICZαA, containing *Eco*R1 and *Not*1 restriction sites. This vector permitted secretion of the recombinant protein into the culture medium. Positive clones were grown in 25 ml BMGY medium containing 100 μg/ml Zeocin at 30°C for 18–24 h. The overnight grown culture (A_{600}, 2–6) was used to inoculate 2-liter flasks containing 500 ml of buffered glycerol medium. Cells were grown for 2 days at 30°C (A_{600}, 16–20), then centrifuged at 500 rpm for 10 min, and resuspended in 300–400 ml of buffered methanol induction medium. The cell-free supernatant was harvested on days 2, 3, and 4 and concentrated using ammonium precipitation (70%) dissolved in 50 mM phosphate buffer, pH 7.4, and dialyzed at 4°C. Protein purification was performed using a lysine-Sepharose 4B column (Pharmacia) equilibrated with 50 mM phosphate buffer, pH 7.4. Recombinant angiostatin was eluted with 0.2 M c-amino-*N*-caproic acid, pH 7.4 at 4°C with 3 changes at 6–8 h. The dialyzed sample was further concentrated by ultrafiltration using an Amicon concentrator (YM 10). Protein concentration was determined using the micro BCA assay (Bio-Rad).

Clonogenic assay. For angiostatin dose–response experiments, 200–1000 HUVEC, HAEC, and BAEC were plated in 100-mm tissue culture dishes. The VEGF normally present in the growth medium was replaced with 10 ng/ml VEGF purchased from R&D Systems (Minneapolis, MN). Eighteen hours after plating, 0, 1, 10, 100, and 1000 ng/ml angiostain was added. For X-ray survival analysis, 200–20,000 HUVEC, HAEC, and BAEC were plated in 100-mm tissue culture dishes. Eighteen hours after plating, cells were irradiated with 100–900 cGy using a GE Maxitron X-ray generator operating at 250 kV, 26 mA, with a 0.5-mm copper filter, at a dose rate of 118 cGy/min. For the combined experiments, 200–20,000 HUVEC, HAEC, and BAEC were plated in 100 mm tissue culture dishes. Eighteen hours after plating 0, 1, 10, 100, and 1000 ng/ml angiostatin was added. Four hours after the addition of angiostatin the cells were treated with 100–900 cGy. For all experiments, cultures were returned to the incubator for 14–17 days, after which they were stained with crystal violet, colonies were counted, and the surviving fraction was determined. Colonies containing >50 cells were scored as positive.

Apoptosis assays. Based on the results reported by Chmura (18), we chose the 7-AAD staining method for the quantitation of apoptosis. 7-AAD staining was performed as follows. HUVEC (10^5 cells) were plated in 60-mm tissue culture dishes and allowed to grow for 2 days. The cultures were treated with 1000 ng/ml angiostatin, 1000 cGy, or the combination of 1000 ng/ml angiostatin followed 4 h later with 1000 cGy. Cells were harvested for 7-AAD staining at 0, 12, 24, and 48 h after treatment by collecting the medium and then disaggregating the adherent cells with trypsin/EDTA and transferred to collection tube containing the medium and all washes. The dish was rinsed with PBS/1% fetal bovine serum/0.05% sodium azide solution and added to the collection tube. Cells were centrifuged at 1200 RPM for 5 min. The supernatant was discarded and the cells washed once with PBS/1% FBS/0.05% sodium azide solution. The cells were centrifuged and the supernatant and excess liquid discarded. The pellet was loosened by flicking the tube and resuspended in 500 μl 7-AAD (20 μg/ml). The cells were stained on ice for 30 min after which the samples were transferred to FACS tubes and analyzed immediately using a Becton Dickinson FACScan analyzer.

Endothelial cell migration assay. HUVEC were cultured in EGM-2 as per the manufacturer's instructions. To measure migration, cells were starved overnight in minimal growth medium containing 0.1% BSA. Cells in angiostatin treatment group were exposed to 100 ng/ml angiostatin for 4 h. The IR treated and the angiostatin/IR combination cultures were then irradiated with 900 cGy. The cells were then harvested, suspended in minimal growth medium with 0.1% BSA (containing 100 ng/ml angiostatin in the angiostatin treated wells), and plated at 7×10^5 per well on the lower surface of a gelatinized 5.0-μm filter (Nucleopore Corp., Pleasanton, CA) in an inverted modified Boyden chamber as previously described (19). After 1–2 h at 37°C, during which time the cells adhere to the filter, the chamber was reinverted, medium containing 20 ng/ml VEGF was added to the top well, and the chamber was incubated for 16 h at 37°C. The chambers were then disassembled, and the filters fixed and stained with Diff-Quick Stain Set (Dade International, Inc., Miami, FL). Migration was scored as the total number of cells that migrated to the top of the membrane as counted in 10 high power fields.

RESULTS AND DISCUSSION

Endothelial Cell Killing Mediated by Angiostatin

We previously reported the results of human umbilical vein endothelial cells (HUVEC) and human aortic endothelial cells (HAEC) treated with 10 and 100 ng/ml angiostatin in combination with IR (0, 100, 200, and 900 cGy) (17). We have extended the investigation of the clonogenic survival of proliferating HUVEC, HAEC, and bovine aortic endothelial cells (BAEC) following exposure to angiostatin at concentrations ranging from 1 to 1000 ng/ml. Figure 1 demonstrates a

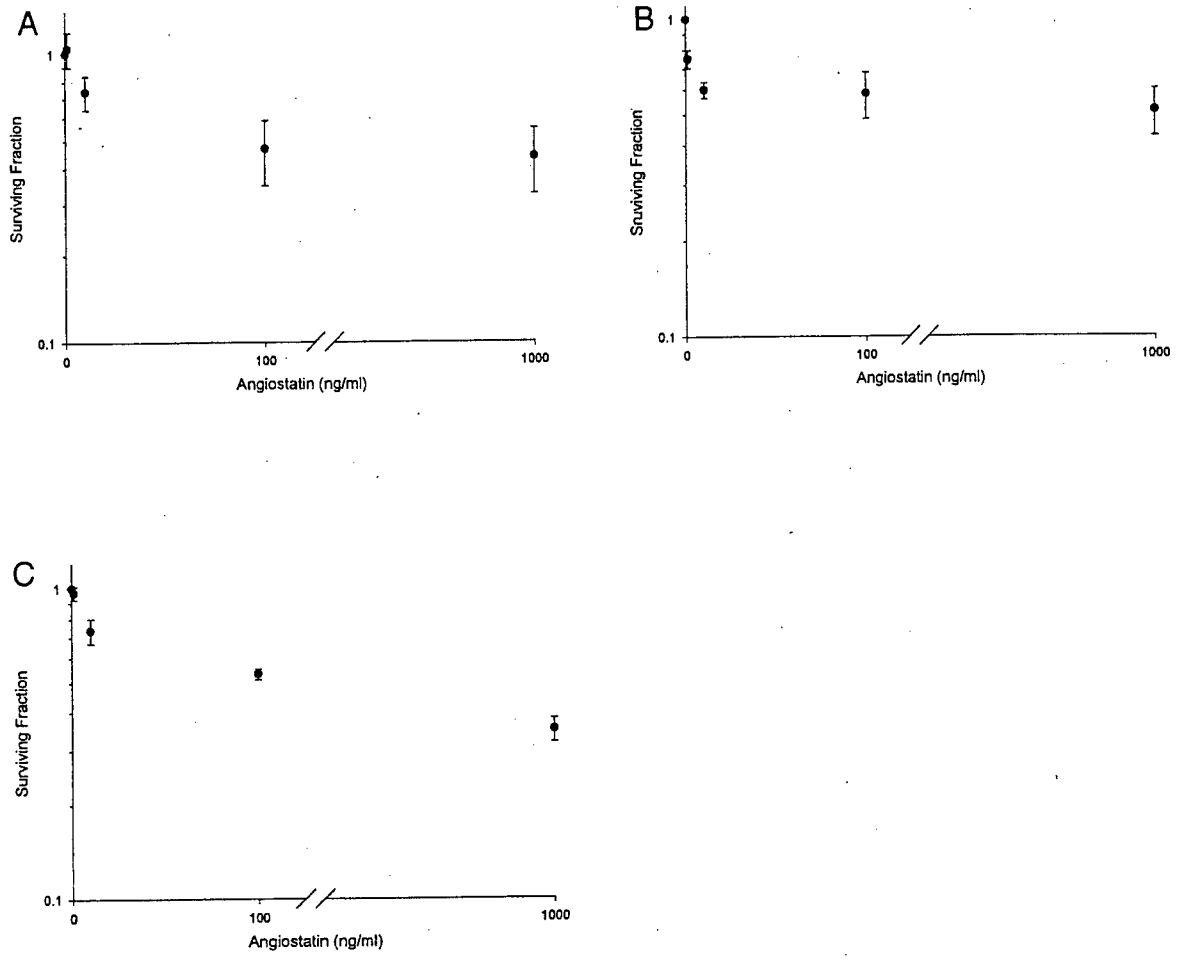

FIG. 1. Clonogenic survival of HUVEC (A), HAEC (B), and BAEC (C) following exposure to 0, 1, 10, 100, and 1000 ng/ml angiostatin (mean ± SEM of three experiments).

steep initial cytotoxic effect of angiostatin on all three endothelial cell lines at 1–10 ng/ml. These cytotoxic effects plateau at 100 ng/ml and remain unchanged to 1000 ng/ml angiostatin. Maximum clonogenic cell death mediated by angiostatin ranges between 40 and 50%. Cell growth was inhibited (27 and 35% in two experiments) in HUVEC 2 days after the addition of 100 ng/ml angiostatin. No changes in any cell cycle compartment were noted in the angiostatin-treated endothelial cells when compared with untreated controls (data not shown). To investigate the possibility of angiostatin causing anoikis (the detachment from the extracellular matrix resulting in apoptosis) in endothelial cells, exponentially growing HUVEC had the medium removed (eliminating all floating cells) and fresh medium containing 100 ng/ml angiostatin added. 3.5 hours later, the culture flask was rapped sharply on the bench and the detached cells collected. The cells were centrifuged and the angiostatin-containing medium discarded. The detached cells were resuspended and plated in fresh medium in 100-mm tissue culture dishes and returned to the incubator for 14 days. Three times as many colonies (each colony derived from a viable, single cell that had detached) were present in the angiostatin-treated HUVEC when compared to untreated control. These results suggest that angiostatin affects the attachment and motility of endothelial cells and thereby decreases their ability to migrate, but does not result in apoptosis. These data demonstrate that angiostatin-mediated cytotoxicity is not a result of anoikis.

To determine whether angiostatin is cytotoxic to nonproliferating or proliferating endothelial cells, plateau phase cultures of BAEC were treated with 100 ng/ml angiostatin for 4 and 28 h and the surviving fractions assessed by colony formation. 85% of the cells were in the G_1 phase of the cell cycle as determined by FACS analysis. At 4 h untreated control cultures demonstrated a surviving fraction of 0.27 ± 0.026, while the culture treated with 100 ng/ml angiostatin had a surviving fraction of 0.21 ± 0.115. At 28 h, the untreated controls had a surviving fraction of 0.256 ± 0.021 and the culture treated with 100 ng/ml had a surviving fraction of 0.326 ± 0.236 (mean ± SEM of

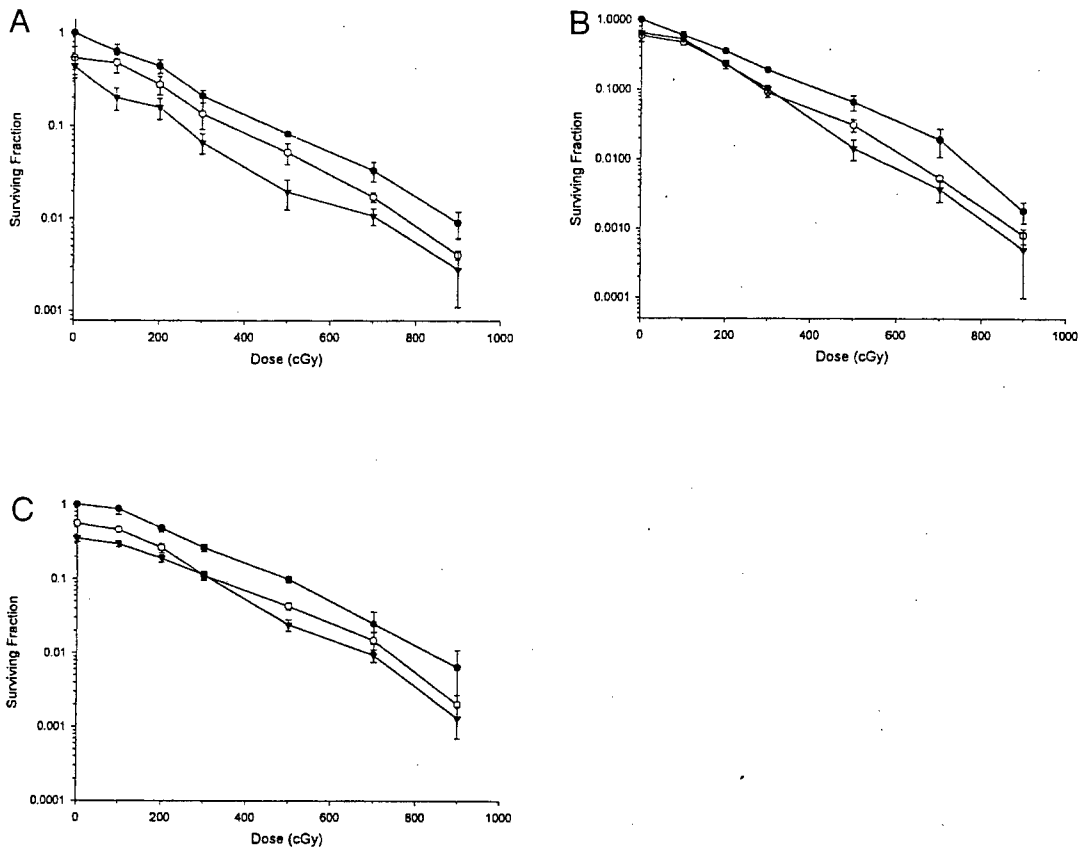

FIG. 2. X-ray survival ± angiostatin in (A) HUVEC, (B) HAEC, and (C) BAEC. ●, control; ○, 100 ng/ml angiostatin; ▼, 1000 ng/ml angiostatin.

two experiments). These results indicate that angiostatin has little if any cytotoxic effect on noncycling plateau phase cells.

To investigate a potential cytotoxic interaction between angiostatin and IR in endothelial cells, we performed X-ray survival analysis (100–900 cGy) in the presence of 0, 1, 10, 100, and 1000 ng/ml angiostatin. An additive cytotoxic interaction between angiostatin and IR at 100 and 1000 ng/ml angiostatin was demonstrated (Fig. 2) in exponentially growing HUVEC, HAEC, and BAEC. By contrast, treatment of confluent BAEC cultures with 100 ng/ml angiostatin and 700 cGy demonstrated that there was no difference in survival of angiostatin-treated plateau phase (G_1) cells when compared to cells treated with IR alone (data not shown). These data suggest that radiation interacts with angiostatin predominantly in dividing endothelial cells.

Previously, we reported no increase in apoptosis when HUVEC cultures were treated with angiostatin (100 ng/ml) and IR (17). Our findings differed from those of another laboratory that reported an increase in apoptosis following exposure of bovine adrenal cortex capillary endothelial cells to 2.5 μg/ml angiostatin (20). We, therefore, increased the angiostatin concentration 10-fold to 1000 ng/ml to assess apoptosis in HUVEC in the present study. We employed 7-AAD staining and FACS analysis to evaluate apoptosis. To investigate the cytotoxic interaction of angiostatin and IR, HUVEC were treated with 1000 ng/ml angiostatin, 1000 cGy, or the combination of 1000 ng/ml angiostatin + 1000 cGy. No difference in percentage of apoptosis was found between controls and angiostatin alone, or between IR alone and the combination of 1000 ng/ml angiostatin + IR (Table 1). These data demonstrate that angiostatin induces endothelial cell killing by a mechanism other than apoptosis.

Whereas these results demonstrate that the cytotoxic interaction between angiostatin and IR is additive *in vitro,* previous studies have shown that antitumor effects of IR and angiostatin are greater than additive *in vivo* (17, 21). We, therefore, investigated whether angiostatin and IR interact at the migration stage of angiogenesis. Our results demonstrate that the combination of angiostatin and IR inhibits endothelial cell migration to a greater degree than either treatment alone (Fig. 3). Although angiostatin and IR result in decreased survival of endothelial cells, the migration assays are completed within 24 h of treatment at which time the endothelial cells are phenotyp-

TABLE 1

Time post-IR (h)	Control	1000 ng/ml angiostatin	1000 cGy	1000 ng/ml angiostatin + 1000 cGy
0	6.3	6.5	9.2	6.9
12	11.9	9.1	11.8	8.2
24	5.5	3.6	4.7	3.7
48	16.7	15.4	18.5	16.2

Note. HUVEC were assayed for % apoptosis by staining with 7-AAD after treatment with 1000 ng/ml angiostatin, 1000 cGy, or the combination of 1000 ng/ml angiostatin added 4 h prior to 1000 cGy.

ically and metabolically functional as measured by trypan blue exclusion and cell cycle analysis. Thus, the differences in migration observed are not a result of cell death. These findings, taken together with the survival data, suggest that the angiostatin/IR interaction occurs at both the proliferation and migration stages of angiogenesis.

We have previously reported that angiostatin and IR produce a significantly greater antitumor effect than either agent alone without an increase in normal tissue toxicity. Histological analysis suggested that these agents interacted on the tumor microvasculature (17). Here we report that angiostatin and IR interact in proliferating endothelial cells and induce mitotic, rather than apoptotic, cell death. In addition, we demonstrate that angiostatin and IR have an additive antivascular interaction at the migration stage of angiogenesis. The combined cytotoxic and antimigratory effects of angiostatin and IR on endothelial cells support a mechanism for the antitumor interaction of these agents. Although the cytotoxic interaction between angiostatin and IR at the proliferation and migration phases is approximately additive, our data suggest that antiangiogenic therapies which block more than one stage of angiogenesis may be highly effective when combined with IR. The present results also demonstrate that treatment of endothelial cells with angiostatin has no detectable effect on induction of apoptosis. These findings are in contrast to reports that angiostatin induces endothelial cell apoptosis (15). In addition, while other studies have reported levels of apoptosis in control and angiostatin-treated endothelial cells that are similar to those found in the present work (20), our conclusions differ. Our results suggest that the percentage of apoptotic cells following angiostatin treatment is not significantly elevated to support a mechanism involving endothelial cell apoptosis.

Our results have several implications for cancer treatment. First, the fraction of proliferating endothelial cells in the tumor microenvironment may determine the efficacy of certain angiogenesis inhibitors when employed alone or in combination with other cytotoxic therapies. Second, different stages of tumor angiogenesis may be targeted by angiogenesis inhibitors when used in combination with cytotoxic agents. Our data also suggest that angiogenesis inhibitors need not be potent endothelial cell cytotoxins to be effective in clinical cancer treatment. In this context, angiostatin or the combination of angiostatin and IR is selectively toxic to a subset of proliferating endothelial cells.

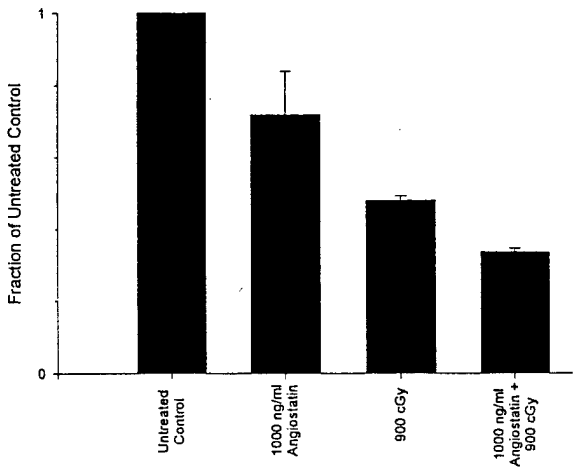

FIG. 3. Migration assay of HUVEC. HUVEC were untreated (control), treated with 1000 ng/ml angiostatin, 9 Gy, or the combination 1000 ng/ml angiostatin + 9 Gy. Reported as fraction of migrated cells when compared to untreated control (mean ± SEM of two experiments).

ACKNOWLEDGMENTS

This research supported by a grant (DAMD17-98-1-8603) from the Department of Defense Prostate Cancer Program, a grant (P50DE/CA11921) from the National Cancer Institute (Oral Cancer Center), the Center for Radiation Therapy, the Chicago Tumor Institute, and gifts from the Passis family and Varian Medical Systems, Inc.

REFERENCES

1. Folkman, J., and Shing, Y. (1992) Angiogenesis. *J. Biol. Chem.* **267,** 10931–10934.
2. Folkman, J. (1995 Angiogenesis in cancer, vascular, rheumatoid and other disease. *Nat. Med.* **1,** 27–31.
3. Denekamp, J. (1991) The current status of targeting tumour vasculature as a means of cancer therapy: An overview. *Int. J. Radiat. Biol.* **60,** 401–408.
4. Harris, A. L., Fox, S., Leek, R., Zhang, H., Scott, P., Bicknell, R., and Gatter, K. (1995) Breast cancer angiogenesis: Therapy target and prognostic factor. *Eur. J. Cancer* **31A,** 831–832.

5. Kerbel, R. S. (1991) Inhibition of tumor angiogenesis as a strategy to circumvent acquired resistance to anticancer therapeutic agents. *BioEssays* **13,** 31–36.
6. Denekamp, J. (1982) Endothelial cell proliferation as a novel approach to targeting tumour therapy. *Br. J. Cancer* **45,** 136–139.
7. O' Reilly, M., Holmgren, L., Shing, Y., Chen, C., Rosenthal, R. A., Cao, Y., Moses, M., Lane, W. S., Sage, E. H., and Folkman, J. (1994) Angiostatin: A circulating endothelial cell inhibitor that suppresses angiogenesis and tumor growth. *Can. J. Nurs. Res.* **26,** 41–53.
8. Cao, Y., Ji, R. W., Davidson, D., Schaller, J., Marti, D., Sohndel, S., McCance, S. G., MS, O. R., Llinas, M., and Folkman, J. (1996) Kringle domains of human angiostatin. Characterization of the anti-proliferative activity on endothelial cells. *J. Biol. Chem.* **271,** 29461–29467.
9. O' Reilly, M., Holmgren, L., Shing, Y., Chen, C., Rosenthal, R. A., Moses, M., Lane, W. S., Cao, Y., Sage, E. H., and Folkman, J. (1994) Angiostatin: A novel angiogenesis inhibitor that mediates the suppression of metastases by a Lewis lung carcinoma [see comments]. *Cell* **79,** 315–328.
10. Soff, G. A., Sanderowitz, J., Gately, S., Verrusio, E., Weiss, I., Brem, S., and Kwaan, H. C. (1995) Expression of plasminogen activator inhibitor type 1 by human prostate carcinoma cells inhibits primary tumor growth, tumor-associated angiogenesis, and metastasis to lung and liver in an athymic mouse model. *J. Clin. Invest.* **96,** 2593–2600.
11. Tanaka, T., Cao, Y., Folkman, J., and Fine, H. A. (1998) Viral vector-targeted antiangiogenic gene therapy utilizing an angiostatin complementary DNA. *Cancer Res.* **58,** 3362–3369.
12. Cao, Y. (1999) Therapeutic potentials of angiostatin in the treatment of cancer. *Haematologica* **84,** 643–50.
13. Griscelli, F., Li, H., Bennaceur-Griscelli, A., Soria, J., Opolon, P., Soria, C., Perricaudet, M., Yeh, P., and Lu, H. (1998) Angiostatin gene transfer: Inhibition of tumor growth in vivo by blockage of endothelial cell proliferation associated with a mitosis arrest. *Proc. Natl. Acad. Sci. USA* **95,** 6367–6372.
14. Moser, T. L., Stack, M. S., Asplin, I., Enghild, J. J., Hojrup, P., Everitt, L., Hubchak, S., Schnaper, H. W., and Pizzo, S. V. (1999) Angiostatin binds ATP synthase on the surface of human endothelial cells. *Proc. Natl. Acad. Sci. USA* **96,** 2811–2816.
15. Lucas, R., Holmgren, L., Garcia, I., Jimenez, B., Mandriota, S. J., Borlat, F., Sim, B. K., Wu, Z., Grau, G. E., Shing, Y., Soff, G. A., Bouck, N., and Pepper, M. S. (1998) Multiple forms of angiostatin induce apoptosis in endothelial cells. *Blood* **92,** 4730–4741.
16. O'Reilly, M. (1997) Angiostatin: An endogenous inhibitor of angiogenesis and of tumor growth. *EXS* **79,** 273–294.
17. Mauceri, H. J., Hanna, N. N., Beckett, M. A., Gorski, D. H., Staba, M. J., Stellato, K. A., Bigelow, K., Heimann, R., Gately, S., Dhanabal, M., Soff, G. A., Sukhatme, V. P., Kufe, D. W., and Weichselbaum, R. R. (1998) Combined effects of angiostatin and ionizing radiation in antitumour therapy. *Nature* **394,** 287–291.
18. Chmura, S. J. (1997) Comparison of TdT, 7-AAD, and propidium iodide staining to detect apoptotic lymphocytes. *In* Immunology Methods Manual: The Comprehensive Sourcebook of Techniques (Lefkovits, I., Ed.), Vol. 3. Academic Press, San Diego.
19. Tolsma, S. S., Volpert, O. V., Good, D. J., Frazier, W. A., Polverini, P. J., and Bouck, N. (1993) Peptides derived from two separate domains of the matrix protein thrombospondin-1 have anti-angiogenic activity. *J. Cell Biol.* **122,** 497–511.
20. Claesson-Welsh, L., Welsh, M., Ito, N., Anand-Apte, B., Soker, S., Zetter, B., O'Reilly, M., and Folkman, J. (1998) Angiostatin induces endothelial cell apoptosis and activation of focal adhesion kinase independently of the integrin-binding motif RGD. *Proc. Natl. Acad. Sci. USA* **95,** 5579–5583.
21. Gorski, D. H., Mauceri, H. J., Salloum, R. M., Gately, S., Hellman, S., Beckett, M. A., Sukhatme, V. P., Soff, G. A., Kufe, D. W., and Weichselbaum, R. R. (1998) Potentiation of the antitumor effect of ionizing radiation by brief concomitant exposures to angiostatin. *Cancer Res.* **58,** 5686–5689.

ORIGINAL ARTICLE

Antitumor Interaction of Short-Course Endostatin and Ionizing Radiation

Nader N. Hanna, MD,[a] Saraswathy Seetharam, PhD,[a] Helena J. Mauceri, PhD,[a] Michael A. Beckett, BS,[a] Nora T. Jaskowiak, MD,[a] Rabih M. Salloum, MD,[a] Danielle Hari, BS,[a] *Chicago, Illinois*, Mohanraj Dhanabal, PhD,[b] Ramani Ramachandran, PhD,[b] Raghu Kalluri, PhD,[b] Vikas P. Sukhatme, MD, PhD,[b] Donald W. Kufe, MD,[c] *Boston, Massachusetts*, Ralph R. Weichselbaum, MD,[a] *Chicago, Illinois*

PURPOSE

The purpose of this study was to evaluate whether endostatin, an antiangiogenic cleavage fragment of collagen XVIII, enhances the antitumor effects of ionizing radiation (IR). Endostatin was injected to coincide with fractionated radiotherapy.

METHODS

Xenografts of radioresistant SQ-20B tumor cells were established in athymic nude mice. Lewis lung carcinoma cells were injected into C57Bl/6 mice. Mice bearing SQ-20B xenografts were injected intraperitoneally with 2.5 mg/kg/day of murine recombinant endostatin 5 times per week for 2 weeks 3 hours before IR treatment (50 Gy total dose). Mice bearing Lewis lung carcinoma tumors were injected intraperitoneally with endostatin (2.5 mg/kg/day) four times; the first injection was given 24 hours before the first IR dose (15 Gy) and then 3 hours before IR (15 Gy/day) for 3 consecutive days. Microvascular density was assessed on tumor tissue sections by use of CD31 immunohistochemistry and light microscopy. Endothelial cell survival analyses was employed to evaluate endostatin effects on human aortic endothelial cells and human umbilical vein endothelial cells. Endothelial cell apoptosis was examined by use of FACS analysis and DAPI microscopy.

RESULTS

In SQ-20B xenografts, combined treatment with endostatin and IR produced tumor growth inhibition that was most pronounced at the nadir of regression (day 21). By day 35, tumors receiving combined treatment with endostatin and IR were 47% smaller than tumors treated with endostatin alone. Interactive cytotoxic treatment effects between endostatin and IR were also demonstrated in mice bearing Lewis lung carcinoma tumors. Significant tumor growth inhibition was observed in the endostatin/IR group at days 11 and 13 compared with IR alone. Histologic analyses demonstrated a reduction in microvascular density after combined treatment with endostatin and IR compared with endostatin treatment alone. Survival analyses confirmed interactive cytotoxicity between endostatin and IR in both human aortic endothelial cells and human umbilical vein endothelial cells but not in SQ-20B tumor cells. Combined treatment with endostatin and IR produced an increase in cultured pulmonary artery endothelial apoptosis compared with either treatment alone.

DISCUSSION

The tumor regression observed after combined treatment with endostatin and IR suggests additive antitumor effects in both human and murine tumors. Importantly, the concentrations of endostatin employed produced little tumor regression when endostatin was employed as a single agent. The results from the clonogenic and apoptosis assays support the hypothesis that the endothelial compartment is the target for the endostatin/IR interaction *(Cancer J 2000;x:xxx-xxx)*.

KEY WORDS
Antiangiogenic therapy, ionizing radiation, targeting, vasculature

From the Departments of [a]Radiation and Cellular Oncology and Surgery, University of Chicago, Chicago, Illinois, [b]Renal Division, Beth Israel Deaconess Medical Center, Boston, Massachusetts; and [c]Dana-Farber Cancer Institute and Harvard Medical School, Boston, Massachusetts.

Received on month day, year; accepted for publication month day, year.

No benefits in any form have been or will be received from a commercial party related directly or indirectly to the subject of this article.

Reprint requests: Ralph R. Weichselbaum, MD, University of Chicago, Department of Radiation and Cellular Oncology, 5758 S. Maryland Ave., MC 9006, Chicago, IL 60637

Supported by a grant (DAMD17-98-1-8603) from the Department of Defense Prostate Cancer Program, a grant (P50DE/CA11921) from The National Cancer Institute (Oral Cancer Center), The Center for Radiation Therapy, The Chicago Tumor Institute, and gifts from the Passis family and Varian Medical Systems, Inc.

Angiogenesis, a critical factor in early tumor development,[1–3] is associated with aggressive behavior of human cancers.[4–8] Traditional cancer treatments with chemotherapy and/or radiotherapy have been directed at malignant cell populations and often fail to achieve tumor control.[9] Targeting tumor vasculature with angiogenic inhibitors has emerged as a new direction for cancer

treatment.[10-12] Potential advantages of employing angiogenic inhibitors are that they target genetically stable normal endothelial cells that are less likely to acquire resistance to cancer therapy agents.[13] In addition, one tumor vessel may supply 10^5 to 10^6 tumor cells, and thus tumor endothelial cell targeting may amplify the antitumor effects.

Endostatin, first isolated from mice bearing hemangioendotheliomas, is a 20-kDa C-terminal proteolytic fragment of collagen XVIII that is localized to the perivascular space.[14] O'Reilly et al[15] demonstrated that treatment with endostatin at a dose of 0.3 mg/kg/day suppressed the growth of lung metastases in the Lewis lung carcinoma (LLC) tumor model. Importantly, no weight loss, systemic toxicity, or drug resistance was observed in animals receiving endostatin treatment. However, tumors recurred at the primary site 5 to 14 days after discontinuation of endostatin therapy. Endostatin is currently under investigation in human trials.

Current antiangiogenic therapy requires continuous and prolonged administration of angiogenic inhibitors. A strategy that targets both tumor cells and/or increases the efficacy of endothelial cell kill might overcome the requirement for prolonged antiangiogenic treatment and address problems associated with the production and availability of angiostatin and endostatin. In the present studies, we demonstrate a modulation of endothelial cell death after exposure to endostatin. We also report an increase in antitumor effects when endostatin treatment is combined with ionizing radiation (IR) when compared with either treatment alone. Histopathologic analyses demonstrate a decrease in tumor angiogenesis, as indicated by a reduction in microvascular density at day 35. These data, combined with our in vitro studies, support interactive cytotoxic effects of endostatin and IR that are specific for endothelial cells that produce antitumor effects without toxicity.

METHODS

Cell Lines

The human aortic endothelial cells (HAEC) and human umbilical vein endothelial cells (HUVEC) that were used for these studies were purchased from Clonetics and maintained in EGM-2 medium (Clonetics Corporation, San Diego, CA). Calf pulmonary artery endothelial (CPAE) cells were obtained from the ATCC (Manassas, VA) and were maintained in Dulbecco's Modified Eagle's Medium (DMEM) (Gibco, Grand Island, NY) supplemented with 10% fetal bovine serum (Intergen, Purchase, NY), 100 units/mL of penicillin (GIBCO), and 100 μg/mL streptomycin (GIBCO). SQ-20B cells, derived from a patient with squamous cell cancer of the larynx after recurrence following primary radiotherapy (D_0 = 239 cGy), were maintained as previously described.[16] Lewis lung carcinoma (LLC-LM) tumor cells, a gift from Dr. Judah Folkman, were grown in DMEM supplemented with 10% heat-inactivated fetal bovine serum, 100 units/mL of penicillin, and 100 μg/mL of streptomycin.

Cloning and Expression of Murine Endostatin in *Escherichia coli*

The sequence encoding the carboxyl terminal portion of the mouse collagen XVIII was amplified by polymerase chain reaction (PCR) by use of Vent DNA polymerase and the endostatin pBAPak 8 vector as a template. PCR was carried out for 30 cycles by use of 94°C for denaturation, 600C for annealing, and 72°C for extension, one minute for each. The amplified DNA fragment (355 base pairs) was purified by use of a QIAquick PCR purification kit, digested with *Nde*I and *Xho*I and ligated into the pET17b his expression vector. Initial transformation was carried out in the HMS 174 host strain. Positive clones were sequenced on both strands and finally transformed into BL21(DE3) for expression. The expression of recombinant protein in the pET system was carried out according to manufacturer specifications.

Murine Endostatin Purification

Recombinant endostatin was purified by use of a Ni-NTA column in the presence of 8 M of urea, as described in the QIA expressionist manual. Briefly, the bacterial pellet was solubilized in equilibration buffer containing 8 M of urea, 10 mM of Tris, and 100 mM of sodium phosphate buffer, pH 8 0, for 1 hour at room temperature. The suspension was sonicated three to four times and centrifuged at 10,000 × g. The soluble fraction was loaded onto a Ni-NTA column operating at a flow rate of 10 to 20 mL/h. The column was washed repeatedly with equilibration buffer. Bound proteins were eluted by sequentially lowering the pH of the buffer from pH 8.0 to 6.3, 4.2, and 3.0. Purified fractions were analyzed by SDS-PAGE. Fractions containing purified endostatin protein were pooled and permitted to slowly refold. During dialysis against phosphate-buffered saline (PBS), pH 7.4, at 4°C, the protein precipitated out of solution. Endostatin was further concentrated and stored in small aliquots at −70°C. Protein concentration was determined by use of the BCA assay (Pierce, Rockford, IL).

Expression and Purification of Murine Endostatin in *Pichia pastoris*

The sequence encoding mouse endostatin was further modified by PCR by use of Vent DNA polymerase. The

amplified fragment containing *Eco*RI and *Not*I restriction sites was subcloned into a predigested yeast expression vector. Initial transformation was performed in the top 10' host strain. The resultant clones were screened for insert, and the positive clones were sequenced. The plasmid was linearized with *Sac* I and used for homologous recombination into the host strain GS115. Transformation was carried by use of the lithium chloride method using standard techniques. Recombinants were selected by plating on Yeast Proteome Database plates containing 100 μg/mL of Zeocin and clones, which grew and were then tested for expression. Protein purification of endostatin was carried out by use of a heparin-agarose column.

Clonogenic Assay

For endostatin dose response experiments, 200 to 1000 HUVECs and HAECs were plated in 100-mm tissue culture dishes. The VEGF normally present in the growth medium was replaced with 10 ng/mL VEGF purchased from R&D Systems (Minneapolis, MN). Eighteen hours after plating, 0, 1, 10, 100,and 1000 ng/mL of murine endostatin was added. For x-ray survival analysis, 200 to 20,000 HUVECs and HAECs were plated in 100-mm tissue culture dishes. Eighteen hours after plating, cells were irradiated with 100 to 900 cGy by use of a GE Maxitron X-ray generator operating at 250 kV, 26 mA, with a 0.5-mm copper filter, at a dose rate of 118 cGy/min. For the combined experiments, 200 to 20,000 HUVECs and HAECs were plated in 100–mm tissue culture dishes. Eighteen hours after plating 0, 10, and 100 ng/mL of murine endostatin was added. Four hours after the addition of endostatin, the cells were treated with 100 to 900 cGy. For all experiments, cultures were incubated for 14 to 17 days, after which they were stained with crystal violet, colonies were counted, and the surviving fraction was determined. Colonies containing more than 50 cells were scored as positive.

Analysis of Apoptosis Using FACS and DAPI Microscopy

HUVECs treated with 100 ng/mL of murine endostatin, IR, or the combination were harvested at 0, 1, 4, 8, 12, 24, 48, 72, and 96 hours. Cells were grown in 100-mm tissue culture dishes and harvested into single-cell suspensions by use of 0.05% trypsin/ethylenediaminetetraacetic acid. CPAE cells were plated in a six-well plate at 100,000 cells/well and treated with 10 μg/mL endostatin, 9 Gy, or the combination on the following day. Endostatin was added 4 hours before IR. Cells were harvested at 0 hours, 24 hours, and 48 hours. Cells were fixed by rinsing twice with PBS. The pellet was broken by tapping, and cells were resuspended in 0.5 mL of paraformaldehyde. After fixation, 1×10^6 cells were washed in PBS and resuspended in 3.8 mM of sodium citrate. RNase A (0.125 mg/mL) was added, and the cells incubated at 37°C for 30 minutes. Propidium iodide (0.01 mg/mL) was added, and cells were incubated on ice for 30 minutes. DNA content was analyzed by use of a Becton-Dickinson FACScan Analyzer.

For morphologic analysis, 5×10^6 cells were washed in PBS and resuspended at a concentration of 1×10^6 cell/mL of PBS. The cell suspension (200 μL) was transferred to a microscope slide coated with poly-L-lysine by use of a CytoSpin centrifuge. Four hundred microliters (0.1 μg/mL) of DAPI was applied to each slide for 15 minutes in the dark. The slides were washed twice with PBS and dried. Cover slips were mounted by use of Vectashield mounting medium. The slides were viewed by use of a Zeiss photomicroscope equipped with a Photometrics digital camera connected to a Power Macintosh running IP Lab Analysis software. Random fields were photographed and 100 nuclei counted for each experimental condition.

Animal Studies

SQ-20B xenografts were grown in the hind limbs of 6- to 8-week-old athymic female nude mice (Frederick Cancer Research Institute, Frederick, MD) by subcutaneous inoculation of 5×10^6 cells suspended in 100 mL of PBS. Tumors were permitted to grow for 11 to 15 days to a mean volume of 470.3 ± 28.1 mm^3 ($n = 51$). LLC tumor cells (1×10^6 in PBS) were injected in the right hind limb of C57Bl/6 female mice and permitted to grow to a mean volume of 305.9 ± 8.2 mm^3 ($n = 35$). At day 0, initial tumor volume was determined by direct measurement by use of calipers, as previously described.[17] Subsequently, tumor volume was determined two to three times per week. Based on the day 0 tumor volume, mice were randomly assigned to treatment groups such that the mean volume of each treatment group was approximately equal. Mice treated with murine recombinant endostatin were injected intraperitoneally with a dose of 2.5 mg/kg at 3 hours before x-irradiation. Mice bearing SQ-20B xenografts were injected five times per week for 2 weeks to coincide with IR exposure (5 Gy/day, 5 days/week to a total dose of 50 Gy). Mice bearing LLC tumors were injected with endostatin 24 hours before the first IR dose and then 3 hours before IR for 3 consecutive days (15 Gy/day to a total dose of 45 Gy). The care and treatment of experimental animals was in accordance with institutional guidelines. Data are reported as percent of original (day 0) tumor volume and are graphed as fractional tumor volume ± SEM.

Immunohistochemistry

At day 35, mice were euthanized, and tumors were excised and fixed in 10% neutral buffered formalin.

After the tumors were embedded in paraffin, 5-μm sections were cut, tissue sections were mounted, and CD31 immunohistochemistry was performed. A total of five high-power fields (400×) per section were examined by use of a Nikon Microphot-FX microscope equipped with a Sony digital camera. Vessel counts were determine by use of Macintosh Image Pro-Plus imaging software as previously described.[18]

Statistical Analysis

Statistical significance was determined by use of one-way analysis of variance (ANOVA) and students *t*-test.

RESULTS

To explore the potential cytotoxic effects of endostatin, survival analysis was performed on HAECs, HUVECs, and SQ-20B tumor cells. Clonogenic assays demonstrated 20% to 40% killing for HAECs and HUVECs exposed to concentrations of 1000 ng/mL of endostatin (Fig. 1a). To explore potential interactive cytotoxicity, HAEC (Fig. 1b) and HUVEC cultures were treated with endostatin and exposed to IR. Both 10 and 100 ng/mL of endostatin produced enhancement of IR killing of HAECs at doses ranging from 100 to 900 cGy. IR killing enhancement of HUVECs occurred at the higher radiation doses (700 and 900 cGy). An interaction between endostatin and IR was present in both HAEC and HUVEC cell lines. By contrast, no interactive killing was observed when SQ-20B tumor cells were treated with the combination of endostatin and IR (data not shown).

To evaluate whether the mechanism of interaction between endostatin and IR involves cell killing mediated by apoptosis, HUVECs were treated with 100 ng/mL of endostatin, 900 cGy, or the combination. There was no increase in apoptosis in cells treated with (1) endostatin alone compared with control cells and (2) endostatin plus IR when compared with IR alone. Dhanabal et al[19] reported significant differences in annexin fluorescence intensity (apoptosis) in CPAE cells treated with 5 and 10 μg/mL of endostatin when compared with control. Examination of CPAE cells 24 hours after treatment with 10 μg/mL of endostatin, 9 Gy, or the combination, showed that the control cells were 7% apoptotic, cells treated with 10 μg/mL of endostatin were 20% apoptotic, cells treated with 9Gy were 20.6% apoptotic, and cells treated with the combination were 34% apoptotic. Forty-eight hours after treatment, control cells were 17.8% apoptotic, cells treated with endostatin were 32% apoptotic, cells treated with 9 Gy were 27.8% apoptotic, and cells treated with the combination were 56.1% apoptotic. These data, considered with data from HAECs and HUVECs, suggest that the mechanism of endothelial cell killing may be both necrotic and apoptotic.

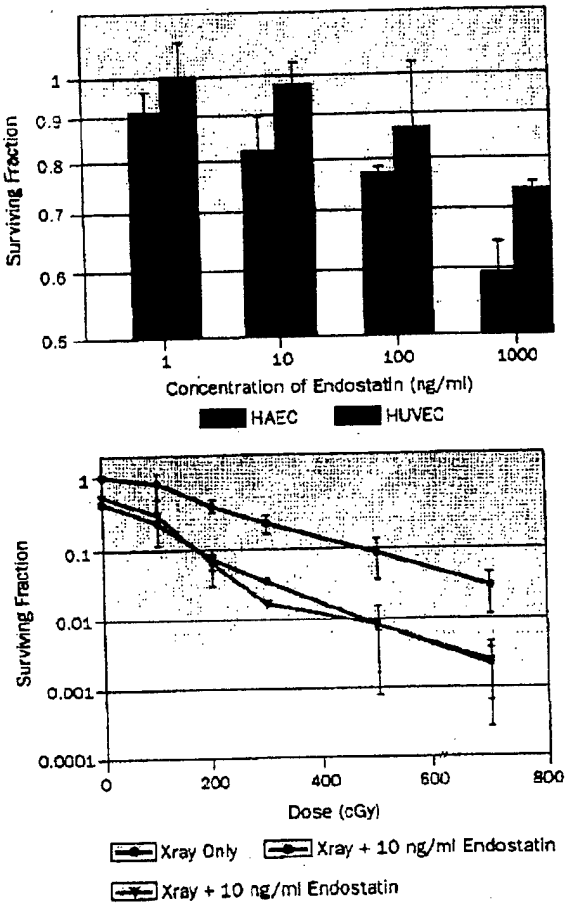

Figure 1(a) Endothelial cells (200–500 human aortic endothelial cells [HAECs] and human umbilical vein endothelial cells [HUVECs]) were plated in EGM-2 medium in 100-mm tissue culture dishes. Eighteen hours later, mouse endostatin (1, 10, 100, or 1000 ng/mL) was added. The dishes were returned to the incubator for 14 to 17 days, after which they were stained with crystal violet, colonies were counted, and the surviving fraction was determined. Colonies containing more than 50 cells were scored as positive. Values represent mean of two experiments ± SEM. (b) Endothelial cells (HAECs) were plated in EGM-2 medium. To account for radiation killing, increasing numbers of cells (200 to 10^4) were plated in 100-mm tissue culture dishes. Eighteen hours later, plating endostatin was added at concentrations of 10 and 100 ng/mL. Four hours later, cells were irradiated with doses of 100–700 cGy by use of a GE Maxitron x-ray generator operating at 26 mA, 250 kV, with a 0.5-mm copper filter, at a dose rate of 118 cGy/min. Cultures were incubated and stained as described earlier. Values represent mean of two experiments ± SEM.

We employed tumor regression and regrowth to evaluate potential interactive cytotoxic effects between endostatin and IR by use of tumor model systems. In animals bearing SQ-20B xenografts (mean volume at day 0 = 470.0 ± 28.1 mm^3, n = 51), combined treatment with endostatin and IR produced tumor

growth inhibition that was most pronounced at the nadir of regression (day 21) when compared with either treatment alone (Fig. 2). Compared with untreated control tumors, 50 Gy produced a 36% reduction in mean tumor volume, whereas treatment with endostatin alone produced a 21% reduction. After combined treatment with endostatin and 50 Gy, mean tumor volume was reduced by 69% ($P = 0.06$, ANOVA). This reduction (69%) was greater than expected (50%), suggesting an interaction between endostatin and IR. Mice in both the control and the IR treatment groups were sacrificed at day 25 because tumor burden. We monitored the remaining two treatment groups (endostatin alone and endostatin plus IR) until day 35, when we collected tumor tissue for immunohistochemical analysis. We noted that the effects of combined treatment were still evident. Tumors receiving combined treatment with endostatin and IR (443 ± 95 mm³) were 47% smaller than tumors treated with endostatin alone (832 ± 342 mm³). We conducted a second experiment (data not shown) employing SQ-20 B xenografts (mean volume at day 0 = 754.1 ± 60.9 mm³, $n = 26$). Again, we observed an increase in regression after combined treatment with endostatin and IR when compared with either treatment alone (day 14, $p = 0.06$, ANOVA). Although the nadir of regression was observed 7 days earlier than in the previous experiment, the antitumor interaction between endostatin and IR was unquestionable. No increase in local (in-field) desquamation effects between animals treated with IR and those treated with endostatin plus IR was noted. Additionally, body weights were maintained equally in all treatment groups compared with control animals (data not shown).

We conducted similar experiments employing the murine LLC model, which differs from the SQ-20B xenograft model in both radiosensitivity and doubling time. We found that in C57Bl/6 mice bearing LLC tumors (mean volume at day 0 = 305.9 ± 8.2 mm³, $n = 35$), injection of endostatin 24 hours before the initiation of IR therapy produced the best interaction between the two treatment modalities. Combined treatment produced tumor growth inhibition that was significant when compared with either treatment alone (day 11, $P = 0.001$, ANOVA, Fig. 3). Tumors in the control group were 11.2 times larger than initial volume (day

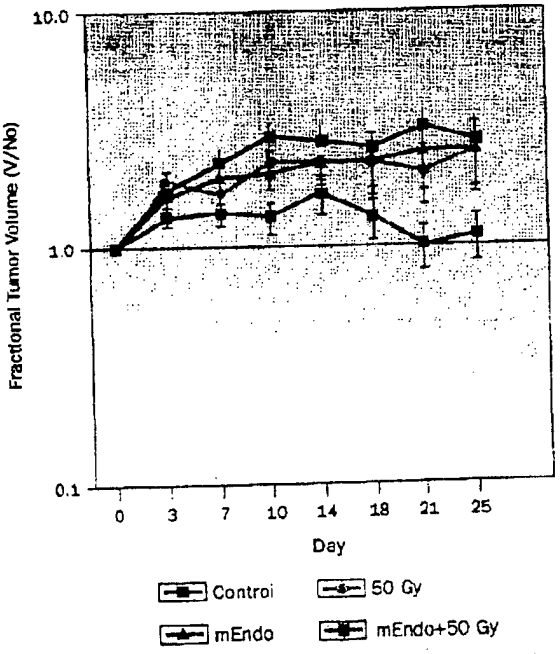

Figure 2 Tumor growth after combined treatment with endostatin and ionizing radiation (IR). Athymic nude mice bearing SQ-20B xenografts (470.3 ± 28.1 mm³) were injected intraperitoneally with murine recombinant endostatin (2.5 mg/kg) 3 hours before x-irradiation (5 Gy/day, 4 days/week, to a total dose of 50 Gy). Data are calculated as the percent of original volume (day 0) tumor volume and are graphed as fractional tumor volume ± SEM. Volumes of xenografts are shown after treatment with control (untreated); IR alone at 50 Gy; murine endostatin alone (mEndo); and murine endostatin and 50 Gy (mEndo + 50 Gy).

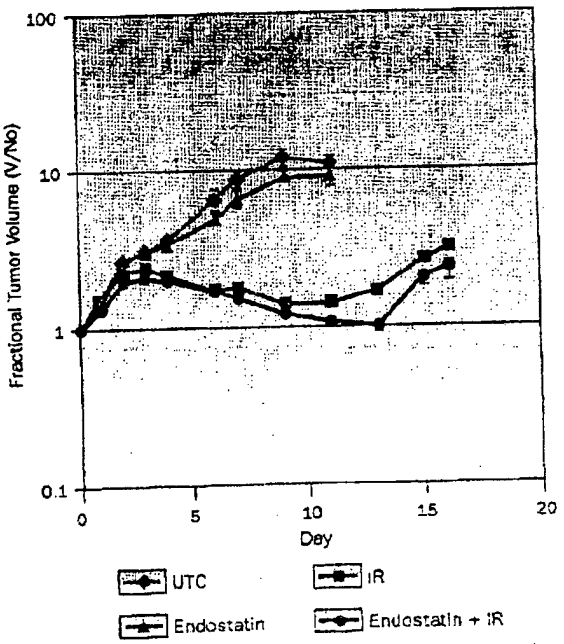

Figure 3 Tumor growth after combined treatment with endostatin and ionizing radiation (IR). C57Bl/6 female mice bearing Lewis lung carcinomas were injected intraperitoneally with murine recombinant endostatin (2.4 mg/kg) 24 hours before the first IR dose and then 3 hours before IR for 3 consecutive days (15 Gy/day to a total dose of 45 Gy). Data are calculated as the percent of original volume (day 0) tumor volume and are graphed as fractional tumor volume ± SEM. Volumes of tumors are shown after treatment with control (untreated); IR alone at 45 Gy; murine endostatin alone (mEndo); and murine endostatin and 45 Gy (mEndo + 45 Gy).

0), whereas those in the endostatin alone group were 9.38 times larger. Tumor growth in the IR and the combined treatment groups was slowed after treatment (IR alone = 1.41, IR plus endostatin = 1.08 times larger than initial volume). In spite of the rapid growth of LLC tumors, the comparatively low dose and short duration of endostatin treatment (2.5 mg/kg × 4 days), and the IR schedule (15 Gy × 3), interactive cytotoxic treatment effects between endostatin and IR were demonstrated in this experiment (expected = 10.5%, observed = 9.6%). Mice in the control and the endostatin alone groups were sacrificed at day 11 because of tumor burden. Mice in the IR and combined treatment groups were monitored until termination of the experiment on day 16. No increase in local (in-field) desquamation effects between animals treated with IR and those treated with endostatin plus IR was noted. Additionally, body weights were maintained equally in all treatment groups compared with control animals (data not shown).

To evaluate the effects of combined treatment with endostatin and IR on the tumor vasculature, we examined SQ-20B tumor tissue sections by use of anti-CD31 antibody and standard immunohistochemical techniques. Tumors were excised from six animals in the two surviving treatment groups (endostatin alone and endostatin plus IR) from the first experiment. The mean number of vessels per five high-power fields was reduced after exposure to combined treatment with endostatin and IR (14 ± 8) compared with endostatin alone (40 ± 11, Table 1). These data suggest an interaction between endostatin and IR.

DISCUSSION

Results from in vivo studies employing tumor model systems support the hypothesis that the tumor endothelium can be converted into a target for cytotoxic effects of IR. The tumor regression observed after combined treatment with endostatin and IR demonstrates interactive antitumor effects that are additive when compared with the effects of either treatment alone. Importantly, the antitumor effects observed were achieved by use of relatively low concentrations of endostatin (2.5 mg/kg/day) when compared with those used in the experiments of Boehm et al,[15] in which tumor-bearing animals were treated with 20 mg/kg/day. Also, in the present studies, endostatin was administered in order to coincide with fractionated radiotherapy. No additional endostatin was administered after the completion of IR therapy. In other published reports, prolonged endostatin treatment was required in order to achieve tumor control and to maintain dormancy.[15] Importantly, no increase in local or systemic side effects was noted in combined treatment groups when compared with animals treated with IR alone.

Further support for the hypothesis that the vasculature represents a target for endostatin/IR interaction comes from the immunohistochemical analyses of SQ-20B xenografts. The number of vessels in tumors treated with endostatin and IR was reduced when compared with the number of vessels in the tumors treated with endostatin alone. It is noteworthy that although a low dose of endostatin (2.5 mg/kg/day) was used in these experiments and endostatin treatment was terminated at day 11 to coincide with the last dose of IR, the effects of combined treatment persisted at day 35. A more dramatic treatment effect on vascular density may have been present at earlier times and during treatment. Also, the limited supply of murine endostatin prevented the use of a higher dose that might have revealed more dramatic tumor regression in the combined treatment group.

The hypothesis that the endothelium is a potential target for the cytotoxic interaction between endostatin and IR is further supported by studies that demonstrate that endostatin enhances the cytotoxic effects of IR on endothelial cells but not on tumor cells. These findings are similar to our previously published report using angiostatin.[18] The mechanism by which the combination of endostatin and IR produces cell killing appears to be a mitotic or an apoptotic mode of cell death, depending on the origin of the endothelial cells investigated. These results highlight potential molecular differences in mechanism or mechanisms of endostatin cell kill in endothelial cells and the interaction with IR.

CONCLUSIONS

The present data, considered with the results of our previous work employing angiostatin, strongly support our hypothesis that combined targeting of the tumor cell population and the endothelial cell population is superior to treatment of either component alone. Treatment with antiangiogenic peptides, such as endostatin

TABLE 1 Intratumoral Microvessel Density in SQ-20B Tumors[a]

Treatment	Microvessel Count Mean ± SEM	Median (range)
Endostatin (n = 6)	40 ± 11	41.5 (0–78)
Endostatin + IR (n = 6)	14 ± 8	7.0 (0–51)

Abbreviation: IR, ionizing radiation.
[a] P = 0.09; t-test.

that interacts with IR, can magnify tumor control by causing endothelial cell killing that deprives the growing tumor cells of an adequate blood supply. Evaluation of the antitumor interaction between short-course, low-dose endostatin and IR requires a different risk/benefit analysis for potential clinical use than a classical isobologram analysis between two toxic agents because substantial therapeutic benefit may be achieved without increased toxicity.[20] Radiotherapy combined with anti-angiogenic therapy offers considerable potential for the treatment of human cancers.

ACKNOWLEDGMENT

Dr. Nader N. Hanna is an Assistant Professor of Surgery at the University of Kentucky.

REFERENCES

1. Folkman J, Shing Y. Angiogenesis. *J Biol Chem* 1992;267: 10931–10934.
2. Folkman J. Angiogenesis in cancer, vascular, rheumatoid and other disease. Nat Med 1995;1:27–31.
3. Hanahan D, Folkman J. Patterns and emerging mechanisms of the angiogenic switch during tumorigenesis. J Natl Cancer Inst 1996;88:1091–1092.
4. Weidner N. Intratumoral vascularity as a prognostic factor in cancers of the urogenital tract. Eur J Cancer 1996;32A:2506–2512.
5. Weidner N, Folkman J. Tumoral vascularity as a prognostic factor in cancer. Important Adv Oncol 1996:167–190.
6. Weidner N, Carroll PR, Flax J et al. Tumor angiogenesis correlates with metastasis in invasive prostate carcinoma. Am J Pathol 1993; 143:401–409.
7. Weidner N, Folkman J, Pozza F et al. Tumor angiogenesis: a new significant and independent prognostic indicator in early-stage breast carcinoma [see comments]. J Biol Chem 1992;267: 26157–26165.
8. Weidner N, Semple JP, Welch WR et al. Tumor angiogenesis and metastasis: correlation in invasive breast carcinoma. N Engl J Med 1991;324:1–8.
9. Suit HD. The scope of the problem of primary tumor control. Cancer 1988;61:2141–47.
10. Gasti G, Hermann T, Steurer M et al. Angiogenesis as a target for tumor treatment. Oncology 1997;54:177–184.
11. Kerbel RS. Inhibition of tumor angiogenesis as a strategy to circumvent acquired resistance to anti-cancer therapeutic agents. Bioessays 1991;13:31–36.
12. Denekamp J, Hill S. Angiogenic attack as a therapeutic strategy for cancer. Radiother Oncol 1991;20[suppl 1]:103–112.
13. Denekamp J. Endothelial cell proliferation as a novel approach to targeting tumour therapy. Br J Cancer 1982;45:136–139.
14. O'Reilly M, Boehm T, Shing Y et al. Endostatin: an endogenous inhibitor of angiogenesis and tumor growth. Cell 1997;88: 277–285.
15. Boehm T, Folkman J, Browder T et al. Antiangiogenic therapy of experimental cancer does not induce acquired drug resistance [see comments]. Nature 1997;390:404–407.
16. Weichselbaum RR, Hallahan DE, Sukhatme VP et al. Gene therapy targeted by ionizing radiation. Int J Radiat Oncol Biol Phys 1992; 24:565–567.
17. Hallahan DE, Mauceri HJ, Seung LP et al. Spatial and temporal control of gene therapy using ionizing radiation. Nat Med 1995; 1:786–791.
18. Mauceri HJ, Hanna NN, Beckett MA et al. Combined effects of angiostatin and ionizing radiation in antitumour therapy. Nature 1998;394:287–291.
19. Dhanabal M, Ramchandran R, Waterman MJ et al. Endostatin induces endothelial cell apoptosis. J Biol Chem 1999;274: 11721–1726.
20. Gessner PK. Isobolographic analysis of interactions: an update on applications and utility. Toxicology 1995;105:161–179.

Bibliography

1. Mauceri, H. J., Hanna, N. N., Beckett, M. A., Gorski, D. H., Staba, M. J., Stellato, K. A., Bigelow, K., Heimann, R., Gately, S., Dhanabal, M., Soff, G. A., Sukhatme, V. P., Kufe, D. W., and Weichselbaum, R. R. (1998). Combined effects of angiostatin and ionizing radiation in antitumour therapy. Nature *394*, 287-291.
2. Gorski, D. H., Mauceri, H. J., Salloum, R. M., Gately, S., Hellman, S., Beckett, M. A., Sukhatme, V. P., Soff, G. A., Kufe, D. W., and Weichselbaum, R. R. (1998). Potentiation of the antitumor effect of ionizing radiation by brief concomitant exposures to angiostatin. Cancer Res *58*, 5686-5689.
3. Gorski, D. H., Beckett, M. A., Jaskowiak, N. T., Calvin, D. P., Mauceri, H. J., Salloum, R. M., Seetharam, S., Koons, A., Hari, D. M., Kufe, D. W., and Weichselbaum, R. R. (1999). Blockage of the vascular endothelial growth factor stress response increases the antitumor effects of ionizing radiation. Cancer Res *59*, 3374-3378.
4. Seetharam, S., Staba M-J., Schumm, L.P., Schreiber, K., Schreiber, H., Kufe, D.W., and Weichselbaum, R.R. (1999) Enhanced eradication of local and distant tumors by genetically produced interleuken-12 and radiation. Int. J. Onc. *15*, 769-773.
5. Mauceri, H.J., Beckett, M.A., Seetharam, S., Kufe, D.W., and Weichselbaum, R.R. (2000) Gene therapy targeted by ionizing radiation targets both tumor cells and tumor vasculature. Proceedings of the 11th International Congress of Radiation Research *2*, 672-675.
6. Colorado, P.C., Torre, A., Kamphaus. G., Maeshima, Y., Hopfer, H., Takahashi, K., Volk, R., Zamborsky, E.D., Herman, S., Sarkar, P.K., Eridksen, M.B., Dhanabal, M., Simons, M., Post, M., Kufe, D.W., Weichselbaum, R.R., Sukhatme, V.P., Kalluri, R. (2000) Antiangiogenic cues from vascular basement membrane collagen. Cancer Res *60*, 2520-2526.
7. Hari, D., Beckett, M.A., Sukhatme, V.P., Dhanabal, M., Lu, H., Mauceri, H.J., Kufe, D.W., and Weichsebaum, R.R. (2000) Angiostatin induces mitotic cell death of proliferating endothelial cells. Mol. Cell. Biol. Res. Commun. *3*, 277-282.
8. Hanna, N.N., Mauceri, H.J., Seetharam, S., Beckett, M.A., Jaskowiak, N.T., Salloum, R.M., Hari, D., Dhanabal, M., Ramchandran, R., Colorado,P.C., Kalluri, R., Sukhatme, V.P., Kufe, D.W., and Weichselbaum, R.R. Antitumor interaction of short course endostatin and ionizing radiation. The Cancer Journal from The Scientific American (In Press).
9. Seetharam, S., Mauceri, H.J., Beckett, M.A., Gupta, V., Koons, A., Schumm, P., Sukhatme, V.P., Dhanabal, M., Lu, H., Kufe, D.W., and Weichsebaum, R.R. Angiostatin in combination with cyclophosphamide inhibits lung metastases but not primary tumor growth. (Manuscript in preparation)

Personnel Receiving Pay From the Research Effort

Ralph R. Weichselbaum, M.D.

Michael Beckett

Amy Cha

Marija Pejovic (Cost Sharing)